

# **Watershed Hydrologic Modeling and Sediment and Nutrient Loading Estimation for the Lake Tahoe Total Maximum Daily Load**

**October, 2005**

**Revised: February 2007**

Prepared for:

Lahontan Regional Water Quality Control Board  
2501 Lake Tahoe Blvd.  
South Lake Tahoe, CA 96150

And

University of California–Davis  
1441 Research Park Drive #171  
Davis, CA 95616

Prepared by:

Tetra Tech, Inc.  
10306 Eaton Place, Suite 340  
Fairfax, VA 22030

# Contents

<b>1. PROJECT DEFINITION</b> .....	<b>1</b>
<b>2. MODEL SELECTION</b> .....	<b>4</b>
2.1. SELECTION CRITERIA .....	5
2.2. LOADING SIMULATION PROGRAM C++ (LSPC) OVERVIEW .....	6
<b>3. MODELING APPROACH</b> .....	<b>8</b>
3.1. WATERSHED SEGMENTATION .....	8
3.2. WATER BODY REPRESENTATION .....	9
3.3. METEOROLOGICAL DATA.....	10
<i>Local Weather Data</i> .....	11
<i>Local Temperature Data</i> .....	13
<i>Lapse Rate Calculations</i> .....	14
<i>Evapotranspiration Calculations</i> .....	15
<i>Synthetic Weather Dataset</i> .....	16
3.4. LAND USE REPRESENTATION .....	24
<i>The Parcel Boundaries Layer</i> .....	27
<i>Hard Impervious Cover Layer</i> .....	27
<i>Upland Erosion Potential</i> .....	28
<i>Land Use Categorization/Reclassification</i> .....	28
<i>GIS Layering Process</i> .....	32
3.5. SOILS .....	37
<b>4. MODEL CALIBRATION AND VALIDATION</b> .....	<b>42</b>
4.1. HYDROLOGY CALIBRATION .....	43
<i>Snow Hydrology Simulation</i> .....	44
<i>Hydrology Simulation</i> .....	47
4.2. WATER QUALITY CALIBRATION .....	51
<i>Estimating Sediment Loads with Log-Transform Regression</i> .....	52
<i>Pollutant Export Analysis Using Regression and Hydrograph Separation</i> .....	55
<i>Estimating Seasonal Pollutant Loading Patterns in the Streams</i> .....	56
<i>Model Parameterization by Land Use</i> .....	60
<b>5. DISCUSSION OF MODEL RESULTS</b> .....	<b>68</b>
<b>6. EXPLORATORY SCENARIO: POTENTIAL IMPACTS ASSOCIATED WITH CLIMATE CHANGE</b> .....	<b>71</b>
<i>Development of Climate Change Projections</i> .....	71
<i>Watershed Model Results - Hydrology</i> .....	75
<b>7. REFERENCES</b> .....	<b>79</b>
<b>APPENDIX A: MODEL CALIBRATION RESULTS</b> .....	<b>82</b>
<b>APPENDIX B: LAKE TAHOE WATERSHED MODEL LAND USE RUNOFF PARAMETERIZATION</b> .....	<b>83</b>
<b>APPENDIX C: WATERSHED MODEL RESULTS</b> .....	<b>86</b>

# FIGURES

FIGURE 1-1. LOCATION OF THE LAKE TAHOE BASIN.....	2
FIGURE 2-1. CONCEPTUAL DATA FLOW AND INTERACTIONS FOR A WATERSHED MODEL.....	4
FIGURE 3-1. SUBWATERSHED DELINEATION AND ELEVATION IN THE LAKE TAHOE BASIN.....	9
FIGURE 3-2. STREAM CHANNEL REPRESENTATION IN THE LSPC MODEL.....	10
FIGURE 3-3. LOCATION OF SNOTEL AND NCDC WEATHER STATIONS IN THE LAKE TAHOE.....	12
BASIN.....	12
FIGURE 3-4. ORIGINAL VS. CORRECTED SNOTEL TEMPERATURE TIME SERIES AT FALLEN LEAF LAKE.....	13
FIGURE 3-5. SCATTER PLOTS OF SNOTEL TEMPERATURE VS. ELEVATION FOR REGIONAL LAPSE RATE ESTIMATE.....	14
FIGURE 3-6. MONTHLY MODELED EVAPOTRANSPIRATION (ET) AT WARD CREEK VS. OBSERVED ET AT TAHOE CITY.....	16
FIGURE 3-7. LOCATION OF THE 142 MM5 WEATHER GRID CELLS IN THE LAKE TAHOE BASIN.....	19
FIGURE 3-8. LOCATION OF SNOTEL GAGES RELATIVE TO SELECTED MM5 CELLS WITH.....	20
COMPARABLE ELEVATION.....	20
FIGURE 3-9. MM5 VS. OBSERVED SNOTEL ELEVATION AND TEMPERATURE.....	21
FIGURE 3-10. PREDICTED MM5 TEMPERATURE VS. OBSERVED SNOTEL TEMPERATURE AND ELEVATION...	22
FIGURE 3-11. PREDICTED MM5 PRECIPITATION VS. OBSERVED SNOTEL PRECIPITATION AND ELEVATION..	23
FIGURE 3-12. SEASONAL MM5 PRECIPITATION VS. OBSERVED SNOTEL PRECIPITATION AT WARD CREEK.	23
FIGURE 3-13. FINAL COMPOSITE LAND USE COVERAGE FOR THE LAKE TAHOE BASIN.....	26
FIGURE 3-14. HARD IMPERVIOUS COVER FOR THE LAKE TAHOE BASIN AND EXAMPLE FOCUS AREA.....	28
FIGURE 3-15. EXAMPLE OF PARCEL REFINEMENTS IN A PORTION OF THE HEAVENLY SKI AREA.....	30
FIGURE 3-16. EXAMPLE OF PARCEL REFINEMENT IN A CAMPGROUND PARCEL BOUNDARY NEAR EMERALD BAY ON THE SOUTHWESTERN SHORE OF LAKE TAHOE.....	31
FIGURE 3-17. EXAMPLE OF PARCEL REFINEMENT FOR HIGHWAY RIGHT-OF-WAY OWNERSHIP (IMAGE ON LEFT) TO ACTUAL HIGHWAY WIDTHS BASED ON HARD-COVER IMPERVIOUS OVERLAY (IMAGE ON RIGHT).....	32
FIGURE 3-18. FOREST FIRE BOUNDARIES SHADED WITH BURN SEVERITY FOR THE GONDOLA FIRE. (THE RIGHT PANEL SHOWS HOW THE AFFECTED AREAS ARE AGGREGATED BY SUBWATERSHED.).....	35
FIGURE 3-19. MAP OF UPLAND EROSION POTENTIAL FOR THE LAKE TAHOE BASIN.....	36
FIGURE 3-20. SSURGO MAP UNITS AND CORRESPONDING SOIL DESCRIPTIONS.....	38
FIGURE 3-21. AVERAGE PERMEABILITY OF LAKE TAHOE BASIN SOILS.....	40
FIGURE 3-22. USLE K EROSION FACTOR FOR SURFACE SOILS.....	41
FIGURE 4-1. HYDROLOGY AND WATER QUALITY CALIBRATION LOCATIONS.....	43
FIGURE 4-3. MODELED VS. OBSERVED DAILY AVERAGE TEMPERATURES AND SNOW WATER EQUIVALENT DEPTHS AT WARD CREEK SNOTEL SITE (OCTOBER 1996–DECEMBER 2004).....	46
FIGURE 4-4. HYDROLOGY CALIBRATION FOR WARD CREEK WITH EMPHASIS ON WATER YEAR.....	49
1997.49	
FIGURE 4-5. HYDROLOGY VALIDATION FOR WARD CREEK WITH SEASONAL MEAN, MEDIAN, AND VARIATION.....	49
.....	49
FIGURE 4-6. SAMPLE FLOW DISTRIBUTIONS FOR SEDIMENT OBSERVATIONS AT WARD CREEK.....	53
FIGURE 4-7. FLOW-SEDIMENT YIELD REGRESSION RELATIONSHIP AND ERROR DISTRIBUTION AT WARD CREEK.....	54
.....	54
FIGURE 4-8. HYDROGRAPH SEPARATION FOR WARD CREEK (USGS 10336676) USING HISTORICAL FLOW DATA COLLECTED BETWEEN 10/1/1972 AND 9/30/2003.....	57
FIGURE 4-9. SEASONAL NITROGEN AND PHOSPHORUS CONSTITUENT DISTRIBUTION FOR WARD CREEK WATER QUALITY SAMPLING DATA COLLECTED BETWEEN 1972 AND 2003, DERIVED FROM HYDROGRAPH SEPARATION AND REGRESSION.....	59
.....	59
FIGURE 4-10. LSPC MODEL RESULTS VS. OBSERVED DATA FOR TSS AT WARD CREEK.....	66
FIGURE 4-11. LSPC MODEL RESULTS VS. OBSERVED DATA FOR TN AT WARD CREEK.....	66
FIGURE 4-12. LSPC MODEL RESULTS VS. OBSERVED DATA FOR TP AT WARD CREEK.....	66
FIGURE 4-13. LSPC MODEL RESULTS VS. OBSERVED DATA FOR DN AT WARD CREEK.....	67
FIGURE 4-14. LSPC MODEL RESULTS VS. OBSERVED DATA FOR DP AT WARD CREEK.....	67

# TABLES

TABLE 3-1. WEATHER STATIONS AND ASSOCIATED DATA USED TO SIMULATE WEATHER.....	11
CONDITIONS .....	11
TABLE 3-2. SNOTEL GAGES AND SUMMARY INFORMATION (OCTOBER 1990- SEPTEMBER.....	21
2000).....	21
TABLE 3-3. AVERAGE PERCENTAGE OF DIFFERENCE BETWEEN SNOTEL AND MM5 TEMPERATURES DURING	
WINTER SEASON.....	22
TABLE 3-4. YEARLY PERCENTAGE OF DIFFERENCE BETWEEN SNOTEL AND MM5 TOTAL PRECIPITATION	
DURING WINTER SEASON.....	24
TABLE 3-5. MODELING LAND USE CATEGORIES DERIVED FROM THE COMPOSITE LAND USE LAYER.....	33
TABLE 3-6. PERCENT COVERAGE FOR EACH OF THE FIVE VEGETATED-UNIMPACTED CATEGORIES .....	37
(BASED ON EROSION POTENTIAL).....	37
TABLE 3-7. FINAL LAND USE DISTRIBUTION FOR THE LAKE TAHOE BASIN .....	37
TABLE 4-1. SUMMARY OF SNOW MODULE CALIBRATION PARAMETERS (ADJUSTED PARAMETERS .....	47
ARE HIGHLIGHTED).....	47
TABLE 4-2. HYDROLOGY VALIDATION SUMMARY STATISTICS FOR WARD CREEK .....	50
TABLE 4-3. SUMMARY OF SEDIMENT LOAD ESTIMATES AT WARD CREEK USING THE MINIMUM.....	55
VALUE UNBIASED ESTIMATOR.....	55
TABLE 4-4. SUMMARY OF MONITORING DATA COLLECTED AT THE WARD CREEK OUTLET .....	56
TABLE 4-5. BASE FLOW AND STORM FLOW SEDIMENT AND NUTRIENT RATING CURVE SUMMARY .....	58
TABLE 4-7. RELATIVE POLLUTANT CONCENTRATIONS FOR MODELED LAND USES (NOTE: APPENDIX B	
DESCRIBES HOW THESE NUMBERS WERE DETERMINED). .....	61
TABLE 6-1. MATRIX SUMMARY OF CLIMATE CHANGE SCENARIOS.....	73
TABLE 6-2. DESCRIPTIONS FOR CLIMATE CHANGE SCENARIOS .....	73
TABLE 6-3. SELECTED MODEL OUTPUT PARAMETERS FOR CLIMATE CHANGE ANALYSIS.....	75

# ACRONYMS

BF – base flow  
BMP – best management practice  
CICU – Commercial/Institutional/Communications/Utilities  
CTC – California Tahoe Conservancy  
DEM – Digital Elevation Model  
DLM – Dynamic Lake Model  
DON – dissolved organic nitrogen  
DOP – dissolved organic phosphorus  
DRI – Desert Research Institute  
D-Team – TMDL Development Team  
ERA – Equivalent Roaded Area  
ET – evapotranspiration  
GIS – geographic information system  
GQUAL – general water quality module  
HIC – hard impervious cover  
HSPF – Hydrologic Simulation Program–FORTRAN  
HYSEP – hydrograph separation  
LRWQCB – Lahontan Region Water Quality Control Board  
LSPC – Loading Simulation Program C++  
LTIMP – Lake Tahoe Interagency Monitoring Program  
MFR – multi-family residential  
MVUE – Minimum Variance Unbiased Estimator  
NCAR – National Center for Atmospheric Research  
NCDC – National Climatic Data Center  
NCEP – National Center for Environmental Prediction  
NDEP – Nevada Department of Environmental Protection  
NH<sub>4</sub> – ammonia  
NHD – National Hydrography Dataset  
NO<sub>3</sub> – nitrate  
NRCS – Natural Resources Conservation Service  
ONRW – Outstanding National Resource Water  
PEVT – potential evapotranspiration  
RO – storm flow  
SFR – single-family residential  
SNOTEL – SNOpack TELelemetry  
SRP – soluble reactive phosphorus  
STATSGO – State Soil Geographic database  
SWE – snow water equivalent  
TKN – total Kjeldahl nitrogen  
TMDL – Total Maximum Daily Load  
TN – total nitrogen  
TP – total phosphorus  
TRPA – Tahoe Regional Planning Agency  
TSS – total suspended sediment  
Tt – Tetra Tech, Inc.  
UC Davis – University of California at Davis  
UCDHRL – Hydrologic Research Laboratory at the University of California at Davis  
USDA – United States Department of Agriculture  
USEPA – United States Environmental Protection Agency  
USGS – United States Geological Survey  
USLE – Universal Soil Loss Equation

---

---



# 1. PROJECT DEFINITION

---

Considered a national treasure, and designated by the United States Environmental Protection Agency (USEPA) as an Outstanding National Resource Water (ONRW), beautiful Lake Tahoe and its surrounding watershed have captured the eyes and imaginations of the public and scientists for many decades. Situated high in the Sierra Nevada Mountains across the California–Nevada state border, the Lake Tahoe Basin covers approximately 315 square miles; the lake elevation is at about 6,220 feet (Figure 1-1). The basin is characterized by steep mountain slopes, evergreen and mixed forests, and urban development at various locations around the perimeter of the lake. Popular recreational activities include skiing, hiking, and camping, as well as other outdoor activities.

Lake Tahoe is one of the most pristine lakes in the world. In recent decades, however, once-pristine portions of the Lake Tahoe Basin have become urbanized. Studies during the past 40 years have shown that many factors have interacted to degrade the basin’s air quality, terrestrial landscape, and water quality. These factors include land disturbance, an increasing resident and tourist population, habitat destruction, air pollution, soil erosion, roads and road maintenance, and loss of natural landscapes capable of detaining and infiltrating rainfall runoff. Since 1968 the lake’s Secchi depth clarity has declined at a rate of nearly 1 foot per year. To stop and reverse this trend, a Total Maximum Daily Load (TMDL) and associated basin management plan are being developed for the Lake Tahoe Basin.

The TMDL process identifies the maximum load of a pollutant a waterbody is able to assimilate while still fully supporting its designated uses. The TMDL process also allocates portions of the allowable load to all sources, identifies the necessary controls that might be implemented voluntarily or through regulatory means, and describes a monitoring plan and associated corrective feedback loop to ensure that uses are fully supported. Watershed modeling is often used during TMDL development to help with one or more of these tasks. Models can be used to help fill in gaps in observed water quality data, estimate existing pollutant sources throughout a watershed, calculate allowable loads, and assess the potential effectiveness of various control options.

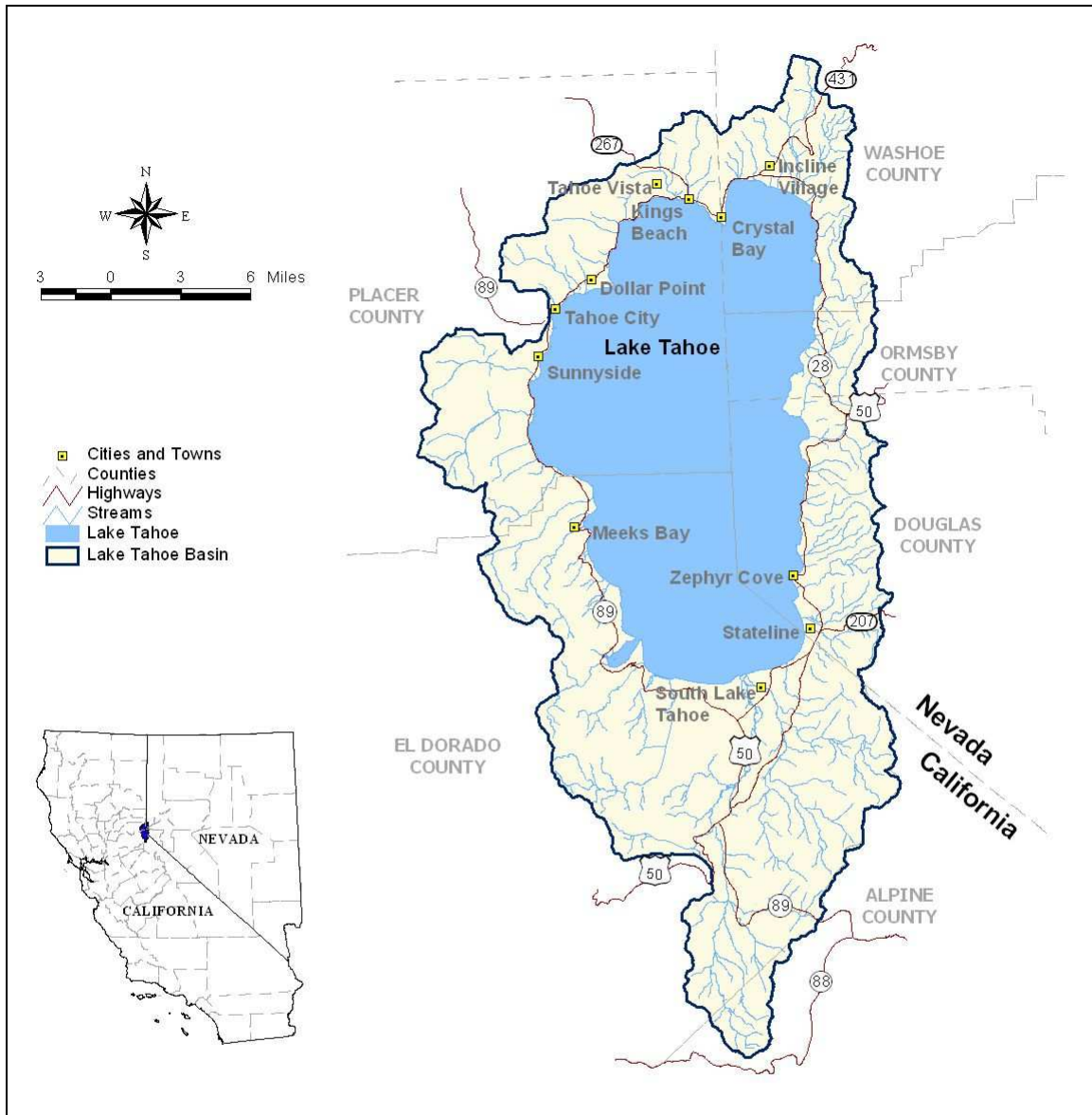


**Figure 1-1. Location of the Lake Tahoe Basin.**

A TMDL for Lake Tahoe is under development; it has an endpoint target of the mean annual water clarity (measured as Secchi depth) during the period 1967–1971. In support of this effort, a comprehensive watershed model has been developed for the Lake Tahoe Basin as part of the 2007 Lake Tahoe technical TMDL initiative (Reuter and Roberts 2004). The primary reasons for developing a watershed model for Lake Tahoe are the following:

- To determine basin-wide estimates for watershed loading of sediment and nutrients to Lake Tahoe based on land use type

- 
- 
- To provide input to the Dynamic Lake Model (DLM) for the Clarity TMDL, developed by the University of California at Davis (Schladow et. al 2004)
  - To create a platform to determine the allowable pollutant load or load allocation from each subwatershed
  - To project load reductions from various best management practices (BMPs) and other management scenarios

No such model had been previously developed for the Lake Tahoe Basin. The physical setting (which includes a complex topography with 63 individual watersheds plus numerous large parcels that drain directly to the lake), climate patterns, hydrologic/geologic characteristics, and pollutant management considerations demanded an innovative solution and approach for watershed modeling. Integral to the Lake Tahoe modeling effort was adaptation of the model to include scientific results from multiple studies by various research institutions, as well as unique subalpine environment considerations. The high level of detail involved in compiling, analyzing, and organizing the required data for the modeling effort not only benefits the current TMDL objectives but also forms a lasting database of information to support other future scientific and water quality planning studies in the basin.

The purpose of this document is to explain the watershed modeling approach and present results for the Lake Tahoe Basin. The model selection process, modeling approach, and model testing or calibration process are detailed. Results of model application to predict existing conditions and alternative loading scenarios are also presented. Detailed results from the watershed model are being used as input data for the DLM.

---

---

## 2. MODEL SELECTION

---

Two different types of models were necessary to simulate conditions in the Lake Tahoe Basin. A watershed model was used to address the generation of pollutant loads over the land surface and through groundwater contributions, as well as to predict the resulting impact on stream water quality. A separate receiving water model was necessary to simulate conditions in Lake Tahoe itself (Perez-Losada 2001, Reuter and Roberts 2004, Swift 2004). This document focuses on the watershed model.

A watershed model is essentially a series of algorithms that integrate meteorological forcing data and watershed characteristics to simulate upland and tributary routing processes, including hydrology and pollutant transport. Once a model has been adequately set up and calibrated, and the dominant unit processes are deemed representative on the basis of comparison with available monitored conditions, it becomes a useful tool to quantify existing flows and loads from tributaries without gages and from diffuse overland flow sources. Figure 2-1 illustrates the conceptual data flow for the Lake Tahoe Watershed Model. Such a model provides an interactive system for evaluating “what-if” scenarios associated with management activities.

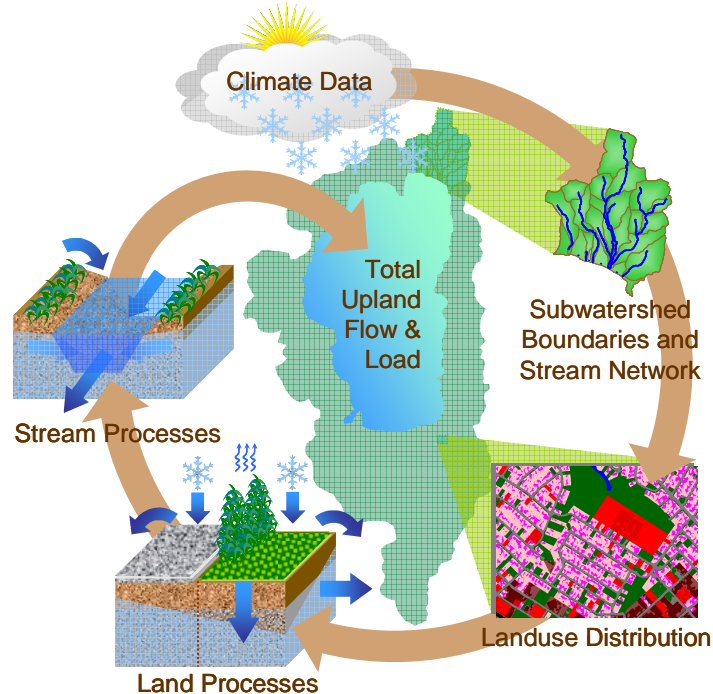


**Figure 2-1. Conceptual data flow and interactions for a watershed model.**

---

---

Like watershed models, receiving water models are composed of a series of algorithms applied to characteristics data to simulate flow/currents and water quality in a water body. The characteristics data, however, represent physical and chemical aspects of a river, lake, or estuary rather than those of the watershed. These models vary from simple 1-dimensional models to complex 3-dimensional models capable of simulating water movement, salinity, temperature, sediment transport, and water quality. The UC Davis Dynamic Lake Model (DLM), coupled with a water quality sub-model and a newly developed optical sub-model (Swift et al. 2006), was chosen to simulate water quality in Lake Tahoe.

## 2.1. Selection Criteria

---

The pollutants of concern for the current modeling application are fine sediment and nutrients, specifically nitrogen and phosphorus. Fine sediment (particles < 63  $\mu\text{m}$ ) is represented as a fraction of the total suspended sediment (TSS) observed in the tributaries. Land use in the Lake Tahoe Basin includes extensive areas of largely undeveloped forest and shrub lands, residential areas with sections of high-intensity development, and areas disturbed by forestry operations and fires. Different potential sources of pollutants are associated with each of the various land uses, and each land use affects the hydrology of the basin in a different way. Some of these sources contribute relatively constant discharges of pollutants, whereas others are heavily influenced by snowmelt and rain events.

The selection criteria for a specific watershed model were based on technical, regulatory, and stakeholder-specified considerations in the Lake Tahoe Basin. Based on these considerations, the following factors were considered critical to selecting an appropriate watershed model. The model should:

- Be able to quantify the pollutants of concern (sediment and nutrients)
- Be able to address a watershed that has a combination of rural and urban land uses
- Be appropriate for simulating a large number of subwatersheds
- Provide adequate time-step estimation of flow and not oversimplify storm events to provide accurate representation of rainfall events/snowmelt and resulting peak runoff
- Be capable of simulating various pollutant transport mechanisms (e.g., groundwater contributions and sheet flow)
- Include an acceptable snowfall and snowmelt routine
- Be flexible enough to accommodate issues such as the mountainous environment, where topography and meteorological conditions can change within a relatively small distance
- Be able to be calibrated and validated with the existing long-term data in the database available through the Lake Tahoe Interagency Monitoring Program (LTIMP)
- Be able to be linked to an appropriate receiving water/lake model

- 
- 
- Be a sound platform for evaluating both existing baseline and hypothetical management decisions
  - Be based on best available data and science
  - Be non-proprietary, tested, and approved by USEPA
  - Be adaptable and available for future applications

## **2.2. Loading Simulation Program C++ (LSPC) Overview**

---

On the basis of the considerations described above and previous modeling experience, the USEPA-approved Loading Simulation Program C++ (LSPC) was selected for Lake Tahoe watershed modeling (<http://www.epa.gov/athens/wwqtsc/html/lspc.html>). LSPC is a watershed modeling system that includes Hydrologic Simulation Program–FORTRAN (HSPF) algorithms for simulating watershed hydrology, erosion, and water quality processes, as well as in-stream transport processes. LSPC integrates a geographic information system (GIS), comprehensive data storage and management capabilities, the original HSPF algorithms, and a data analysis/post-processing system into a convenient PC-based Windows environment. The algorithms of LSPC are identical to a subset of those in the HSPF model. LSPC is maintained by the USEPA Office of Research and Development in Athens, Georgia, and is a component of USEPA's National TMDL Toolbox (<http://www.epa.gov/athens/wwqtsc/index.html>). A brief overview of the HSPF model is provided below; a detailed discussion of HSPF-simulated processes and model parameters is available in the HSPF user's manual (Bicknell et al. 1997).

HSPF is a comprehensive watershed and receiving water quality modeling framework that was originally developed in the mid-1970s. During the past several years it has been used to develop hundreds of USEPA-approved TMDLs, and it is generally considered the most advanced hydrologic and watershed loading model available. The hydrologic portion of HSPF/LSPC is based on the Stanford Watershed Model (Crawford and Linsley 1966), which was one of the pioneering watershed models. The HSPF framework is developed in a modular fashion with many different components that can be assembled in different ways, depending on the objectives of the individual project. The model includes these major modules:

- PERLND for simulating watershed processes on pervious land areas
- IMPLND for simulating processes on impervious land areas
- SEDMNT for simulating production and removal of sediment
- RCHRES for simulating processes in streams and vertically mixed lakes
- SEDTRN for simulating transport, deposition, and scour of sediment in streams

All of these modules include many submodules that calculate the various hydrologic, sediment, and water quality processes in the watershed. Many options are available for both simplified and complex process formulations. Spatially, the watershed is divided into a series of subbasins or subwatersheds representing the drainage areas that contribute to each of the stream reaches. These subwatersheds are then further subdivided into segments representing different land uses. For the developed areas, the land use segments

---

---

are further divided into pervious and impervious fractions. The stream network links the surface runoff and subsurface flow contributions from each of the land segments and subwatersheds and routes them through the water bodies using storage-routing techniques. The stream-routing component considers direct precipitation and evaporation from the water surfaces, as well as flow contributions from the watershed, tributaries, and upstream stream reaches. Flow withdrawals and diversions can also be accommodated. The stream network is constructed to represent all the major tributary streams, as well as different portions of stream reaches where significant changes in water quality occur.

Like the watershed components, several options are available for simulating water quality in the receiving waters. The simpler options consider transport through the waterways and represent all transformations and removal processes using simple first-order decay approaches. Decay may be used to represent the net loss due to processes like settling and adsorption. Judging from the relatively high delivery efficiency of the Lake Tahoe tributaries, water quality constituents are likely to remain somewhat conservative. The LSPC framework is flexible and allows different combinations of constituents to be modeled depending on data availability and the objectives of the study.

The advantages of choosing LSPC as the watershed model for the Lake Tahoe Basin include the following:

- It simulates all the necessary constituents and applies to rural and urban watersheds.
- It has a comprehensive modeling framework that uses the proposed LSPC approach, thereby facilitating development of TMDLs not only for this project but also for potential future projects to address other impairments throughout the Lake Tahoe Basin/
- It allows for customization of algorithms and subroutines to accommodate the particular needs of the Lake Tahoe Basin.
- The time-variable nature of the modeling enables a straightforward evaluation of the cause-effect relationship between source contributions and water body response, as well as direct comparison to relevant water quality criteria.
- The proposed modeling tools are in the public domain and approved by USEPA for use in TMDLs.
- The model includes both surface runoff and base flow (groundwater) conditions.
- It provides storage of all physiographic, point source/withdrawal data and process-based modeling parameters in a Microsoft Access database and text file formats to provide for efficient manipulation of data.
- It presents no inherent limitations with respect to the size and number of watersheds and streams that can be modeled.
- It provides flexible model output options for efficient post-processing and analysis designed specifically to support TMDL development and reporting requirements.
- It can be linked to the Lake Tahoe receiving water model (DLM).



---

## **3. MODELING APPROACH**

---

This section of the report describes the LSPC modeling approach used for the Lake Tahoe Basin. Developing and applying the LSPC model to address the project objectives involved the following important steps:

1. Watershed segmentation
2. Water body representation
3. Configuration of key model components—meteorological data, land use representation, and soils
4. Model calibration and validation (for hydrology, sediment, and nutrients)
5. Model simulation for existing conditions and scenarios

The first three steps are discussed in this section of the report. The fourth and fifth steps are discussed in Sections 4 and 5, respectively.

### **3.1. Watershed Segmentation**

---

LSPC was configured to simulate the entire Lake Tahoe Basin as a series of hydrologically connected subwatersheds. The delineation of subwatersheds was based primarily on topography, but it also considered spatial variation in sources, hydrology, jurisdictional boundaries, and the location of water quality monitoring and stream flow gaging stations. The spatial division of the watersheds allowed for a more refined resolution of pollutant sources and a more representative description of hydrologic variability.

Representing elevation change in gradual increments was an important consideration for subwatershed delineation. Because air temperature at a monitoring station is adjusted according to mean watershed elevation during snow simulation (see Section 3.3), subwatershed delineation alone can affect spatially predicted snowfall.

The great variation in topography and land uses in the Lake Tahoe Basin required that the subwatersheds be small enough to minimize these averaging effects and to capture the spatial variability. Lake Tahoe's drainage area was divided into 184 subwatersheds representing 63 direct tributary inputs to the lake. The average size of each subwatershed was 1,100 acres. Areas between stream mouths that directly drain into the lake (intervening zones) were modeled separately. Ten groups of intervening zones were represented in the model. Figure 3-1 shows elevation change and the subwatershed delineation for the watershed model.

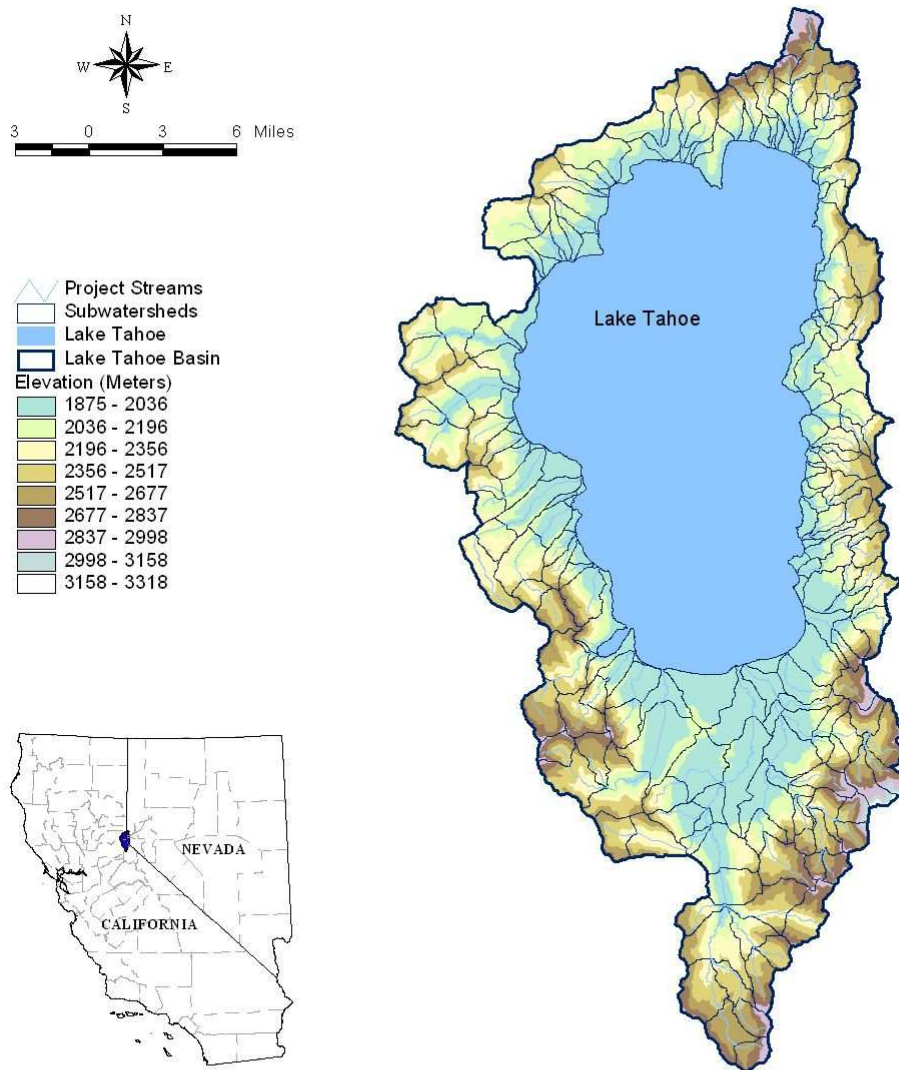


**Figure 3-1. Subwatershed delineation and elevation in the Lake Tahoe Basin.**

### **3.2. Water Body Representation**

Each delineated subwatershed in the LSPC model is conceptually represented; a single stream is assumed to be a completely mixed, one-dimensional segment with a constant trapezoidal cross-section (Figure 3-2). The National Hydrography Dataset (NHD) stream reach network was used to determine the representative stream length for each subwatershed. Once the representative reach was identified, slopes were calculated based on Digital Elevation Model (DEM) data and stream lengths were measured from the original NHD stream coverage. Mean depths and channel widths for a number of

segments were available from field surveys conducted by the United States Department of Agriculture (USDA)–Agricultural Research Service (Simon et al. 2003). Assuming representative trapezoidal geometry for all streams, mean stream depth and channel width were estimated, using regression curves that relate upstream drainage area to stream dimensions, and were compared with stream surveys at selected locations—General Creek (a wetter west shore of the basin) and Logan House Creek (a drier east shore of the basin). The rating curves consisted of a representative depth-outflow-volume-surface area relationship. An estimated Manning’s roughness coefficient of 0.02 was applied to each representative stream reach based on typical literature values (Schwab et al. 1993).

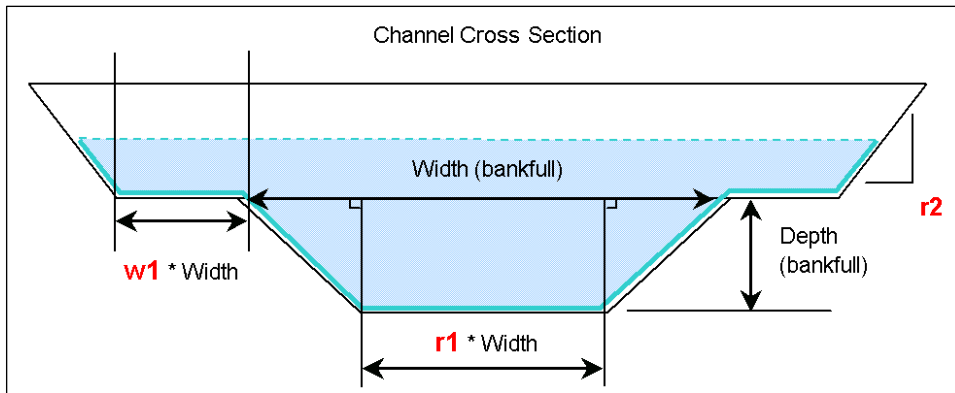


**Figure 3-2. Stream channel representation in the LSPC model.**

### 3.3. Meteorological Data

Hydrologic processes are time-varying and depend on changes in environmental conditions, including precipitation, temperature, and wind speed. As a result, meteorological data are a critical component of watershed models.

Meteorological conditions are the driving force for nonpoint source transport processes in watershed modeling. Generally, the finer the spatial and temporal resolution available for meteorology, the more representative the associated watershed processes will be. As a minimum, precipitation and evapotranspiration are required as forcing functions for most watershed models. For the Lake Tahoe Basin, where the snowfall/snowmelt process is the most significant factor in basin-wide hydrology, additional data were required for snow simulation. These data are temperature, dew point temperature, wind speed, and solar radiation. The physical setting of the basin and the topographic relief cause significantly high variability in weather patterns over a relatively short distance in the same basin. In addition, orographic effects at Lake Tahoe result in a pronounced rain shadow reaching from the much wetter west side to the drier east side. This section discusses local observed weather data used for model calibration; customization of observed data to local influences; and a high-resolution, grid-based synthetic dataset (MM5) originally planned for use during the TMDL scenario runs.

## Local Weather Data

An hourly time step for weather data was required to properly reflect diurnal temperature changes. For snow simulation, the model uses temperature to decide whether precipitation should be considered as rainfall or snowfall. Proper prediction of this trigger is required to ensure proper timing of water delivery to the rest of the hydrologic cycle. The timing of rainfall and snowmelt events directly relates to the timing of predicted sediment and nutrient loading. Likewise, the DLM requires proper timing of watershed boundary conditions for predictive accuracy.

There were two primary data sources for locally observed weather data. One source was a series of nine Snowpack Telemetry (SNOTEL) gages in and around the Lake Tahoe Basin maintained by USDA’s Natural Resources Conservation Service (NRCS). The SNOTEL sites record air temperature, precipitation, and snow water equivalent data (used for snowfall/snowmelt calibration). The other data source was the National Climatic Data Center (NCDC), which maintains a network of long-term weather stations in the region. South Lake Tahoe Airport was the only hourly surface air gage inside the basin.

Table 3-1 lists the weather datasets used to generate the weather forcing files for watershed modeling, and Figure 3-3 shows the location of the SNOTEL and NCDC weather stations in the watershed.

**Table 3-1. Weather stations and associated data used to simulate weather conditions**

Station Name	Code	Agency <sup>a</sup>	Data Type <sup>b</sup>	Elevation (ft)	Available Data
Echo Peak	ECOC1	NRCS	SNOTEL	7800	precipitation, temperature
Fallen Leaf	FLFC1	NRCS	SNOTEL	6300	precipitation, temperature
Hagan’s Meadow	HGNC1	NRCS	SNOTEL	8000	precipitation, temperature
Heavenly	HVNC1	NRCS	SNOTEL	8850	precipitation, temperature
Marlette	MRLN2	NRCS	SNOTEL	8000	precipitation, temperature
Mount Rose Ski <sup>c</sup>	MRSN2	NRCS	SNOTEL	8850	precipitation, temperature
Rubicon	RUBC1	NRCS	SNOTEL	7500	precipitation, temperature
Tahoe Crossing	THOC1	NRCS	SNOTEL	6750	precipitation, temperature
Ward Creek	WRDC1	NRCS	SNOTEL	6750	precipitation, temperature
South Lake Tahoe AP	93230	NCDC	Hourly	6314	dew point, wind, solar radiation
Reno AP <sup>c</sup>	23185	NCDC	Hourly	4410	dew point, wind, solar radiation
Emigrant Gap AP <sup>c</sup>	23225	NCDC	Hourly	5276	dew point, wind, solar radiation

<sup>a</sup>NRCS is the National Resource Conservation Service; NCDC is the National Climatic Data Center.

<sup>b</sup>SNOTEL indicates data from Snowpack Telemetry stations (available as daily and hourly).

<sup>c</sup>These weather stations are outside the Lake Tahoe Basin.

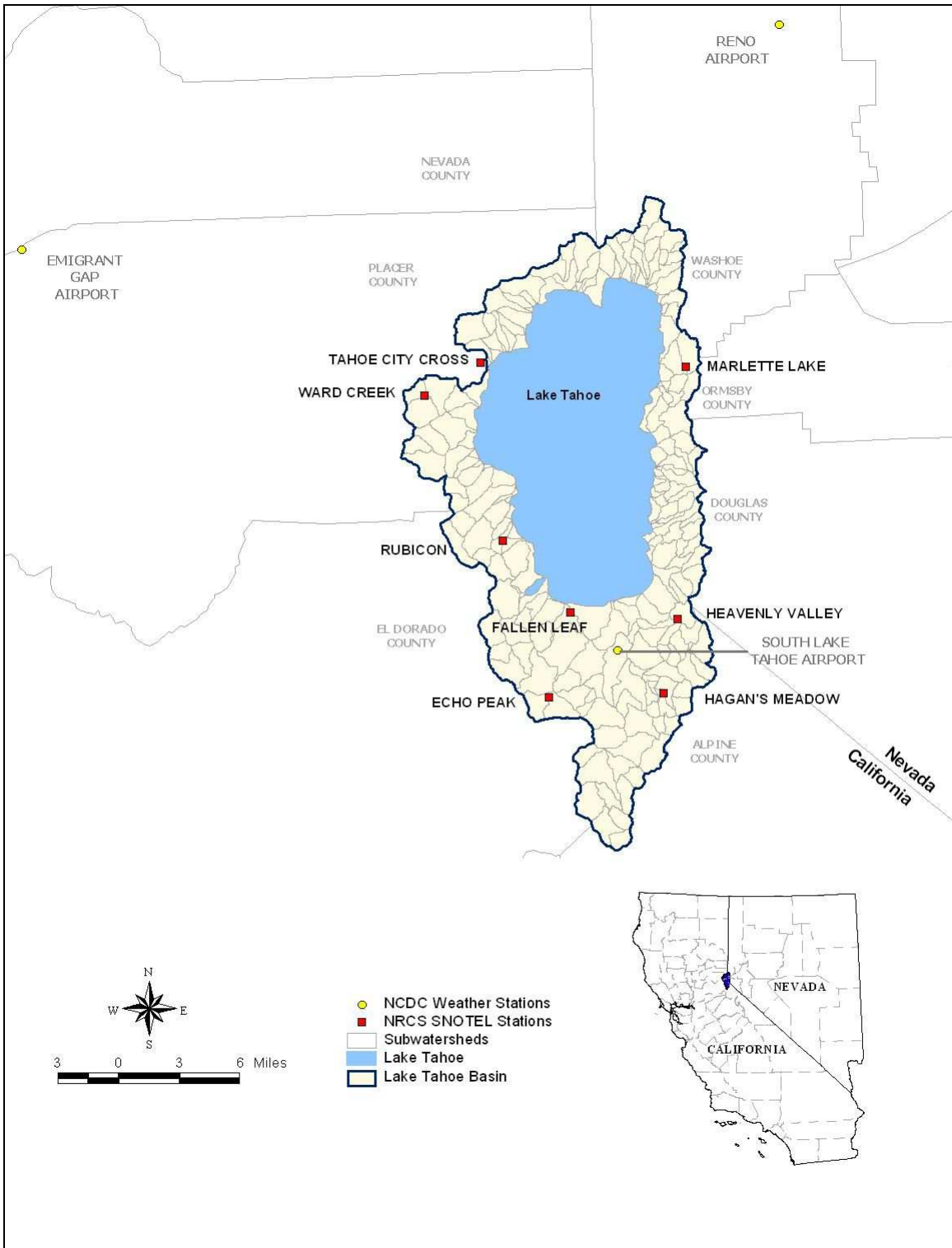


**Figure 3-3. Location of SNOTEL and NCDC weather stations in the Lake Tahoe Basin.**

---

---

## Local Temperature Data

Model testing revealed some inconsistencies in the hourly SNOTEL temperature and precipitation observations when first applied directly. These discrepancies needed to be addressed to perform snow and hydrology calibration. As previously described, the snowfall simulation module was especially sensitive to air temperature data because temperature determines whether precipitation is considered as rain or snow. The implications of just a few degrees of error were significant. Missing a single fairly sizable snowfall event could disrupt the entire snowpack dynamics for the year, causing melting when snow accumulation should be occurring. Conversely, if rainfall was incorrectly considered as snow, pack accumulation occurred instead of the expected rain-on-snow response. These inconsistencies became especially evident when snowfall was predicted in July and August of 2000 at the Fallen Leaf station during a model testing run. Consequently, discrepancies in these data were carefully reviewed and corrected. Figure 3-4 shows the corrected SNOTEL temperature time series at Fallen Leaf station.

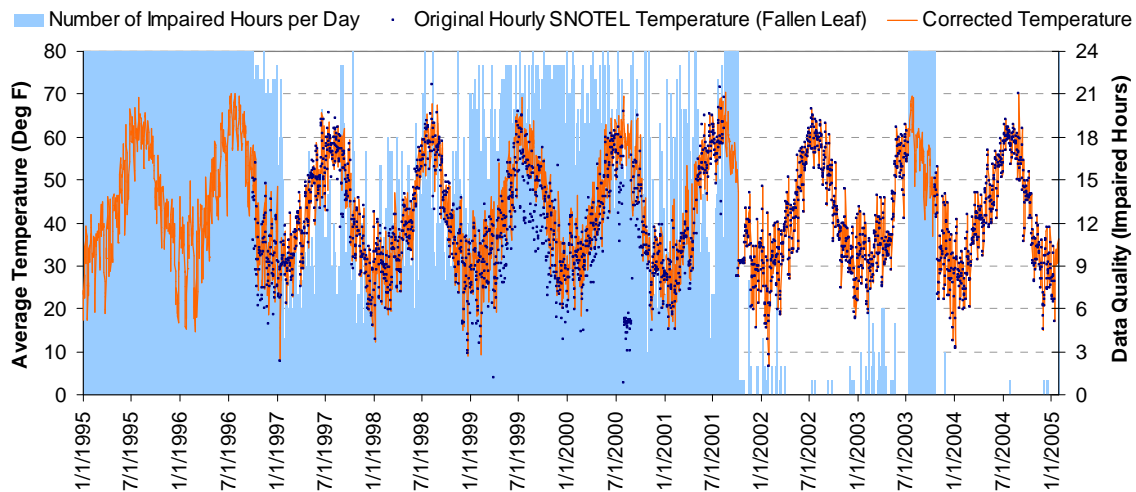


**Figure 3-4. Original vs. corrected SNOTEL temperature time series at Fallen Leaf Lake.**

Through conversations with NRCS staff regarding the data-reporting procedures, it was learned that daily precipitation totals and minimum/maximum temperatures were more rigorously validated than the hourly datasets. Furthermore, although the SNOTEL dataset included quality flags for impaired values, some of the reportedly unimpaired values were outside the minimum and maximum temperature range. Those values were flagged as impaired. A rigorous quality assurance procedure was developed and applied to consistently process all hourly SNOTEL data from all sites into an acceptable condition for watershed modeling. From Figure 3-4, one can discern gage reporting history, including changes in reporting frequencies, periods of missing or impaired datasets, and

periods of missing or impaired hourly data. For example, before October 1996 only daily values were recorded. Diurnal disaggregating of NRCS-validated minimum and maximum temperature was used to patch missing or impaired hourly values.

## Lapse Rate Calculations

Another critical model parameter for snow simulation is the temperature correction for elevation changes (lapse rate).

Temperature lapse rate—the rate at which temperature decreases with increasing elevation—significantly influences snowfall prediction, especially when extrapolating snow behavior to subwatersheds without gages. This rate is particularly important in the Lake Tahoe Basin, where elevation changes rapidly with distance from the lake. LSPC estimates lapse rate as a function of the elevation difference between the mean subwatershed elevation and the elevation at the location where temperature is gaged. Figure 3-5 shows scatter plots and linear regression for temperature versus elevation for SNOTEL gages in the basin. The slope of the line is the Tahoe-specific lapse rate approximation, which averages about 0.0022 degrees Fahrenheit (°F) per foot difference in elevation (with an *R*-squared value of 0.875).

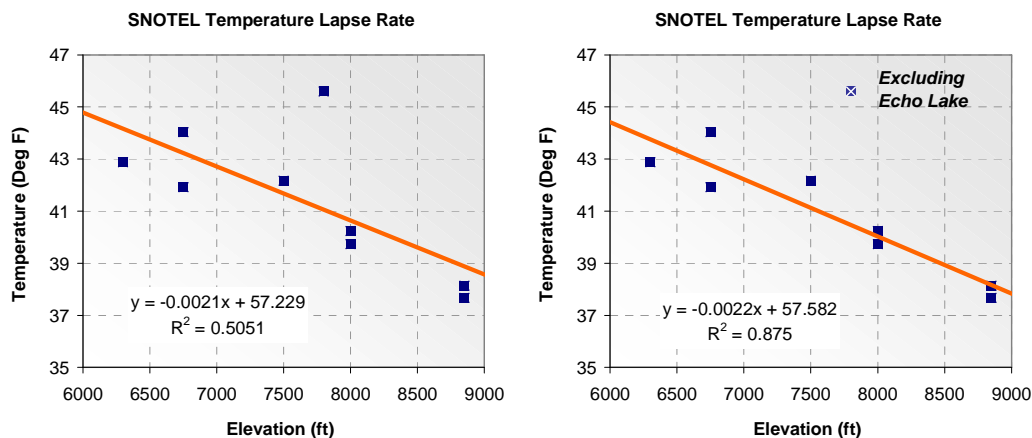


**Figure 3-5. Scatter plots of SNOTEL temperature vs. elevation for regional lapse rate estimate.**

One outlier to the trend was the Echo Peak gage. Although that gage was at a relatively high elevation, it had the highest overall temperature of all the compared gages. At the same time, Echo Peak experiences the second-highest amount of precipitation and snowfall despite its high temperatures. Data analysis showed that snow accumulation frequently occurred even while temperatures approached 40 °F. An explanation for this might be found by examining the areas immediately surrounding the gage. Photographs of the gage show that it is on a crest with very little surrounding vegetation. Another

---

---

factor that was not considered in this lapse rate adjustment exercise is the local topography surrounding the gage. East-facing versus west-facing slopes might tend to shade the gage or expose it to solar radiation. It is possible that this combination of factors exposes the gage to unimpaired heat from solar radiation. At the same time, the surrounding mountains at Echo Peak are probably responsible for inducing more precipitation. The snowpack most likely persists because it easily reflects solar radiation and the rocky ground beneath remains cold. Consequently, the lapse rate for data excluding Echo Peak was used in LPSC.

The watershed model simulates both a wet- and dry-weather lapse rate. HSPF and LPSC assume a default wet lapse rate of 0.0035 °F per foot difference in elevation. The default hourly dry lapse rates vary between 0.0035 and 0.005 °F per foot (Bicknell et al. 1997). Data analysis indicated that actual temperature lapse rates in the Lake Tahoe Basin are probably about 40 to 60 percent lower than the default values used in the model. During snow simulation, a user-defined parameter (ELDAT) is the mean difference between watershed elevation and the temperature gage elevation. The original values were derived from GIS analysis; however, since ELDAT and lapse rate are linearly related, a 40 to 60 percent ELDAT reduction properly corrected for Tahoe-specific conditions.

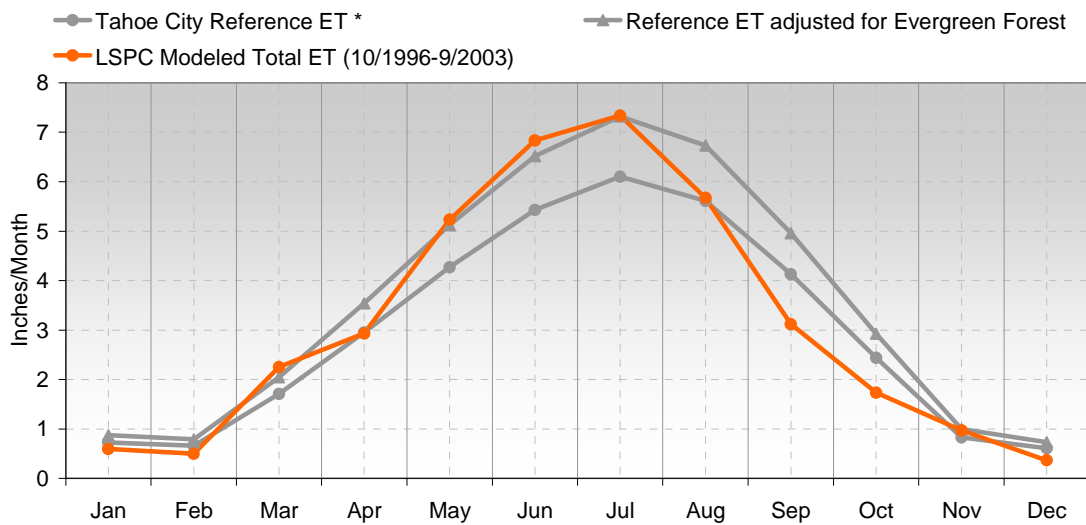
## Evapotranspiration Calculations

Following snowfall/snowmelt simulation, evapotranspiration is arguably the second most important factor influencing Lake Tahoe Basin hydrology. Evapotranspiration in the model is used to represent the sum of the evaporation and transpiration that occur due to plants in their natural environment. LPSC requires, as a weather input, the potential evapotranspiration (PEVT), which is the maximum naturally achievable amount of evapotranspiration at any given moment. Model testing revealed that the method selected for computing PEVT in Lake Tahoe was of great significance.

Although some methods for actually measuring evapotranspiration in the field are available, most practitioners estimate evapotranspiration using empirical formulations that are a function of other related (and more commonly observed) weather data. Three widely used methods are the Hamon method (1961), the Jensen-Haise method (1963), and the Penman pan-evaporation method (1948). The Penman method, which is the earliest of these three methods, computes evaporation as a function of temperature, solar radiation, dew point or relative humidity, and wind movement. The other two methods, Hamon and Jensen-Haise, are simplified empirical representations that require fewer observed datasets to compute. The Hamon method is a function of only temperature, while the Jensen-Haise method requires solar radiation and temperature.

The Penman method (1948) was most suitable for Lake Tahoe. An average vegetation (crop) factor of 0.875 (based on calibration to observed Tahoe City reference evapotranspiration) was used to translate Penman pan-evaporation to PEVT. Figure 3-6 shows monthly modeled evapotranspiration plotted against reference monthly evapotranspiration at Tahoe City. The annual observed evapotranspiration at Tahoe City

is between 35.5 and 42.5 inches per year for reference crop (crop factor of 1.0) and evergreen forest (crop factor of 1.2).



\* Historical average monthly reference crop evapotranspiration for Tahoe City, California  
UC Davis Division of Agriculture and Natural Resources, Publication 21454

**Figure 3-6. Monthly modeled evapotranspiration (ET) at Ward Creek vs. observed ET at Tahoe City.**

## Synthetic Weather Dataset

As previously mentioned, a synthetic weather dataset (MM5) was developed for TMDL scenario runs. It was not used for model calibration; only actual observed data were used during calibration. The TMDL target for lake clarity is defined as the mean annual Secchi depth during the period 1967–1971. However, with a hydraulic residence time of approximately 650 years, a nutrient doubling time on the scale of a few decades, and paleolimnologic data that show a lake recovery time on the order of many decades (Heyvaert 1998, Jassby et al. 1995), the existing spatial and temporal coverage for meteorological data was not adequate to model future conditions over an appropriate ecological time scale.

High-temporal-resolution weather observations for a long period of record are rarely available at a small enough scale to reflect the high degree of spatial climate variability known to exist in the Lake Tahoe Basin. A traditional way of overcoming this difficulty is to statistically interpolate values between existing weather stations where actual observations are available. Although this type of approach works well for a geographically dense monitoring network with fairly homogenous meteorological characteristics, it can prove problematic in a setting like Lake Tahoe, where the network

---

---

of stations has low spatial density and the physical setting naturally causes high spatial variability in meteorology. There are numerous distinct micro-climate pockets throughout the drainage area.

To accomplish the goals of this modeling project, TMDL strategists envisioned using 42 years of reconstructed meteorological input as the basis for extrapolating future conditions, taking the potential influence of climate change into account to the extent possible. To perform this research and development effort, the Lahontan Regional Water Quality Control Board (LRWQCB) contracted with a team from the Hydrologic Research Laboratory at the University of California at Davis (UCDHRL) led by Dr. M. Levent Kavvas.

The strategy for the TMDL developers was to use the previous 42 years of weather data to drive watershed modeling into the future (by extrapolating likely weather conditions). The UC Davis research team developed a 42-year history, with 1-hour time steps, of meteorological conditions at a 3- by 3-kilometer square resolution for the entire drainage area, resulting in 142 unique sets of meteorological information. This state-of-the-art meteorological reconstruction process was performed using a regional atmospheric model called MM5 (Anderson et al. 2004). MM5, the fifth-generation atmospheric model developed jointly by the National Center for Atmospheric Research (NCAR) and Pennsylvania State University, is particularly well suited for steep mountainous terrains like the Lake Tahoe Basin (Anderson et al. 2004).

The MM5 meteorological data represent a synthetically generated coverage of the basin. Because MM5 is a model, it is an approximation of what might actually be occurring at a particular location. The primary purpose of this information is to support long-term hypothetical modeling scenarios. It is important to note that MM5 calibration was actually performed using real data observations at select locations throughout the basin and at nearby sites outside the basin. While the UC Davis meteorological output included precipitation, surface air temperature, dew point temperature, downward longwave radiation, downward solar radiation, relative humidity, latent heat flux, and wind speed, calibration focused on air temperature and precipitation data from the period 1996–2000 (Anderson et al. 2004). The MM5 output is not suitable for calibrating processes and response within the LSPC watershed model. As previously described, locally observed data from meteorological gages in and around the Lake Tahoe Basin were applied for model calibration.

Inputs for the MM5 model included a dataset from the National Center for Environmental Prediction (NCEP), which consisted of 12-hour time interval records from 1958 to 2000 taken over a 285- by 285-kilometer area covering parts of California and Nevada, and orographic information about the region (Anderson et al. 2004). Through extensive computational demand, MM5 scales down the larger/coarser NCEP data to a 3- by 3-kilometer resolution considering orographic changes throughout the modeling area.

A significant amount of processing and translation was required to convert the MM5 regional weather predictions into a format suitable for watershed modeling. Five types of

---

---

weather information directly extracted from the MM5 output are precipitation, air temperature, dew point temperature, wind speed, and solar radiation. Evapotranspiration, represented as a function of air and dew point temperature, wind movement, and solar radiation, was derived for the entire Lake Tahoe Basin area using the Penman method (Penman 1948). These six different types of weather information predicted at 142 locations resulted in a set of 852 unique hourly time series for driving the watershed model scenarios. Figure 3-7 shows the spatial position of the 142 weather grid cells in relation to the Lake Tahoe watershed area. Because the original MM5 model output was formatted in terms of spatial snapshots reported over time, it was necessary to transpose the entire dataset into temporal profiles at each location in space for the model. After the information at each of the 142 weather grids was processed into the required format for direct linkage to the Lake Tahoe watershed model, data were assigned to each of the 184 subwatersheds using the Thiessen polygon method. Because climate was predicted at the grid centroids, and all the grid cells were 3- by 3-kilometer squares uniformly distributed over the drainage area, the Thiessen polygon method was equivalent to a straight intersect between the weather grids and the subwatershed boundaries. Weights were assigned to each of the 142 grid cells and aggregated to a subwatershed basis using the area fractions of grid cells intersecting each subwatershed boundary. This approach provided a very high degree of spatial and time resolution not typically seen in watershed modeling.

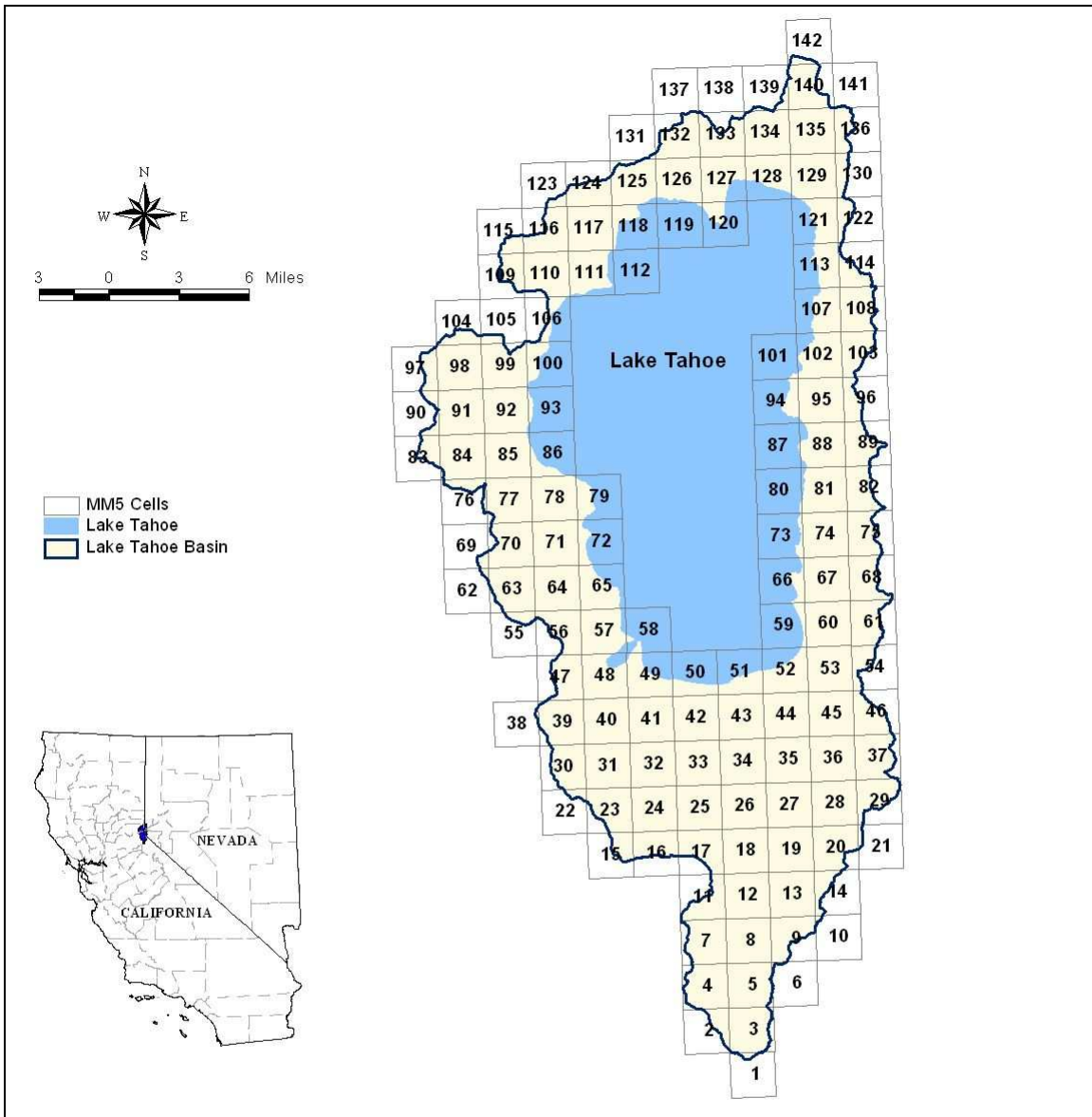


**Figure 3-7. Location of the 142 MM5 weather grid cells in the Lake Tahoe Basin.**

During MM5 model development, the model was guided by data from several gages spanning a wide area in and around outside the Lake Tahoe Basin (Anderson et al., 2004). To gage the predictive ability of the MM5 meteorology to drive the Lake Tahoe watershed model, further validation of long-term MM5 summaries against observed SNOTEL summaries was performed. There were nine SNOTEL gages within the domain of the MM5 spatial grid coverage. Data from the nearest SNOTEL station were compared with the synthetic data at the nearest MM5 grid with similar elevation to assess predictive comparability throughout the basin. Figure 3-8 shows the location of the SNOTEL gages relative to selected MM5 cells with comparable elevation. Table 3-2 contains additional information about the nine SNOTEL gages.

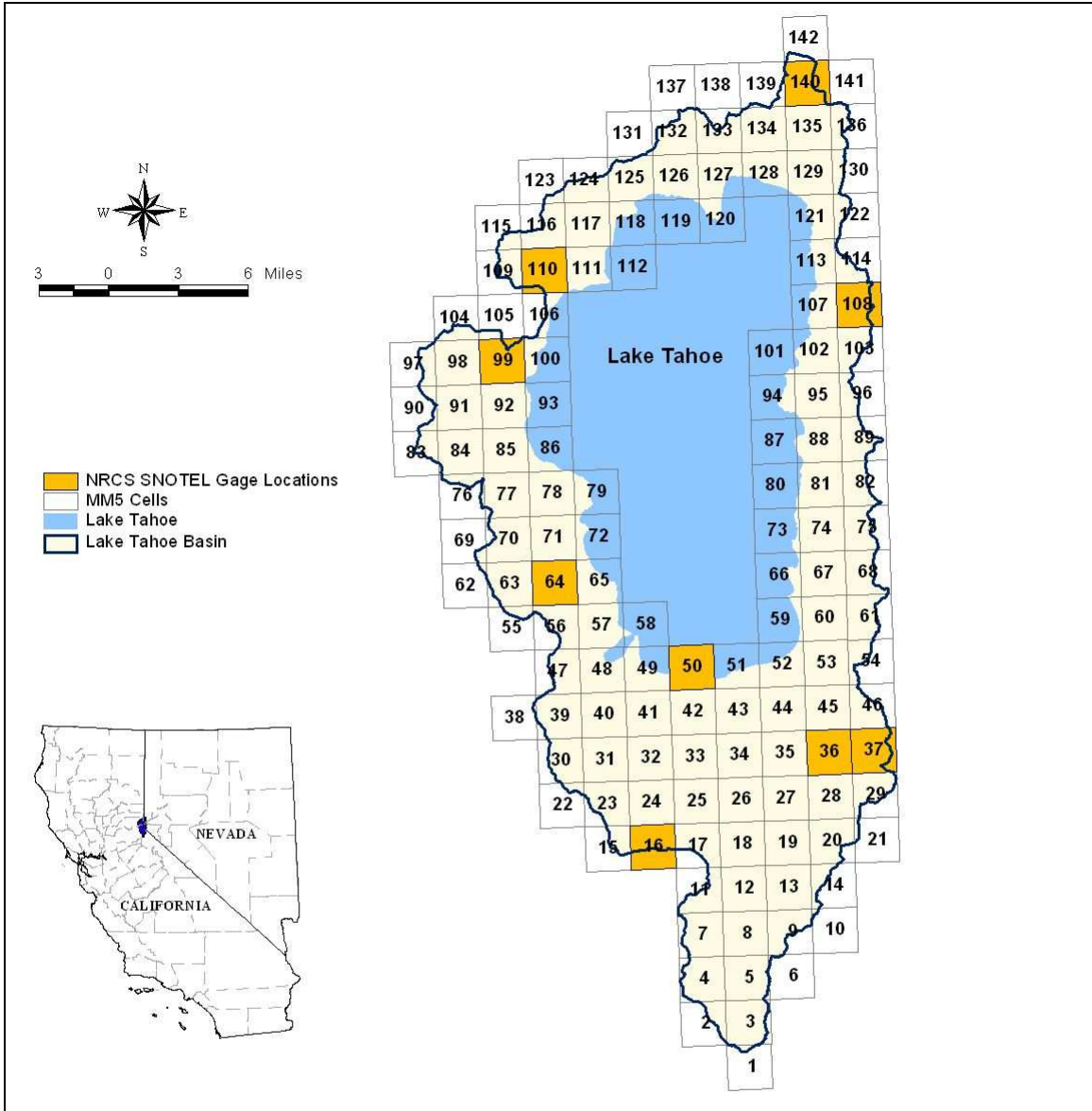
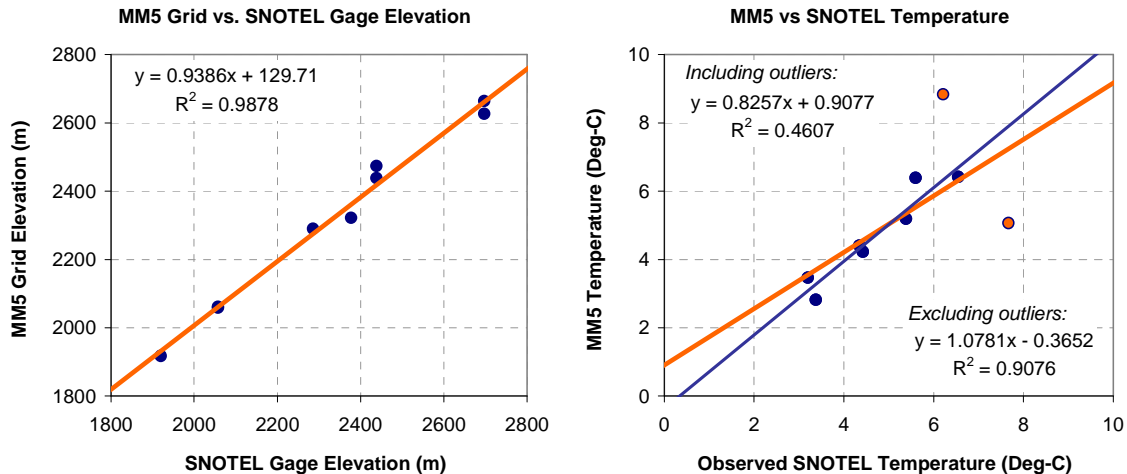


**Figure 3-8. Location of SNOTEL gages relative to selected MM5 cells with comparable elevation.**

**Table 3-2. SNOTEL gages and summary information (October 1990- September 2000).**

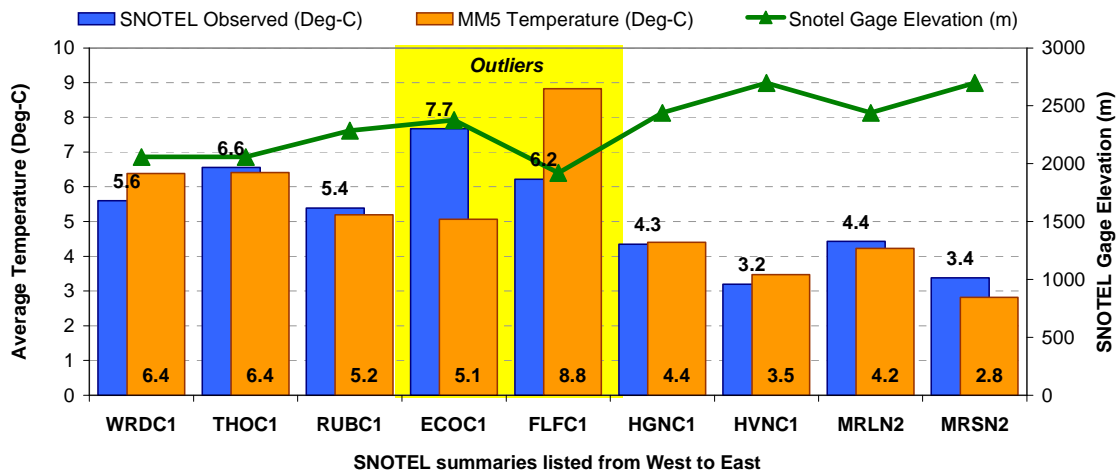
Station Name	Code	Elevation (m)	Precipitation (in/yr)	Temperature (Deg C)
Echo Peak	ECOC1	2,377	62	7.7
Fallen Leaf	FLFC1	1,920	37	6.2
Hagens Meadow	HGNC1	2,438	34	4.3
Heavenly	HVNC1	2,698	41	3.2
Marlette	MRLN2	2,438	43	4.4
Mount Rose Ski	MRSN2	2,698	61	3.4
Rubicon	RUBC1	2,286	44	5.4
Tahoe Crossing	THOC1	2,057	37	6.6
Ward Creek	WRDC1	2,057	71	5.6

Figure 3-9 shows both modified MM5 versus observed SNOTEL gage elevation and annual average temperature graphs. The Fallen Leaf and Echo Peak SNOTEL data showed temperature trend deviations from what was predicted at the other seven gages. When Fallen Leaf and Echo Peak pairs are excluded, there is very good agreement between long-term MM5 and SNOTEL temperature. The MM5 versus observed data summaries span January 1990 through December 2000.



**Figure 3-9. MM5 vs. observed SNOTEL elevation and temperature.**

Figure 3-10 further shows comparisons between observed SNOTEL and MM5 temperature predictions. The observed temperature monitored at Echo Peak (ECOC1) is higher than what might be expected to occur at its relatively high elevation; and although the Fallen Leaf (FLFC1) SNOTEL gage is at the lowest elevation in the basin, there might be a slight cooling effect because the gage is situated between two water bodies (Fallen Leaf Lake and Lake Tahoe itself). This discrepancy might propagate error into predicted watershed response for the associated region of the Upper Truckee watershed. Table 3-3 presents the percentage of difference between SNOTEL and MM5 temperatures for the winter season.



**Figure 3-10. Predicted MM5 temperature vs. observed SNOTEL temperature and elevation.**

**Table 3-3. Average percentage of difference between SNOTEL and MM5 temperatures during winter season**

Date	Weather Stations					
	Ward Creek	Rubicon #2	Marlette Lake	Hagans Meadow	Fallen Leaf	Echo Peak
1/1990–4/1990	No data	No data	2%	4%	No data	-15%
11/1990–4/1991	-9%	-1%	1%	7%	18%	-15%
11/1991–4/1992	1%	2%	3%	9%	18%	-7%
11/1992–4/1993	-4%	3%	0%	7%	16%	-7%
11/1993–4/1994	-1%	2%	3%	7%	18%	-8%
11/1994–4/1995	-1%	4%	6%	8%	17%	-6%
11/1995–4/1996	-3%	1%	1%	7%	15%	-7%
11/1996–4/1997	-2%	1%	3%	5%	13%	-7%
11/1997–4/1998	-5%	2%	2%	4%	14%	-8%
11/1998–4/1999	-2%	3%	6%	5%	17%	-7%
11/1999–4/2000	-2%	2%	0%	2%	15%	-7%
11/2000–4/2000	8%	0%	-4%	13%	22%	No data

The MM5 precipitation prediction is consistently lower than the observed SNOTEL-reported precipitation, although the relative spatial variation approaches the observed trends. Figure 3-11 shows predicted MM5 precipitation, observed SNOTEL precipitation, and SNOTEL gage elevations. Figure 3-12 illustrates seasonal precipitation patterns at Ward Creek for the 10 years between October 1990 and September 2000. The same trend is observed at other MM5 grid cells around the basin. The composite seasonal comparison reveals that the under-predicting months of the year coincide with snowfall-dominated months. One potential limitation of the MM5 predictions is a reduced predictive ability to represent snowfall volumes during fall, winter, and spring. Summer rainfall predictions by MM5 are relatively close in magnitude compared with observed SNOTEL totals. Table 3-4 shows the percentage of difference between SNOTEL and MM5 total precipitation for the winter season.

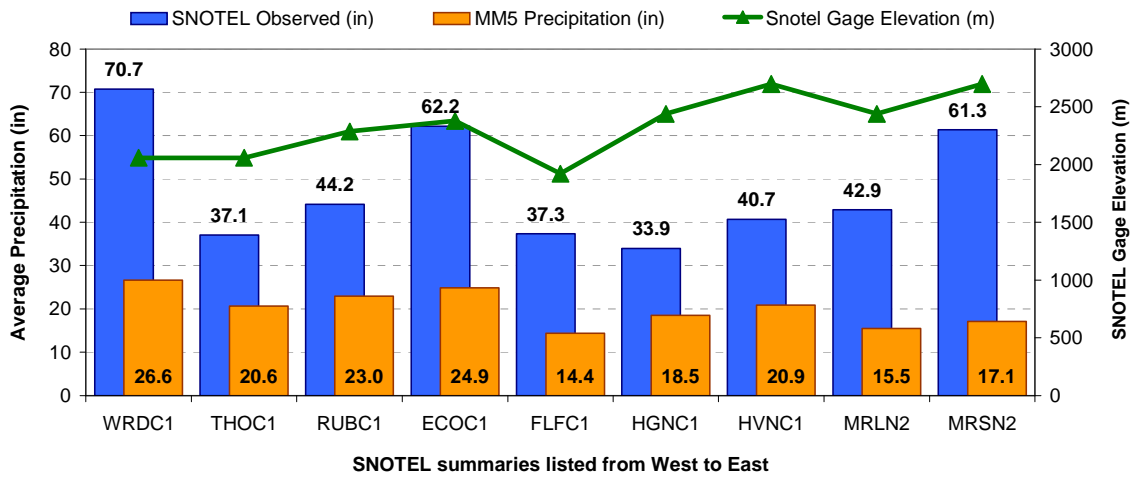


**Figure 3-11. Predicted MM5 precipitation vs. observed SNOTEL precipitation and elevation.**

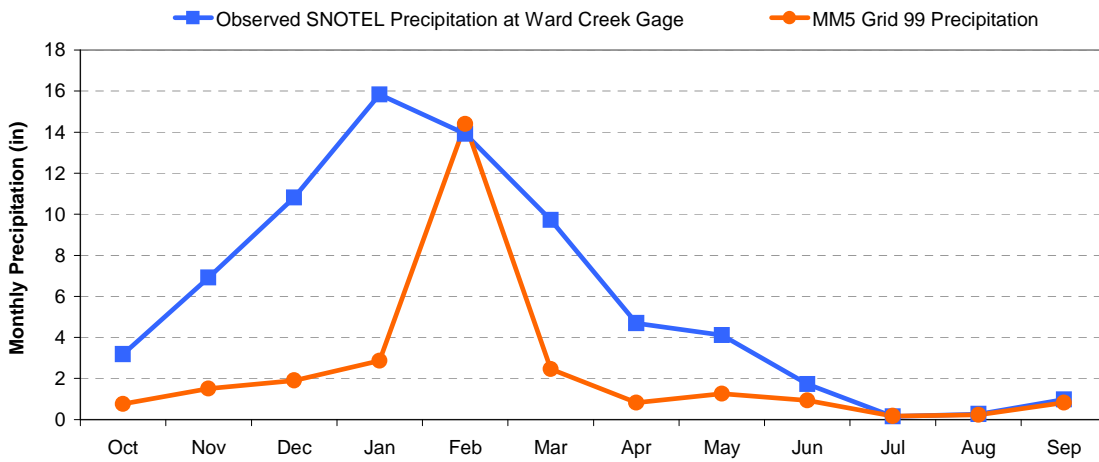


**Figure 3-12. Seasonal MM5 precipitation vs. observed SNOTEL precipitation at Ward Creek.**

**Table 3-4. Yearly percentage of difference between SNOTEL and MM5 total precipitation during winter season**

Date	Weather Stations					
	Ward Creek	Rubicon #2	Marlette Lake	Hagans Meadow	Fallen Leaf	Echo Peak
1/1990–4/1990	-55%	-50%	-56%	-29%	-45%	-67%
11/1990–4/1991	-53%	-44%	-54%	-20%	-31%	-67%
11/1991–4/1992	-46%	-35%	-48%	-31%	-42%	-70%
11/1992–4/1993	-59%	-54%	-67%	-36%	-38%	-67%
11/1993–4/1994	-62%	-51%	-58%	-45%	-37%	-69%
11/1994–4/1995	-60%	-64%	-61%	-11%	-46%	-62%
11/1995–4/1996	-62%	-69%	-78%	-59%	-67%	-72%
11/1996–4/1997	-67%	-63%	-56%	-38%	-44%	-69%
11/1997–4/1998	-56%	-47%	-64%	-31%	-49%	-62%
11/1998–4/1999	-58%	-57%	-71%	-42%	-63%	-70%
11/1999–4/2000	-57%	-50%	-66%	-23%	30%	-57%
11/2000–12/2000	-77%	-77%	-83%	-73%	-69%	-76%

The snowfall module includes a parameter called SNOWCF, which accounts for water volume losses due to poor snow catch efficiency at the gages. Although SNOWCF can be adjusted to achieve satisfactory agreement for long-term water volumes, the general timing of the snowpack buildup does not resemble the general shape of observed snowpack buildup. Further refinement of the precipitation predictions might be required to better represent the nature of snowpack buildup.

Overall, although the MM5 data represented spatial variation throughout the basin very well, it tended to under-predict precipitation between October and May. The MM5 model developers stated that snow recognition is a limitation of the model. One proposed solution for resolving this difference is to generate and apply spatially derived monthly snow correction between MM5 and observed SNOTEL predictions. Keep in mind that the primary purpose of the MM5 data is to support long-term hypothetical modeling scenarios. The MM5 output is not suitable for calibrating processes and response within the LSPC watershed model, and therefore it was not used for calibration. As previously explained, locally observed data from meteorological gages in and around the Lake Tahoe Basin were applied for model calibration. The model has been successfully calibrated using observed meteorology from the SNOTEL sites. Further refinement of MM5 is required to apply it for running 40-year hypothetical model scenarios; however, no such refinement has been made at this point in time.

### 3.4. Land Use Representation

LSPC requires a basis for distributing hydrologic and pollutant loading parameters. Such a basis is necessary to appropriately represent hydrologic variability throughout the basin, which is influenced by land surface and subsurface characteristics. It is also necessary to represent variability in pollutant loading, which is highly related to land practices.

---

---

Land use typically represents the primary unit for computing water quantity and quality. Rural and urban land use areas in individual subwatersheds each contribute runoff containing pollutant loads to a stream that flows to the lake. Lands adjacent to the lake contribute pollutants directly to it.

Land use categories were defined in the watershed model for the purpose of evaluating pollutant loading from the Lake Tahoe Basin. The total area of each land use category in each subwatershed was computed and amounts of pollutants generated by land use categories were calculated based on characteristics like soil type, slope, and vegetation.

In addition to the need for land use data in computing water quantity and quality, nonpoint source management decisions are also frequently based on land use-related activity at the subwatershed level. Therefore, it was important to have a detailed land use representation with classifications that were meaningful for load allocation and load reduction.

For the Lake Tahoe Basin, no single GIS data source was available that could adequately represent land use variability and impacts by itself to a degree high enough to support a detailed water quality modeling effort. Therefore, it was determined that the best approach would be to build a composite layer that included the best aspects of all available components.

Developing the Lake Tahoe land use layer required a major effort relying on significant input from several local experts and agencies responsible for land management around the basin. A TMDL Development Team (D-Team) was formed. The D-Team included key staff from the LRWQCB, Nevada Department of Environmental Protection (NDEP), USDA Forest Service Lake Tahoe Basin Management Unit, Desert Research Institute (DRI), the Tahoe Regional Planning Agency (TRPA), California Tahoe Conservancy (CTC), UC Davis, and Tetra Tech, Inc. (Tt). The D-Team located and compiled the most current and representative GIS land use coverage layers available, identified advantages and limitations inherent in each data source, and produced a composite layer that maximized the overall accuracy for representing land use throughout the Lake Tahoe Basin. Figure 3-13 presents the final composite land use coverage.

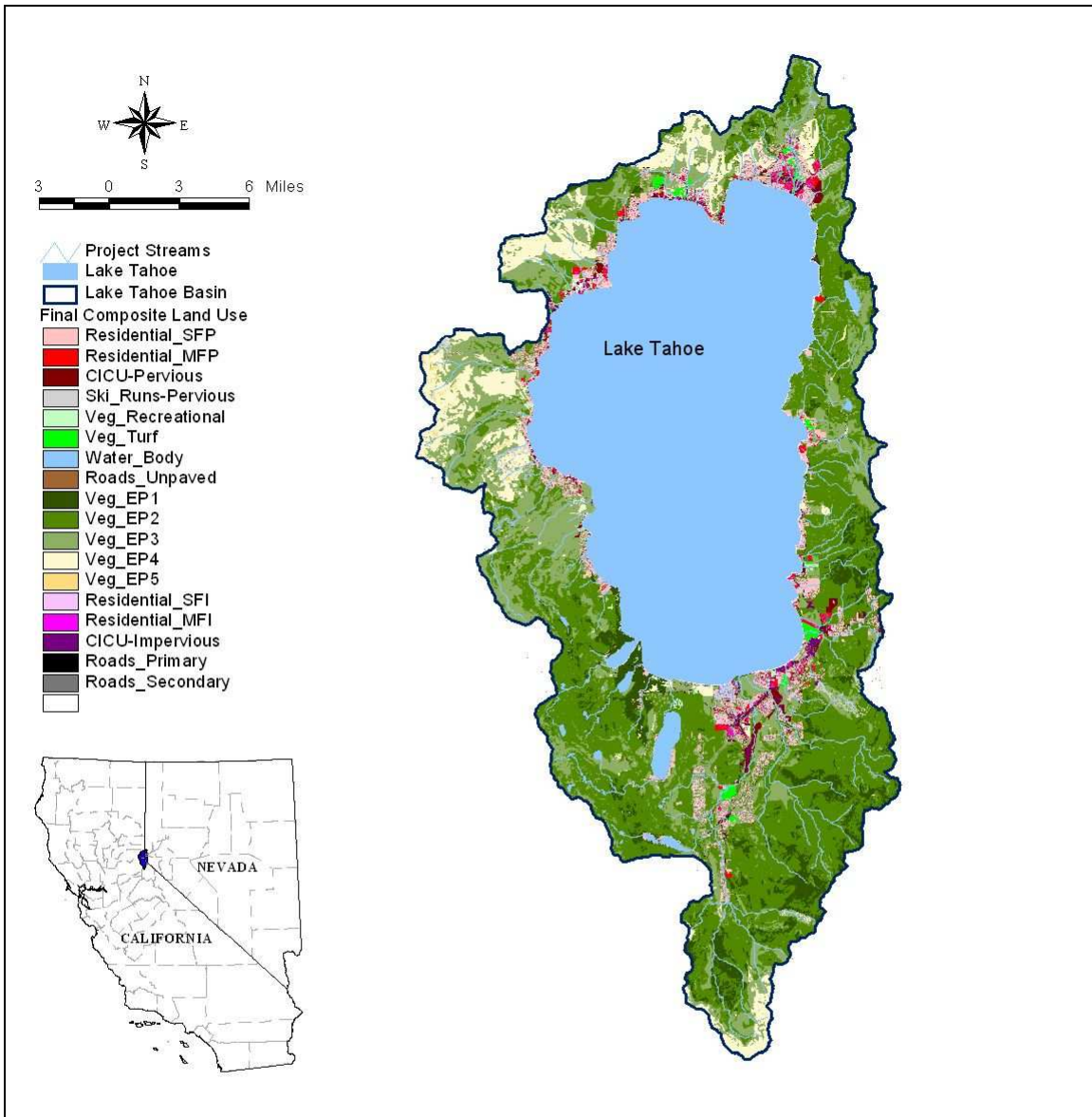


**Figure 3-13. Final composite land use coverage for the Lake Tahoe Basin.**

From a large set of GIS layers that varied in resolution and quality, a plan of action evolved through the data review process. A number of the most critical GIS layers became available only after this project had already begun. The D-Team had to determine a manageable and representative set of land use categories and identify relevant spatial information available for representing each category. Over the course of the development process, certain categories and layers were included or excluded on the basis of ground-truth comparisons, data duplication/exclusion, and site-specific information about the significance of the impact. For example, the initial list of land uses was modified to exclude grazing (a practice that has almost disappeared from the basin and whose historical or legacy impacts are not significant for water quality) and to further refine the

---

---

open space recreational category into turf and non-turf vegetated areas (e.g., golf-courses versus campgrounds).

The final land use layer was based on three primary sources of spatial data: (1) an updated parcel boundaries layer from a number of agencies that compose the Tahoe Basin GIS User's Group, (2) a detailed 1-square-meter-resolution Hard Impervious Cover (HIC) layer that was developed using remote sensing techniques from IKONOS satellite imagery (Minor and Cablk 2004), and (3) a map of upland erosion potential developed by Andrew Simon (Simon et al. 2003).

### The Parcel Boundaries Layer

A number of agencies composing the Tahoe Basin GIS User's Group funded the acquisition of the updated parcel boundaries layer. This layer is a highly detailed GIS coverage that all stakeholders can use for a variety of planning purposes. The new coverage was greatly needed because the older parcel layers had been developed using the best available technology and resources at the time, both of which have been significantly improved in recent years. The fundamental advantage of the new parcel layer was the high resolution with which the individual parcels were delineated, classified, and ground-truthed. This new parcel coverage, accurate to within 10 feet (from TRPA correspondence), was used to develop a basin-wide land ownership coverage for TRPA.

### Hard Impervious Cover Layer

Developed by DRI using spectral mapping and transformation techniques on IKONOS satellite images from 2002 (Minor and Cablk 2004), the HIC layer is a 1-meter-resolution grid map of all anthropogenic impervious surfaces throughout the basin. This high-resolution layer allows for a detailed spatial accounting of impervious surfaces in the basin, including rooftops and paved roads in both urbanized and rural or vegetated areas. Because the degree of directly connected imperviousness significantly affects runoff volume, timing, and pollutant load, it is desirable to accurately represent imperviousness at the parcel scale over the entire basin area. Figure 3-14 shows the hard impervious cover in the Lake Tahoe Basin and an example focus area.

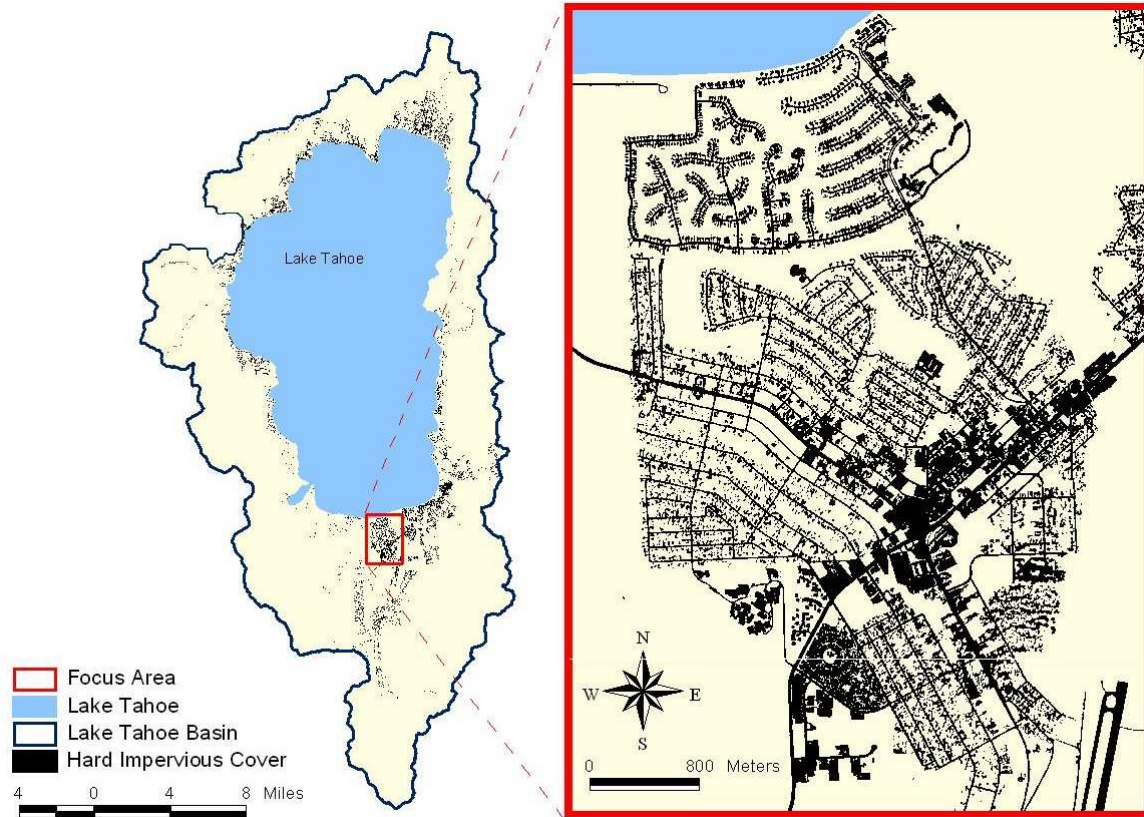


**Figure 3-14. Hard impervious cover for the Lake Tahoe Basin and example focus area.**

### Upland Erosion Potential

During model development it became evident that the land use category classified as vegetated-unimpacted was too broad and did not reflect significant differences in the erodibility of the soils. Further definition of this category became necessary for successful model calibration. Using the GIS coverage Upland-Erosion Potential for the Lake Tahoe Basin developed by Simon et al. (2003), the land uses previously categorized as Vegetated-Unimpacted were subdivided into five erosion potential categories. A more detailed description of the modeled land uses is included in the following section.

### Land Use Categorization/Reclassification

It was neither practical nor possible to gather enough hydrology and pollutant loading information to represent each of the 140 land use classifications for 60,000 individual parcel polygons. Furthermore, certain potential disturbance areas could not be directly mapped from the parcel boundaries alone. The D-Team determined the land use categories based on collective agreement from the various agencies involved as to areas with relatively similar response from a water quality modeling perspective and areas for which local or national pollutant runoff reference information could support model

---

---

representation. The 140 original land use types indicated by the parcel boundary codes were reclassified into the following six general land use categories:

- Single-family residential (SFR)
- Multi-family residential (MFR)
- Commercial/Institutional/Communications/Utilities (CICU)
- Transportation
- Vegetated
- Water body

The D-Team recognized that vegetated (non-urbanized) areas deserved special attention because they constitute over 80 percent of the basin area. Furthermore, the general vegetated lands category included a number of different land uses (e.g., ski resorts and other recreational areas), management activities (e.g., harvesting to control overgrowth and fire hazard), and/or natural conditions (e.g., naturally burned forests) that have differing hydrologic and sediment and nutrient loading characteristics. As a result, six subcategories of vegetated land use were initially defined as follows:

1. *Unimpacted*: Forested areas that have been minimally affected in the recent past
2. *Turf*: Land use types with large turf areas and little impervious coverage, such as golf courses, large playing fields, and cemeteries, with potentially similar land management activities
3. *Recreational*: Lands that are primarily vegetated and are characterized by relatively low-intensity uses and small amounts of impervious coverage; these include the unpaved portions of campgrounds, visitor centers, and day use areas
4. *Ski Areas*: Lands within otherwise vegetated areas for which some trees have been cleared to create a run
5. *Burned*: Areas that have been subject to controlled burns and/or wildfires in the recent past
6. *Harvested*: Lands that management agencies have thinned in the recent past for the purpose of forest health and defensible space (areas cleared to reduce the spread of wildfire)

Once the D-Team had agreed on the classifications, team members identified and categorized each parcel on the basis of their agencies' activities and knowledge of the Lake Tahoe Basin. Selected refinements to the parcel boundary layer were performed to include known areas of disturbance in the basin that had not been identified in the available GIS layers. These areas were ground-truthed and hand-delineated by GIS technicians from the Forest Service, CTC, and NDEP. Through this process, the D-Team identified a complication: the parcel boundary layer often represented ownership jurisdiction better than the actual land use occurring within the selected properties. Therefore, some modifications were required to translate legal or jurisdictional boundaries into actual land uses. Ski areas, campgrounds, parking areas, and primary and secondary roads were all modified.

Because the impact from ski areas stems from the disturbance (clearing) of steep slopes, a

---

---

new GIS category and layer for Ski Runs was developed and used as a refinement for the ski area boundaries previously identified. Land within ski area boundaries that was otherwise fully vegetated and relatively unimpacted was added to the Vegetated Unimpacted land use category, which was collectively refined into five erosion potential categories as described in a following section. Figure 3-15 shows an example of the resulting refinements to the previously defined Vegetated Ski Areas category.

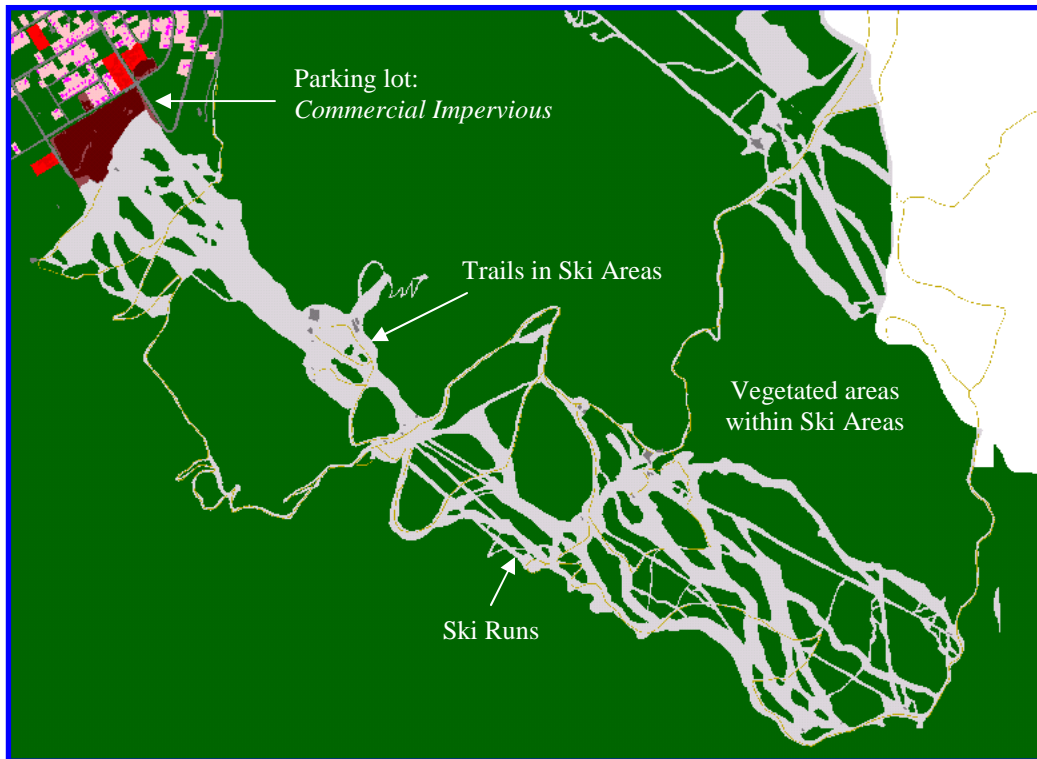


**Figure 3-15. Example of parcel refinements in a portion of the Heavenly Ski Area.**

Campgrounds were hand-delineated based on Forest Service guidance that camping activity typically occurs within 80 feet of roads inside camping areas such as California and Nevada state parks and Forest Service campgrounds. Members of the D-Team obtained supplemental site-specific information from campground brochures and visual confirmation through visits to selected locations. The refined campgrounds were added to the Vegetated-Recreational subcategory. Figure 3-16 illustrates an example of this refinement for campgrounds near Emerald Bay on the southwestern shore of Lake Tahoe.

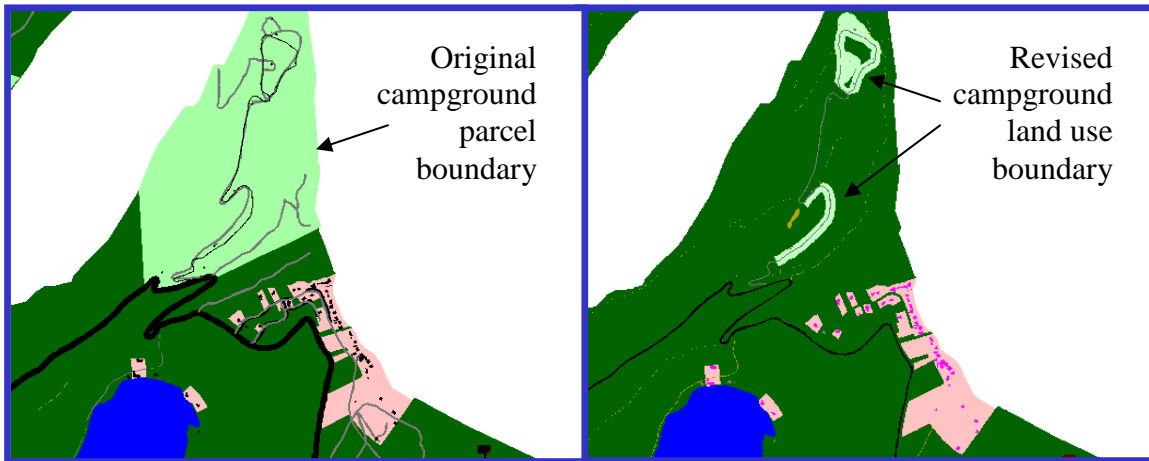


**Figure 3-16. Example of parcel refinement in a campground parcel boundary near Emerald Bay on the southwestern shore of Lake Tahoe.**

Parking areas in high-traffic recreational facilities, beach areas, and ski resorts were hand-delineated and classified as Commercial or Institutional because of the intensity of usage. Figure 3-15, which shows the Heavenly Ski Area, illustrates the result of this type of refinement.

Primary and secondary roads contained in the TRPA parcel coverage delineate the jurisdictional right-of-way, a much wider area than that occupied by the paved road surface. These categories were more accurately represented using the IKONOS HIC layer, by means of a GIS layering and intersecting process (which is described in more detail in the following section, GIS Layering Process). Figure 3-17 illustrates this refinement at the US Route 50 and Route 28 intersection south of Spooner Lake in Nevada.

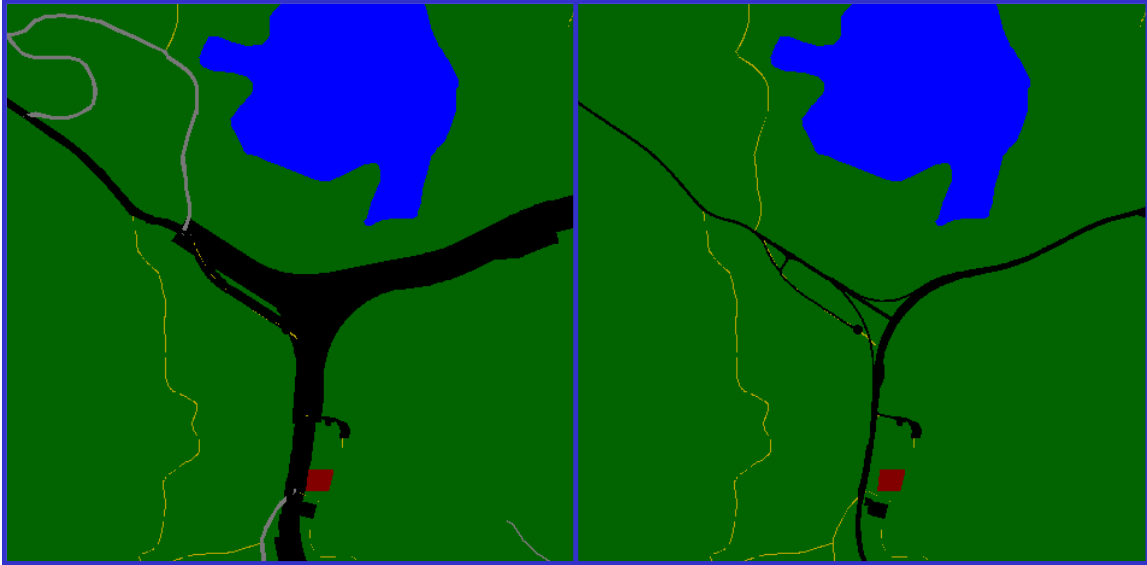


**Figure 3-17. Example of parcel refinement for highway right-of-way ownership (image on left) to actual highway widths based on hard-cover impervious overlay (image on right).**

Supporting GIS layers included Forest Service roads and trails, recreational areas (ski runs and campgrounds), water bodies, and boundaries and dates for forest fires/prescribed burns and harvesting activities. These latter two subcategories were not explicitly represented in the composite layer because they represent episodic impacts. Harvested forest and burned areas were accounted for based on location and calibration time. The GIS Layering Process section below describes how the HIC coverage and fire and timber harvest maps were included in the composite land use coverage for the Lake Tahoe Basin.

### GIS Layering Process

To produce the land use grid that forms the framework for the LSPC watershed model, a layering and intersecting process for the various land use GIS data sources in the Tahoe Basin was performed. The objective of this effort was to develop one composite grid layer that maximized the overall accuracy in representing land use areas in the Lake Tahoe Basin. Table 3-5 shows the final modeling land use categories derived from the composite land use layer.

**Table 3-5. Modeling land use categories derived from the composite land use layer**

Land Use Description	Pervious/Impervious	Subcategory Name	Number
Water body	Impervious	Water_Body	1
Single-family residential	Pervious	Residential_SFP	2
	Impervious	Residential_SFI	3
Multi-family residential	Pervious	Residential_MFP	4
	Impervious	Residential_MFI	5
Commercial/institutional/ communications/utilities	Pervious	CICU-Pervious	6
	Impervious	CICU-Impervious	7
Transportation	Impervious	Roads_Primary	8
	Impervious	Roads_Secondary	9
	Impervious	Roads_Unpaved	10
Vegetated	Pervious	Ski_Areas-Pervious	11
	Pervious	Veg_Unimpacted <sup>a</sup>	12
	Pervious	Veg_Recreational	13
	Pervious	Veg_Burned	14
	Pervious	Veg_Harvest	15
	Pervious	Veg_Turf	16

<sup>a</sup>This subcategory was further refined into five new subcategories based on erosion potential.

GIS layering was performed after all required corrections and refinements to individual parcels had been performed for the entire Basin. Before application of the HIC land use and forest and timber harvesting regions in the GIS layering process, only the categories listed as Pervious in Table 3-5 (excluding Harvested and Burned Vegetated lands) were included in the land use GIS coverage. The incorporation of the separate HIC layer and forest and timber harvest GIS coverages, as well as erosion potential for vegetated areas, is explained below.

#### **Incorporating the HIC Layer**

Based on visual and tabular/quantitative comparisons of transportation areas as represented in the TRPA land use layer, it was determined that the HIC layer represented road surfaces better than buffering existing road widths with average width information. Therefore, the HIC layer was combined with the TRPA land use layer as described below.

First, all existing fields associated with transportation in the TRPA layer were essentially turned off (temporarily) by converting them to Vegetated-Unimpacted. The entire TRPA land use layer was then converted into a 1-meter grid so that it would be compatible with the HIC grid resolution. Doing so made it possible to intersect these two grids, resulting in a unique determination of pervious and impervious grid cells for each land use type. Impervious road surfaces became a fictitious Vegetated-Impervious surface, which could at that point be reclassified as roads.

The transportation category was further subdivided into Primary Roads, Secondary Roads, and Unpaved Roads. The first two subcategories are paved surfaces and are

---

---

represented in the HIC grid. Before merging the HIC grid to the parcel boundary grid, it was necessary to distinguish Primary Road grid cells from other impervious grid cells. To achieve this, a separate highway roads line-theme layer was first uniformly buffered to a width wide enough to span the width of any HIC highway segment (60 feet) and converted into a grid. The new highway grid was intersected with the HIC grid to create Primary Roads HIC grids and Other HIC grids.

After isolating Primary Roads HIC grid cells from Other HIC grids, the HIC grid was intersected with the parcel boundary grid. This process was done to distinguish pervious and impervious SFR, MFR, and CICU land use types. Resulting by-products of this merge were a few Vegetated-Impervious cells. Because the right-of-way-influenced transportation categories in the TRPA land use layer were converted to Vegetated before the merge, and because the Primary Roads were already distinguished within the HIC grid, the process of elimination meant that the resulting Vegetated-Impervious land areas would largely represent the remaining Secondary Roads. A few small structures and objects on vegetated land were also discernible, however, because there were very few of these occurrences, they were still included in the Secondary Roads category.

The final layer incorporated into the composite land use was Unpaved Roads. Because none of the previously added layers had included unpaved road surfaces (the HIC layer considered only hard-impervious areas like pavement and structures), this merge was the most straightforward. The Unpaved Roads layer was created by buffering the unpaved Forest Service and California and Nevada state park roads by each segment's specified width from metadata, and merging in recreational trails that were buffered to a 2-foot width (based on basin-wide average trail width). The buffered Unpaved Roads layer was converted to a grid and intersected with the HIC and parcel boundary composite. All the cells intersected by the unpaved roads layer were directly converted to represent Unpaved Roads.

#### **Incorporating Forest Fire and Harvest Areas**

The remaining vegetated disturbance categories that were not explicitly represented in the TRPA land use coverage included burned and harvested vegetated land and vegetated urban lots. The Forest Service and CTC compiled map layers for fire and timber harvest regions for different events over time. These map layers also represented the degree of burning and harvesting in each affected area. For each burned or harvested zone, an Equivalent Roaded Area (ERA) was computed. The ERA represented the percentage of land in a particular area that was affected by that activity. For example, a harvest ERA of 0.1 indicated that 10 percent of the area within the associated boundary was disturbed due to timber harvesting. Figure 3-18 shows the Gondola Fire, which was a significant forest fire that occurred in 2002 near Heavenly Ski Resort. Subwatershed boundaries are also shown to depict how ERAs were computed at the subwatershed level.

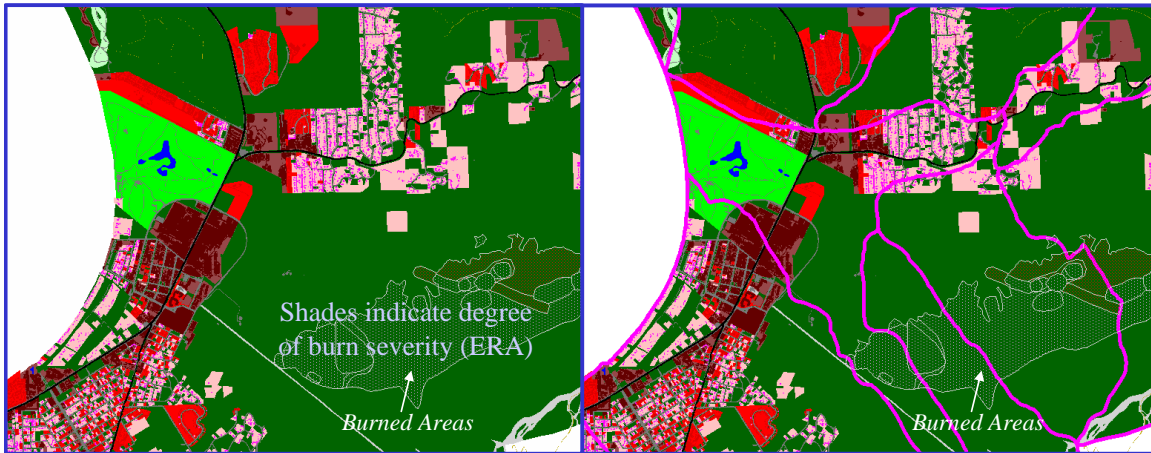


**Figure 3-18. Forest fire boundaries shaded with burn severity for the Gondola Fire. (The right panel shows how the affected areas are aggregated by subwatershed.)**

### **Incorporating Erosion Potential for Vegetated Areas**

The land use category classified as Vegetated-Unimpacted was too broad to reflect significant differences in the erodibility of the soils. Therefore, further definition of this category was necessary. The GIS coverage of Upland-Erosion Potential for the Lake Tahoe Basin developed by Simon et. al (2003) (Figure 3-19) was used to subdivide the land uses previously categorized as Vegetated-Unimpacted into five erosion potential categories. The scale, which goes from a low of 1 to a high of 5, refers to the erosion potential ability of the soil: the higher the value, the higher the erosion potential.

The map of upland-erosion potential for the Lake Tahoe Basin was developed using an upland-erosion-potential index based on the following parameters:

- Soil erodibility factor (K factor)
- Land use
- Paved and unpaved roads, trails and streams
- Surficial geology
- Slope steepness

Each land segment was assigned a representative value for each of the previously listed parameters. Finally, the values of each of the five selected parameters were added and reclassified at a scale of 1 to 5.

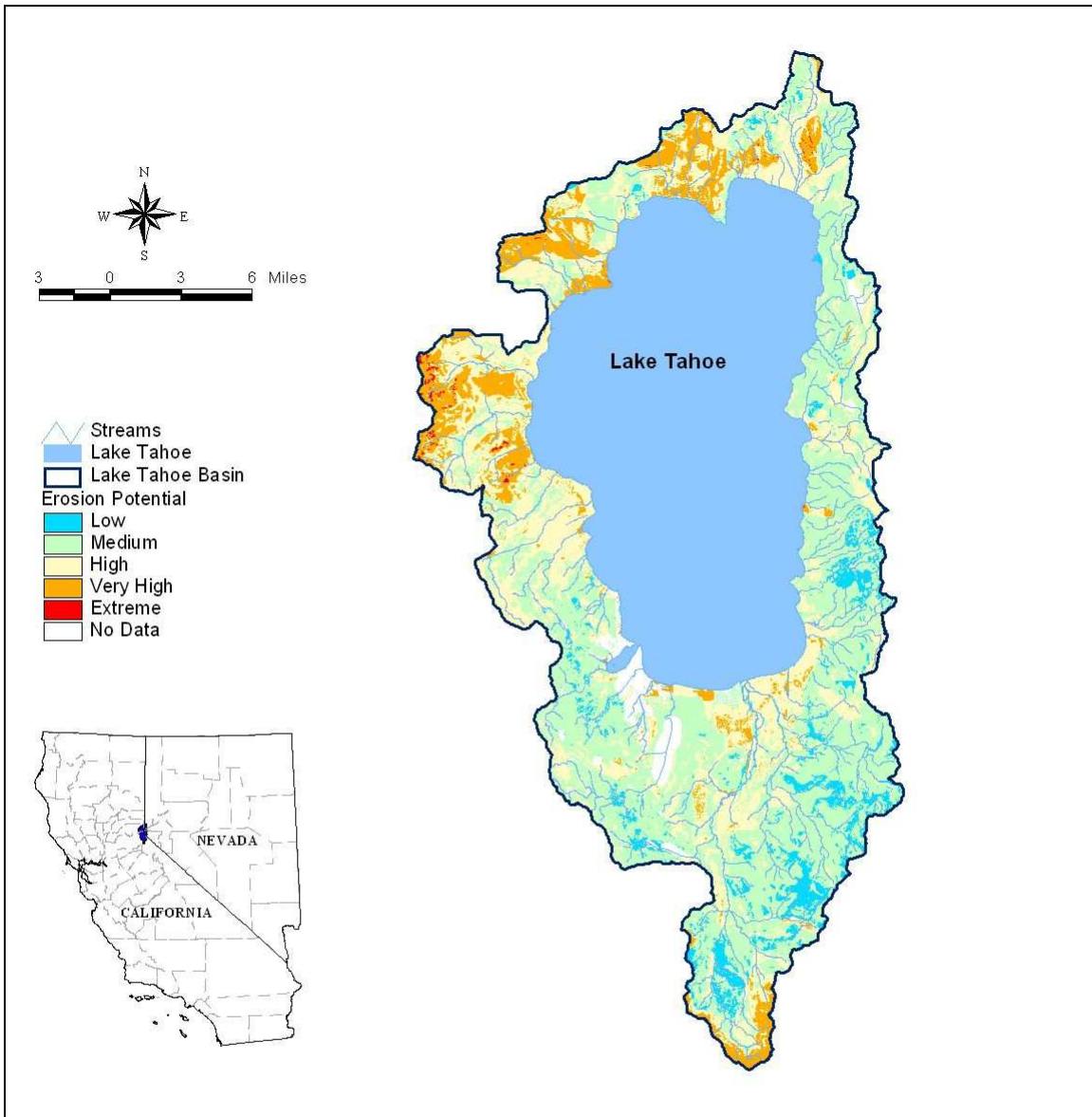


**Figure 3-19. Map of upland erosion potential for the Lake Tahoe Basin.**

The map of upland erosion potential was used to subdivide the broad vegetated-unimpacted category into five vegetated land use categories: Veg\_EP1, Veg\_EP2, Veg\_EP3, Veg\_EP4, and Veg\_EP5. Table 3-6 shows the resulting breakdown of coverage in the Tahoe Basin for the 5 categories.

**Table 3-6. Percent coverage for each of the five Vegetated-Unimpacted categories (based on erosion potential)**

Vegetated Land Use	Percent Cover
Veg_EP1	5.72%
Veg_EP2	46.28%
Veg_EP3	26.14%
Veg_EP4	8.88%
Veg_EP5	0.22%
Total	87.02%

Finally, Table 3-7 shows the final land use distribution for the Lake Tahoe Basin in descending order of percent area.

**Table 3-7. Final land use distribution for the Lake Tahoe Basin**

Land Use	Percentage of Watershed Area	Land Use	Percentage of Watershed Area
Veg_EP2	46.28%	Veg_Turf	0.55%
Veg_EP3	26.14%	Ski_Runs	0.54%
Veg_EP4	8.88%	CICU-Impervious	0.48%
Veg_EP1	5.72%	Residential_MFI	0.38%
Residential_SFP	4.00%	Roads_Primary	0.28%
Water_Body	1.70%	Veg_EP5	0.22%
Roads_Secondary	1.34%	Veg_Burned	0.20%
Residential_MFP	1.00%	Veg_Harvest	0.20%
Residential_SFI	0.89%	Veg_Recreational	0.17%
CICU-Pervious	0.86%	Roads_Unpaved	0.15%

Once the erosion potential was incorporated into the land use coverage, the composite land use coverage was complete and ready to be used in the LSPC model (Figure 3-13).

### 3.5. Soils

Soils data and GIS coverages from the 2004 NRCS Soil Survey were originally used to characterize soils in the Lake Tahoe Basin. General soils data and map unit delineations for the United States are provided as part of the State Soil Geographic (STATSGO) database. As of January 2007, a more detailed NRCS Soil Survey Geographic (SSURGO) database has been completed. The following discussion has been revised based on the updated SSURGO database, which will be considered for any potential future model updates. A map unit is composed of several soil series having similar properties. Identification fields in the GIS coverages can be linked to the database that provides information on chemical and physical soil characteristics. Figure 3-20 shows the general map units in the Lake Tahoe Basin, and the following paragraphs summarize relevant soils data.

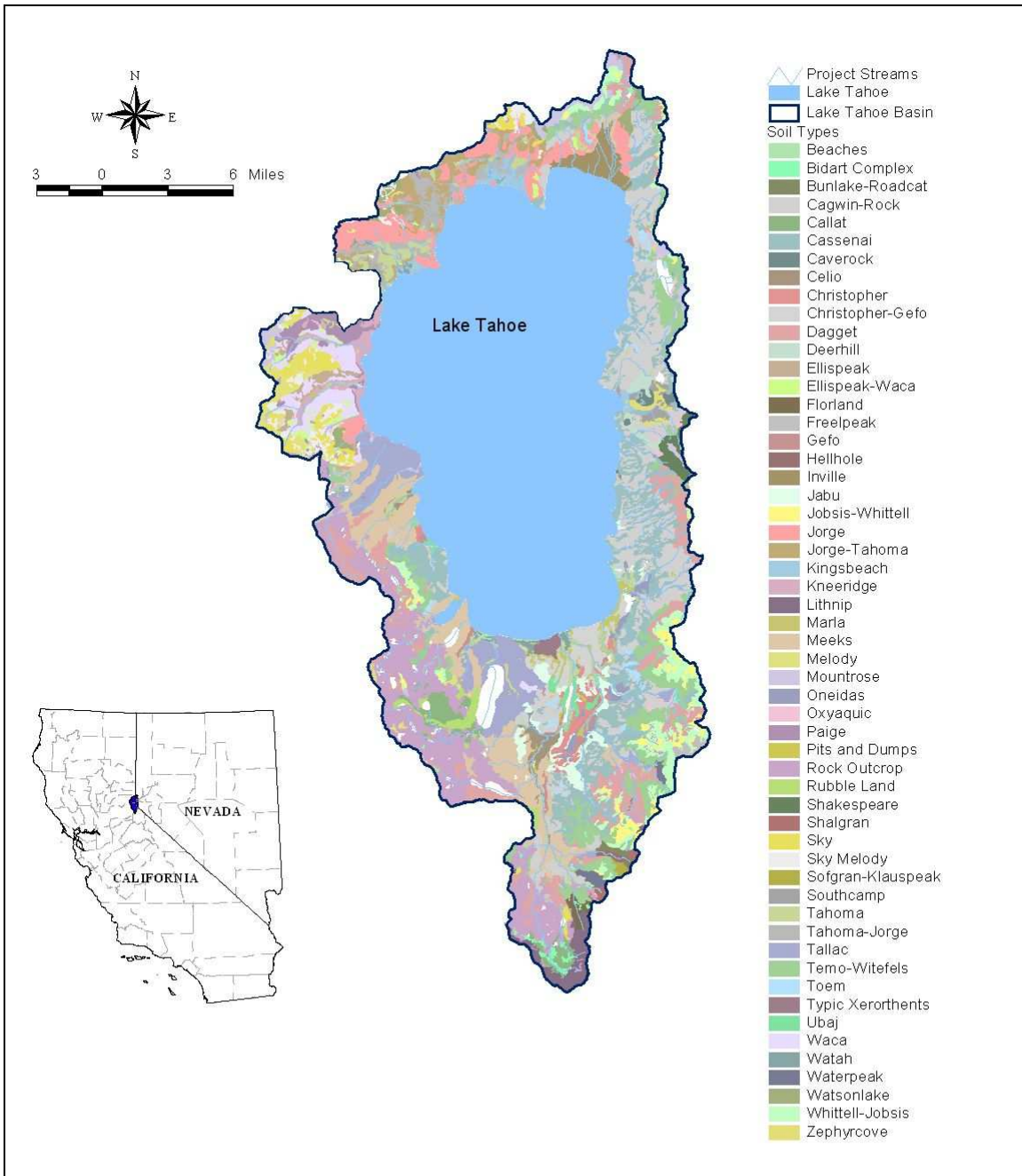


**Figure 3-20. SSURGO map units and corresponding soil descriptions.**

*Permeability* is defined as the rate at which water moves through soil. It is measured in centimeters per second and varies with soil texture, structure, and pore sizes. Soil uses, such as agriculture, septic systems, and construction, can be limited when permeability is too slow. Clays are usually the least permeable soils and sands and gravels the most permeable. NRCS has provided the minimum and maximum ranges for permeability in the Lake Tahoe Basin in the SSURGO database. For the purpose of this analysis, permeabilities are shown as average values for the entire soil layer of each SSURGO map

---

---

unit present in the Lake Tahoe Basin. Figure 3-21 shows that permeability in the Lake Tahoe Basin ranges from a moderate 0.42 cm/s to a very rapid 44 cm/s. The soils with the lowest permeabilities are in the northwest quadrant of the basin.

A commonly used soil attribute is the K-factor, which is a component of the Universal Soil Loss Equation, or USLE (Wischmeier and Smith 1978). The K-factor is a dimensionless measure of a soil's natural susceptibility to erosion, and factor values may range from 0 to 1.00. In practice, maximum factor values generally do not exceed 0.67. Large K-factor values reflect greater inherent soil erodibility. The distribution of K-factor values of the surface soil layers in the Lake Tahoe Basin is shown in Figure 3-22. K-factors and permeability were both included in the database. The figure indicates that, on average, the soils in the basin have K-factors ranging from 0.05 to 0.49, suggesting a wide range of soil erosion potential. The figure also shows several areas lacking K-factor values; these are areas of rock outcrops or water bodies. A number of other factors, including rainfall and runoff, land slope, vegetation cover, and land management practices, influence actual erosion.

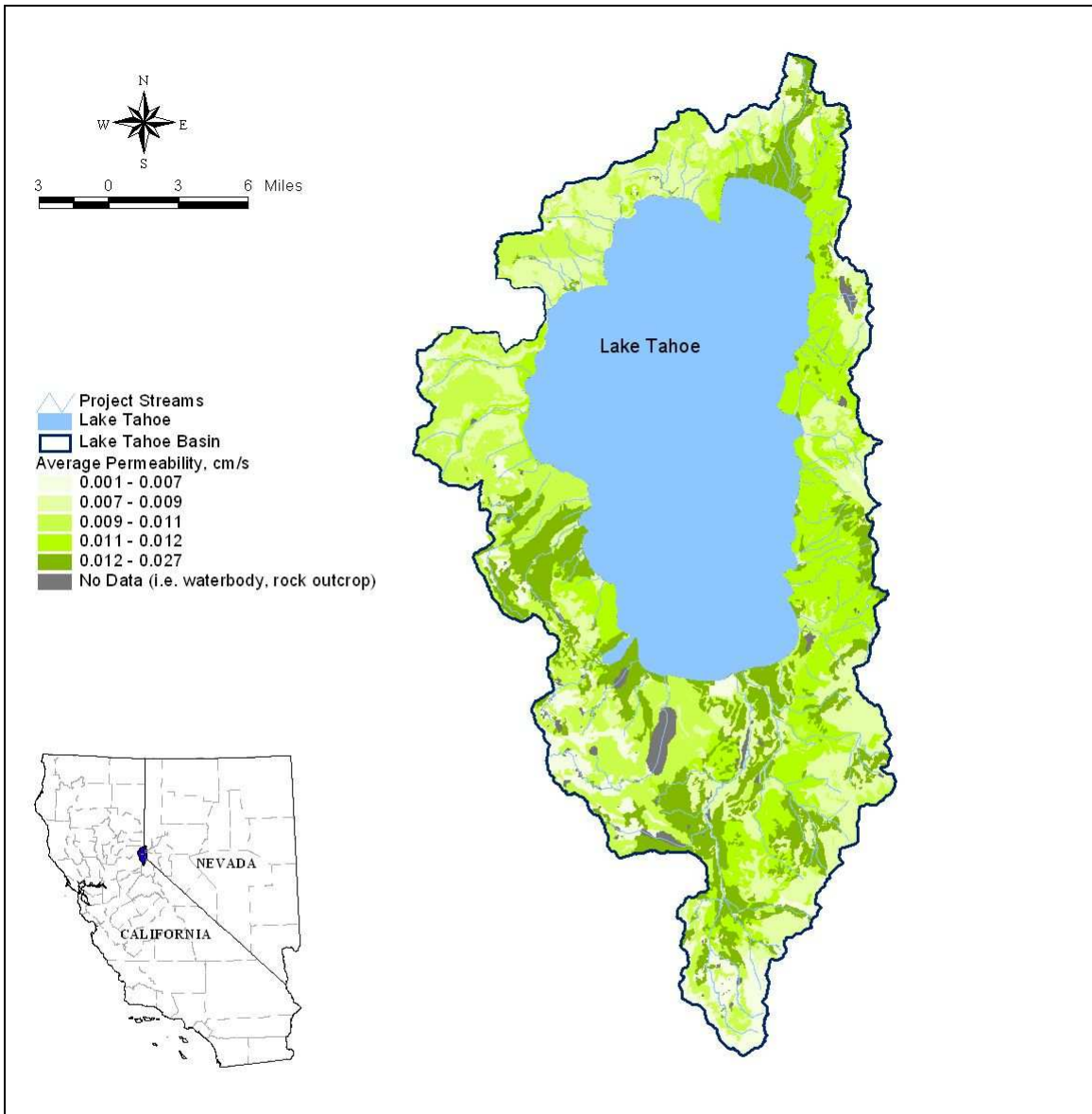


**Figure 3-21. Average permeability of Lake Tahoe Basin soils.**

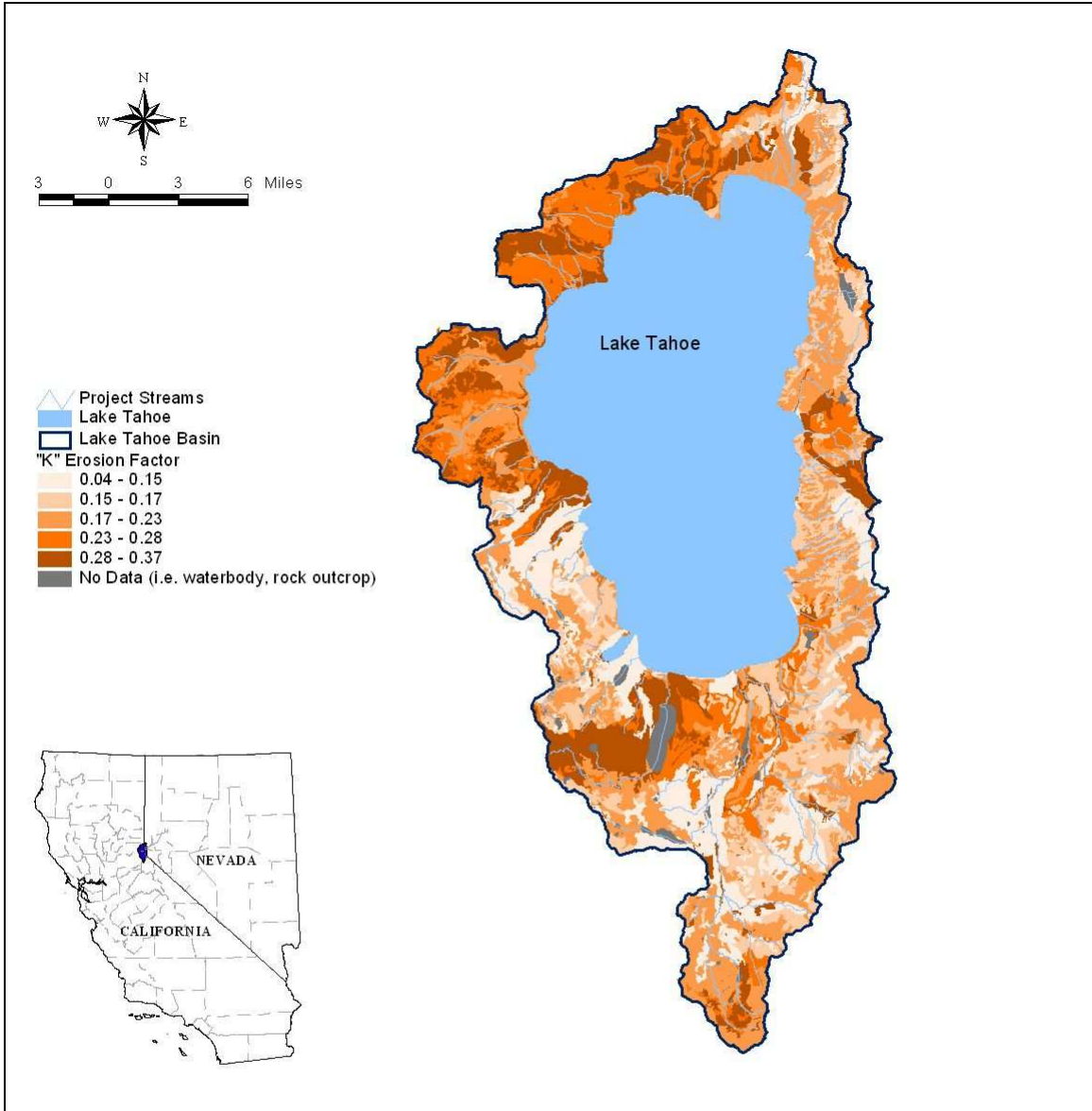


**Figure 3-22. USLE K erosion factor for surface soils.**

---

---



## **4. MODEL CALIBRATION AND VALIDATION**

---

Calibration of the LSPC watershed model for the Lake Tahoe Basin followed a sequential, hierarchical process that began with hydrology, followed by calibration of water quality. Because inaccuracies in the hydrology simulation propagate forward into the water quality simulation, the accuracy of the hydrologic simulation has a significant effect on the accuracy of the water quality simulation. The model was calibrated using both historical stream monitoring data and locally observed stormwater runoff monitoring data.

Ten United States Geological Survey (USGS) stream flow gages and 11 LTIMP water quality gages around the perimeter of Lake Tahoe were used for model calibration. Figure 4-1 shows the location of the monitoring stations. Calibration graphs for Ward Creek are included in this section for illustrative purposes. The remaining calibration graphs and tables are in Appendices A and B.

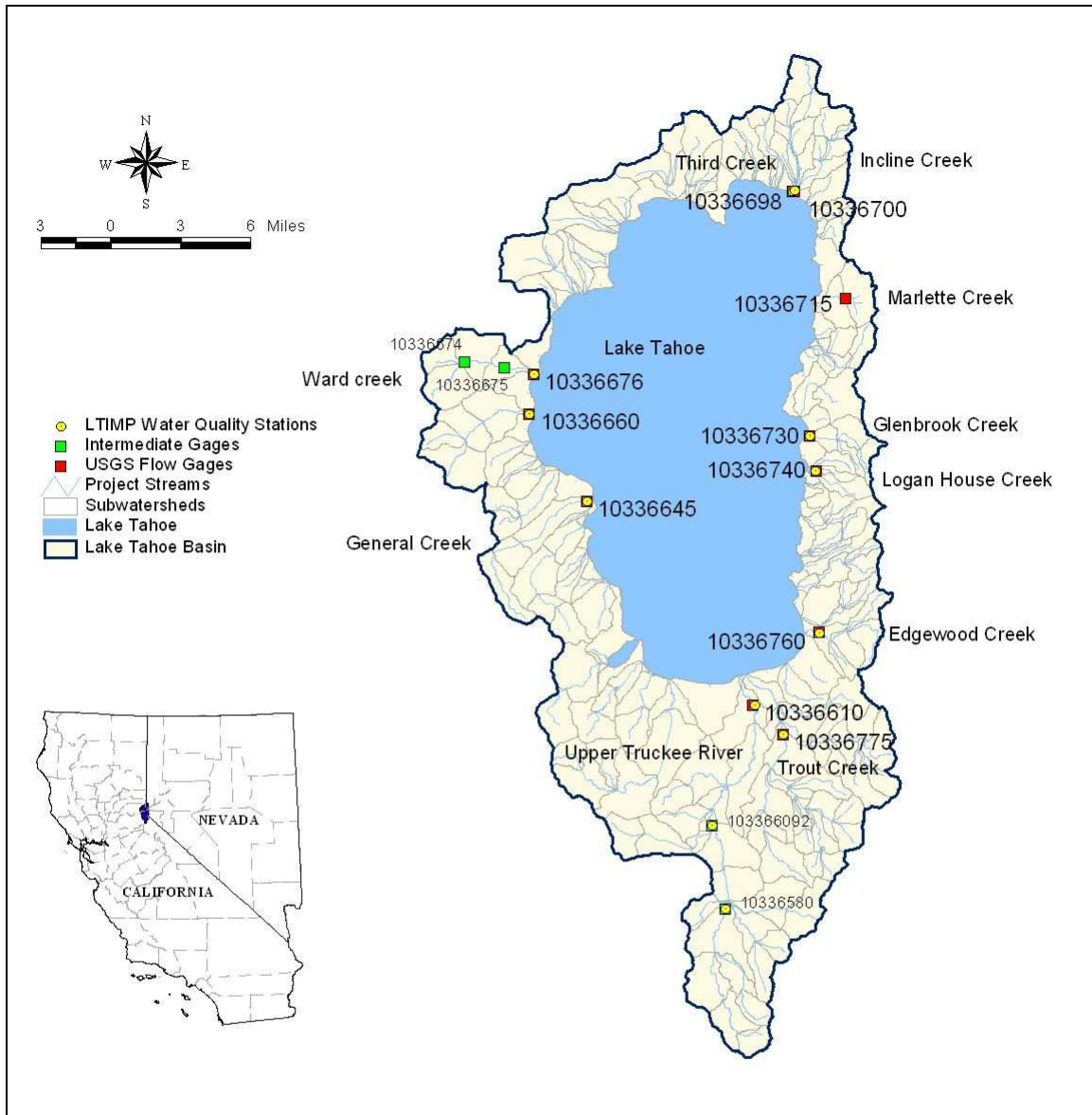


**Figure 4-1. Hydrology and water quality calibration locations.**

## 4.1. Hydrology Calibration

Calibration refers to the adjustment or fine-tuning of modeling parameters to reproduce observations based on field monitoring data. This section describes the modeling and calibration of the snow and hydrology components of the watershed model. Simulation of hydrologic processes, including snow, is an integral part of developing an effective watershed model for Lake Tahoe. The goal of the calibration was to obtain physically realistic model predictions by selecting parameter values that reflect the unique characteristics of the watersheds around the lake. Spatial and temporal aspects were evaluated through the calibration process.

---

---

Hydrologic calibration was performed after configuring the LSPC model. For LSPC, calibration is an iterative procedure of parameter evaluation and refinement as a result of comparing simulated and observed values of interest. It is required for parameters that cannot be deterministically and uniquely evaluated from topographic, climatic, physical, and chemical characteristics of the watershed and compounds of interest. Hydrology calibration was based on several years of simulation to evaluate parameters under a variety of climatic conditions. The calibration procedure resulted in parameter values that produce the best overall agreement between simulated and observed stream flow values throughout the calibration period. Calibration included a time series comparison of daily, monthly, seasonal, and annual values, and individual storm events. Composite comparisons (e.g., average monthly stream flow values over the period of record) were also made. All of these comparisons must be evaluated for a proper calibration of hydrologic parameters.

The LSPC hydrology algorithm follows a strict conservation of mass, with various compartments available to represent different aspects of the hydrologic cycle. Sources of water are direct rainfall or snowmelt. Potential sinks from a land segment are total evapotranspiration, flow to deep groundwater aquifers, and outflow to a reach. From the reach perspective, sources include land outflow (runoff and base flow), direct precipitation, and flow routed from upstream reaches. Sinks include surface evaporation, mechanical withdrawals, and reach outflow.

## Snow Hydrology Simulation

Snowfall and snowmelt have a dominant impact on hydrology, water quality, and management practice requirements in the Lake Tahoe Basin. Therefore, calibrating snow hydrology was critical to the accuracy of the overall hydrology calibration for the basin.

The method used to simulate snow behavior was the energy balance approach. The LSPC SNOW module uses the meteorological forcing information to determine whether precipitation falls as rain or snow, how long the snowpack remains, and when snowpack melting occurs. Heat is transferred into or out of the snowpack through net radiation heat, convection of sensible heat from the air, latent heat transfer by moist air condensation on the snowpack, rain, and conduction from the ground beneath the snowpack. Figure 4-2 is a schematic of the snow process. The snowpack essentially

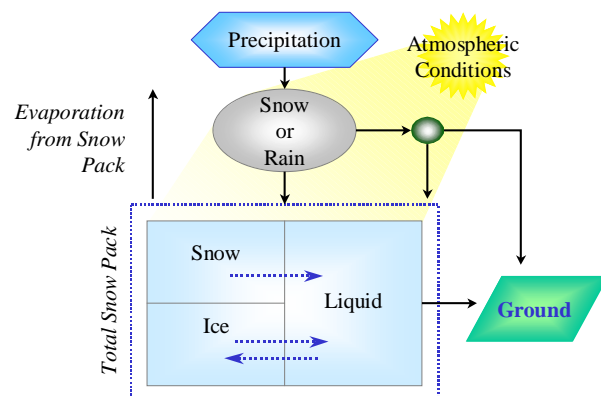


**Figure 4-2. Snow simulation schematic.**

---

---

acts like a reservoir that has specific thermodynamic rules for how water is released. Melting occurs when the liquid portion of the snowpack exceeds the snowpack's holding capacity; melted snow is added to the hydrologic cycle.

Daily average snow water equivalent (SWE) data at the SNOTEL sites were directly compared with modeled SWE output. Emphasis was given to overall volumes and the shape of the SWE curve. Figure 4-3 shows an example of modeled versus observed daily average temperatures and SWE depths at Ward Creek. The upper graph shows temperature (right axis), volume (left axis), and precipitation type. When the temperature falls below the solid brown line, precipitation becomes snowfall; rainfall volumes are the dark blue bars, and snowfall volumes are the light blue bars. The lower graph, which shows modeled SWE in gray and observed SWE as blue dots, demonstrates consistently good agreement year after year through eight annual snowfall/snowmelt cycles.

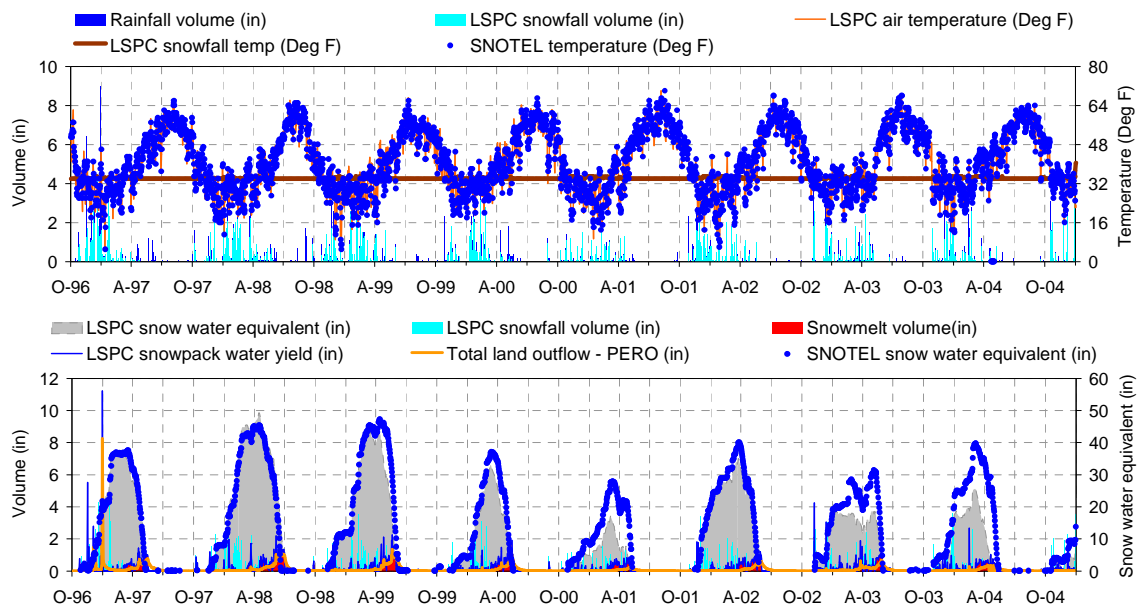


**Figure 4-3. Modeled vs. observed daily average temperatures and snow water equivalent depths at Ward Creek SNOTEL site (October 1996–December 2004).**

During model testing and calibration, it became evident that the most important factor influencing the model snow predictions was not parameterization but the quality of the input temperature time series. The SNOTEL quality assurance process for temperature, together with the lapse rate correction, noticeably reduced overall model error. The calculation of the lapse rate (the rate at which temperature decreases with increasing elevation) in the Lake Tahoe Basin was critical to the accuracy of the watershed model because it influences snowfall prediction, which significantly affects the hydrology of the basin. The lapse rate was particularly important in the Lake Tahoe Basin because of the rapid elevation changes throughout the basin. See Section 3.3 for more detail on the quality assurance process for temperature and calculation of the lapse rate for the Lake Tahoe Basin. Of the 14 available snow parameters in the LSPC model, 4 required adjustment from default values. Table 4-1 summarizes the snow parameters and adjusted ranges from around the basin.

**Table 4-1. Summary of snow module calibration parameters (adjusted parameters are highlighted)**

Parameter	Description	Status	Default	Calibrated
ICEFG	Ice simulation switch, 1 = on or 0 = off	Turned on	1	1
FOREST	Forested land for winter transpiration (fraction)	By land use	N/A	0.2–0.75
LAT	Latitude of land segment (degrees)	From GIS	N/A	By location
MELEV	Mean elevation of land segment (ft)	From GIS	N/A	By location
ELDAT <sup>a</sup>	Difference between MELEV and gage elevation (ft)	From GIS	N/A	By location
SHADE <sup>a</sup>	Land shaded from solar radiation (fraction)	By land use	N/A	0.2–0.75
SNOWCF <sup>a</sup>	Precipitation-snow catch efficiency (multiplier)	By location	1.1–1.5	0.55–1.5
COVIND	Water equivalent for complete land coverage (in)	Constant	1.0–3.0	0.5–1.0
RDCSN	Density of new snow relative to water (in/in)	Constant	0.1–0.2	0.2
TSNOW <sup>a</sup>	Air temperature for snowfall (degrees F)	By location	31–33	34
SNOEVP	Snowpack sublimation coefficient (unitless)	Constant	0.1–0.15	0.15
CCFACT <sup>a</sup>	Condensation/convection coefficient (unitless)	By location	1.0–2.0	0.2–0.35
MWATER	Maximum water content of snow (in/in)	Constant	0.01–0.05	0.03
MGMELT	Maximum ground snowmelt rate (in/day)	Constant	0.01–0.03	0.01

<sup>a</sup> Most sensitive parameters for snow calibration in Lake Tahoe Basin.

## Hydrology Simulation

LSPC hydrology algorithms follow a strict conservation of mass. The sources of water to the land surface are direct precipitation and snowmelt. Some of this water is intercepted by vegetation, man-made structures, or other means. The interception is represented in the model as a land use-specific reservoir that must be filled before any excess water is allowed to overflow to the land surface. The water in the reservoir is also subject to evaporation. The size (in inches per unit of area) of this reservoir can be varied monthly to represent the level of each compartment (above and below the land surface).

Water that is not intercepted is placed in surface detention storage. If the land segment is impervious, no subsurface processes are modeled, and the only pathway to the stream reach is through direct surface runoff. If the land segment is pervious, the water in the surface detention storage can infiltrate, be categorized as potential direct runoff, or be divided between runoff and infiltration. This decision is made during simulation as a function of soil moisture and infiltration rate. The water that is categorized as potential direct runoff is partitioned into surface storage/runoff or interflow, or kept in the upper-zone storage. The amount of surface runoff that flows out of the land segment depends on the land slope and roughness and on the distance it has to travel to a stream. Interflow outflow recedes based on a user-defined parameter.

Water that does not become runoff or interflow or is not lost to evaporation from the upper-zone storage infiltrates. This water becomes part of the lower-zone storage or

---

---

active groundwater storage, or it is lost to the deep/inactive groundwater. The lower-zone storage acts like a reservoir of the subsurface. This reservoir needs to be full for water to reach the groundwater storage. Groundwater is stored and released based on the specified groundwater recession, which can be made to vary nonlinearly.

The model attempts to meet the evapotranspiration demand by evaporation of water from base flow (groundwater seepage into the stream channel), interception storage, upper-zone storage, active groundwater, and lower-zone storage. How much of the evapotranspiration demand may be met from the lower-zone storage is determined by a monthly variable parameter. Finally, water can exit the system in three ways—through evapotranspiration, through loss to deep/inactive groundwater, or by entering the stream channel. The water that enters the stream channel can come from direct overland runoff, interflow outflow, and groundwater outflow.

Some of the hydrologic parameters can be estimated from measured properties of the watersheds, whereas others must be estimated by calibration. Model parameters adjusted during calibration are associated with evapotranspiration, infiltration, upper- and lower-zone storages, recession rates of base flow and interflow, and losses to the deep groundwater system.

During hydrology calibration, land segment hydrology parameters were adjusted to achieve agreement between daily average simulated and observed USGS stream flow at selected locations throughout the basin, as previously shown in Figure 4-1. The average of the 24 hourly model predictions per day was compared with daily mean flow values measured at USGS stream flow gages throughout the basin. The 4-year calibration period was from October 1, 1996, to September 30, 2000. Although the model was run from January 1996 through December 2004, the first 9 months were disregarded to allow for model predictions to stabilize from the effects of estimated initial conditions.

During calibration, agreement between observed and simulated stream flow data was evaluated on an annual, seasonal, and daily basis using quantitative and qualitative measures. Specifically, annual water balance, groundwater volumes and recession rates, and surface runoff and interflow volumes and timing were evaluated. The hydrologic model was calibrated by first adjusting model parameters until the simulated and observed annual and seasonal water budgets matched. Then the intensity and arrival time of individual events were calibrated. This iterative process was repeated until the simulated results closely represented the system and reproduced observed flow patterns and magnitudes. The model calibration was performed using the guidance of error statistics criteria specified in HSPEXP (Lumb et al. 1994). Output comparisons included mean runoff volume for simulation period, monthly runoff volumes, daily flow time series, and flow frequency curves.

The insights gained from calibration are that about 70 percent of the total annual water budget arrives during spring snowmelt and that base flow (or flow from groundwater that has infiltrated into the subsurface regime) accounts for more than 90 percent of the annual in-stream water budget. Most of this groundwater is from snowmelt, which has

the ability to infiltrate rather than immediately enter the stream channel as surface runoff because the snowmelt process occurs relatively slowly. The timing of the hydrograph was directly related to the modeling of the snow component. It became clear that the level of detail achieved in the snow calibration was absolutely necessary for a good calibration of stream flows.

Groundwater recession rates had spatial and seasonal variability. The rates were found to be nonlinear, with a steep curve during the spring that tapered off during summer and fall. The use of a model parameter that allows for nonlinear recession rates was necessary to represent this variability in the recession rates.

Figure 4-4 shows example results over the model calibration period at Ward Creek, with emphasis on water year 1997. Hydrology calibration results for all other stations in the basin are presented in Appendix A. Figure 4-4 also shows that the model is robust enough to predict an extreme 100-year rain-on-snow event (January 1, 1997) while also capturing low-flow variability, as seen by exaggerating low flows using a log scale. Validation was performed for a longer time period (October 1, 1996, through December 31, 2004). Figure 4-5 shows model results for the full validation period at Ward Creek. Results are month-aggregated to evaluate the model's ability to reproduce consistent seasonal trends. Model performance statistics are shown in Table 4-2.

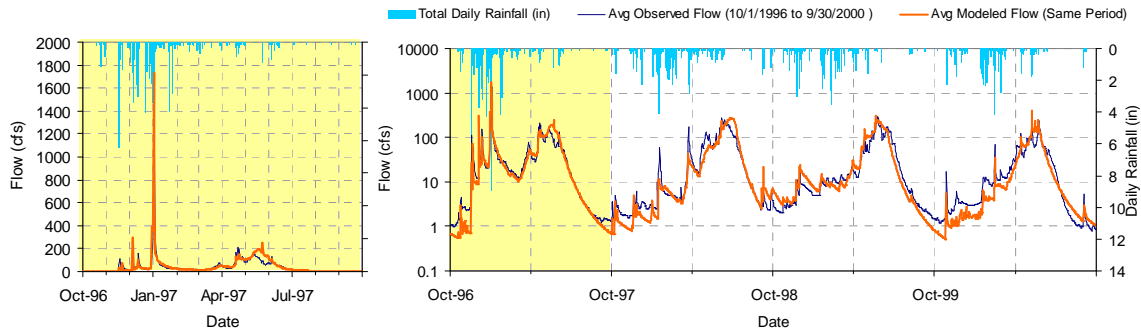


**Figure 4-4. Hydrology calibration for Ward Creek with emphasis on water year 1997.**

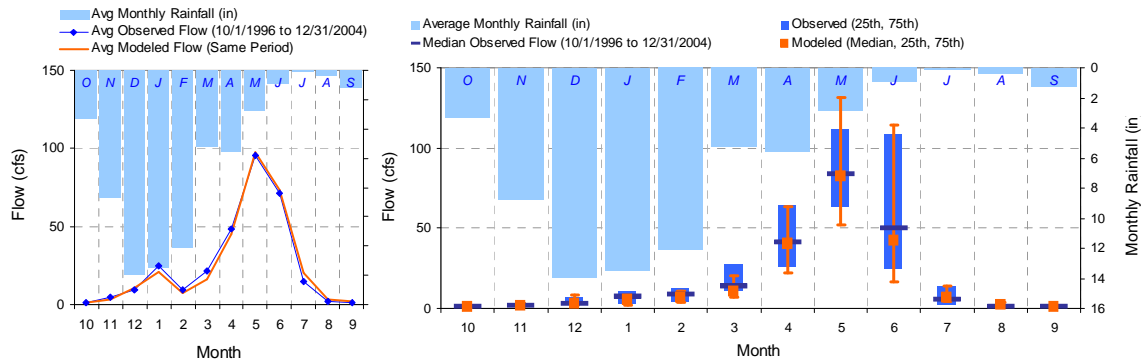


**Figure 4-5. Hydrology validation for Ward Creek with seasonal mean, median, and variation.**

**Table 4-2. Hydrology validation summary statistics for Ward Creek**

LSPC simulated flow		Observed flow gage	
<b>REACH OUTFLOW FROM SUBBASIN 8060</b> 8.25-year analysis period: 10/1/1996 - 12/31/2004 Flow volumes are (inches/year) for upstream drainage area		<b>USGS 10336676 WARD C AT HWY 89 NR TAHOE PINES CA</b> Hydrologic Unit Code: 16050101 Latitude, Longitude: 39.1321292, -120.1576913 Drainage area (sq-mi): 9.7	
Total simulated in-stream flow:	<b>99.19</b>	Total observed in-stream flow:	<b>100.00</b>
Total of simulated highest 10% flows:	<b>58.50</b>	Total of observed highest 10% flows:	<b>53.93</b>
Total of simulated lowest 50% flows:	<b>4.54</b>	Total of observed lowest 50% flows:	<b>4.21</b>
Simulated summer flow volume (months 7-9):	<b>8.49</b>	Observed summer flow volume (7-9):	<b>6.02</b>
Simulated fall flow volume (months 10-12):	<b>5.70</b>	Observed fall flow volume (10-12):	<b>5.59</b>
Simulated winter flow volume (months 1-3):	<b>14.46</b>	Observed winter flow volume (1-3):	<b>18.24</b>
Simulated spring flow volume (months 4-6):	<b>70.54</b>	Observed spring flow volume (4-6):	<b>70.15</b>
Total simulated storm volume:	<b>7.03</b>	Total observed storm volume:	<b>8.29</b>
Simulated summer storm volume (7-9):	<b>0.54</b>	Observed summer storm volume (7-9):	<b>0.40</b>
<i>Errors (simulated-observed)</i>	<i>% Errors</i>	<i>Recommended criteria</i>	
Error in total volume:	-0.81	10	
Error in 50% lowest flows:	-7.32	10	
Error in 10% highest flows:	7.80	15	
Seasonal volume error - Summer:	29.12	30	
Seasonal volume error - Fall:	2.01	30	
Seasonal volume error - Winter:	-26.12	30	
Seasonal volume error - Spring:	0.55	30	
Error in storm volumes:	18.06	20	
Error in summer storm volumes:	26.03	50	

In general, the model produced excellent snow and hydrology results when model inputs were spatially derived from site-specific data and when weather data quality was validated. Performance statistics show that the model reproduced observed trends very well. Table 4-3 shows the validation summary statistics for the other flow gages in the Lake Tahoe Basin.

**Table 4-3. Hydrology validation summary statistics for USGS flow gages in the Lake Tahoe Basin**

Watershed	USGS Station	Location Description	Area (mi <sup>2</sup> )	% Error in Total Volume	Flow % Error in 50% Lowest	Flow % Error in 10% Highest
Upper Truckee	10336610	South Lake Tahoe, CA	54.9	4.1	-14.6	5.0
Upper Truckee	103366092	Hwy 50 above Meyers, CA	34.3	9.1	-26.0	9.7
Upper Truckee	10336580	South Upper Truckee Rd, Meyers, CA	14.1	0.8	2.6	-13.0
Blackwood	10336660	Near Tahoe City, CA	11.2	-6.2	-8.7	7.4
Ward Ck.	10336676	Hwy 89, Tahoe Pines, CA	9.7	-0.8	7.4	7.8

Watershed	USGS Station	Location Description	Area (mi <sup>2</sup> )	% Error in Total Volume	Flow % Error in 50% Lowest	Flow % Error in 10% Highest
General Ck.	10336645	Near Meeks Bay, CA	7.4	-4.3	-7.3	1.0
Incline Ck.	10336700	Near Crystal Bay, NV	6.7	1.7	-2.6	8.8
Edgewood	10336760	At Stateline, NV	5.6	2.1	0.7	21.8
Glenbrook	10336730	At Glenbrook, NV	4.1	7.8	-0.6	3.4
Logan House	10336740	Near Glenbrook, NV	2.1	10.7	30.1	6.1

As a final validation, the annual hydrologic budget estimates from stream flow into Lake Tahoe were compared with previously published estimates. Table 4-4 shows the results of this comparison. The LSPC modeled flows fall right between the other estimates.

**Table 4-4. Hydrologic budget estimates for Lake Tahoe (stream flow component)**

Reference	Period Considered	Estimated Annual Stream Flow into Lake Tahoe (acre-ft)
McGauhey and others 1963	1901–1962	308,000
Crippen and Pavelka 1970	1901–1966	312,000
Dugan and McGauhey 1974	1960–1969	372,000
Myrup and others 1979	1967–1970	413,000
Marjanovic 1987		379,562
<b>LSPC Watershed Model 2006</b>	<b>1990–2002</b>	<b>376,211</b>

## 4.2. Water Quality Calibration

LSPC water quality is a function of the hydrology. Sediment production is directly related to the intensity of surface runoff. Sediment yield varies by land use and spatially throughout the basin. In addition to meteorology and the resulting hydrology, sediment yield is influenced by factors like soil type, surface cover, and soil erodibility. Sediment is delivered to the tributaries and to Lake Tahoe through surface runoff erosion and in-stream bank erosion.

Nutrients are delivered to the tributaries with surface runoff and subsurface flow. They can be observed in both organic and inorganic forms, and they can exist in both dissolved and particulate forms. Some nutrient forms are also associated with sediment runoff. LSPC provides mechanisms for representing all of these various pathways of pollutant delivery. A detailed water quality analysis was performed using statistically based load estimates with observed flow and in-stream monitoring data. The confidence in the calibration process increases with the quantity and quality of the monitoring data. The LTIMP stream database provides very good spatial and temporal coverage that focuses

---

---

primarily on nutrients and sediment. This analysis provides the necessary information to inform the model parameterization and calibration.

This section describes the statistical analysis, model parameterization, and model calibration process. As with the hydrology calibration, example plots are included for Ward Creek. The remaining calibration graphs and tables are included in Appendix A.

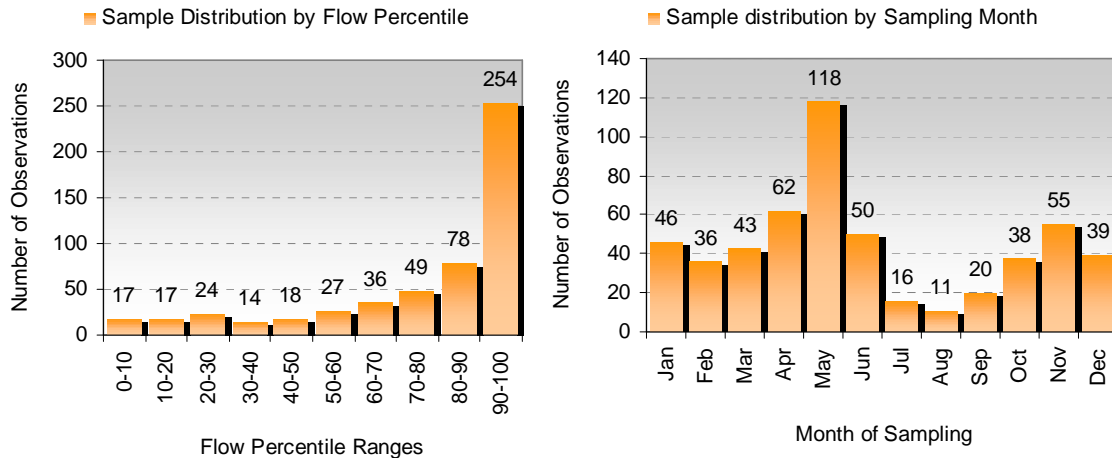
### Estimating Sediment Loads with Log-Transform Regression

Because a primary objective of the Lake Tahoe watershed model is to estimate pollutant loads to be used as input to the DLM, accurate estimates of loads based on the LTIMP monitoring data had to be developed to aid in the water quality calibration process.

Suspended sediment loads are typically estimated using linear regression of observed sediment load versus stream flow datasets. Since sediment load and stream flow are storm-driven, observed values often span several orders of magnitude. Consequently, the in-stream sediment load versus flow relationship tends to be linear in logarithmic space. For practical application of the regression model, estimated loads must be retransformed from log space back to the original units. This retransformation process can be statistically biased, and therefore bias correction was needed. One of the methods that the USGS recommended for bias correction is the Minimum Variance Unbiased Estimator, or MVUE (Cohn and Gilroy 1991). The objective of the method is to yield an unbiased estimate with the smallest possible variance.

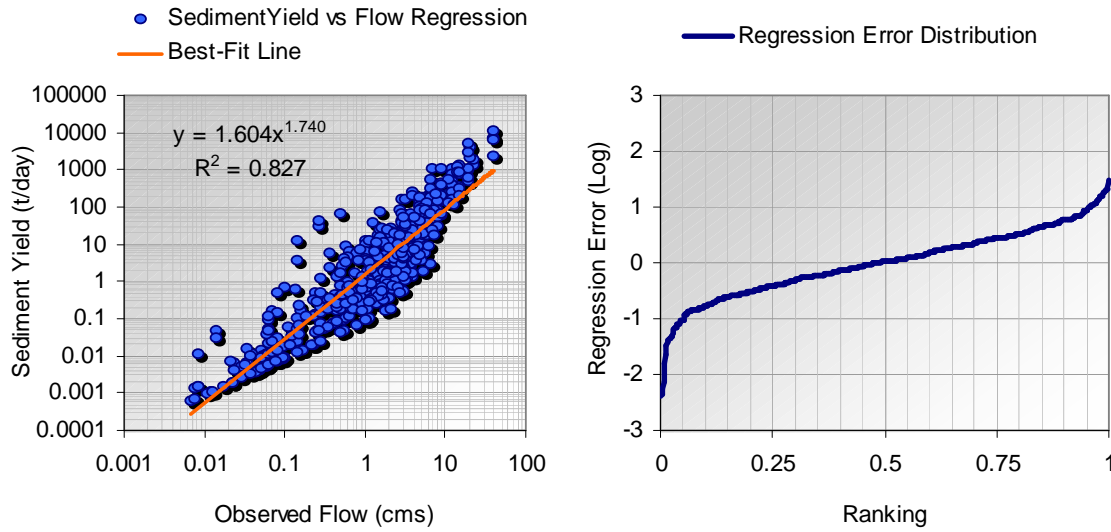
Many years of research have refined this statistical retransformation method and made it practical for estimating loads for environmental engineering applications (Finney 1941, Bradu and Mundlak 1970, Cohn et al. 1989). In addition to sediment, the MVUE retransformation has also been applied in numerous studies to other pollutants that exhibit lognormal relationships, including total and dissolved nitrogen and phosphorus species (MDNR and USGS 2001, Green and Haggard 2001). It is important to note that this method is unbiased only if the regression errors are normally distributed in log space.

Figure 4-6 shows the distribution of sediment samples arranged by associated daily-average-flow percentiles and by sampling month for Ward Creek, a tributary to Lake Tahoe. These samples were collected between December 1972 and September 2003. The sampling distribution is directly related to the observed flow magnitude in the stream, meaning that the month with the highest observed flows (May, when the spring snowmelt peaks occur) also has the highest number of samples collected. Initial evaluation suggests that the Ward Creek sampling distribution is well suited for sediment load versus flow regression analysis.



**Figure 4-6. Sample flow distributions for sediment observations at Ward Creek.**

Figure 4-7 shows a lognormal regression relationship between observed flow and instantaneous sediment yield in the left panel and shows sample error distribution (difference between *log* regression estimated load and *log* instantaneous load) in the right panel. For this example it is assumed that instantaneous sediment yield is represented by the product of sediment concentration and the average daily flow for the sample date. The best-fit regression model or sediment rating curve for this dataset is  $y = 1.604x^{1.740}$ , where  $x$  is flow in cubic meters per second and  $y$  is sediment load in metric tons per day. Figure 4-7 also illustrates that the log errors for this distribution are largely linear or, in other words, that the regression relationship follows a lognormal distribution. The regression model used for prediction is more refined than this depiction because separate equations were derived for surface runoff and base-flow-associated loads.



**Figure 4-7. Flow-sediment yield regression relationship and error distribution at Ward Creek.**

Once an acceptable sediment rating curve has been developed, daily observed flow data are used to estimate a continuous time series of sediment yield for a desired period. The rating curve relationship alone is not statistically consistent and has been shown to systematically underestimate sediment loads in excess of 50 percent in some cases (Cohn 1995). The MVUE is computed daily and applied as a multiplier to the value predicted by the regression model, as shown in equation 1 below:

$$\hat{L}_{MVUE} = L_{RC(t)} \times g_m \quad (1)$$

where

$L_{RC(t)}$  = sediment load estimated from the rating curve for day  $t$  and  
 $g_m$  = Finney (1941) and Bradu and Mundlak (1970) function.

The  $g_m$  function is a Bessel function with the variables of estimated variances. Equations 2 and 3 represent the initial value for  $g_m$ .

$$g_m = \frac{(n-1)}{2(n-2)} (1-V)s^2 \quad (2)$$

$$V = \frac{1}{n} + \left( \frac{(\ln(Q_i) - \overline{\ln(Q)})^2}{\sum_{i=1}^n (\ln(Q_i) - \overline{\ln(Q)})^2} \right) = \frac{1}{n} + \left( \frac{(\ln(Q_i) - QBAR)^2}{QVAR} \right) \quad (3)$$

where

- $n$  = number of observations used to develop the rating curve;  
 $s^2$  = mean square error for the regression;  
 $Q_t$  = observed flow for day  $t$ ;  
 $QBAR$  = average of all  $n$  observed flow values in logarithmic space; and  
 $QVAR$  = sum of  $n$  squares of logarithmic observed flow minus  $QBAR$ .

The  $g_m$  function iterates through additional computational terms until it converges to a reasonably constant value. This function can be evaluated using FORTRAN code developed by Cohn et al. (1989, USGS 2005). Because the MVUE is computed daily, it is especially helpful for cases where there is a large variance in daily discharges, the prediction interval changes greatly over the range of the data, or many of the predictions are made near the extremes of the relationship (USGS 2005). Table 4-3 is a summary of sediment load estimates for the straight rating curve versus the rating curve plus MVUE adjustment for the Ward Creek dataset.

**Table 4-3. Summary of sediment load estimates at Ward Creek using the Minimum Value Unbiased Estimator**

Summary Period	Computed Regression Load (tonnes)		Percent Difference Between Estimates
	Rating Curve Values	Using Daily MVUE	
Summer (months 7–9)	58	158	172.55%
Fall (months 10–12)	20	55	172.42%
Winter (months 1–3)	234	636	171.38%
Spring (months 4–6)	772	2,102	172.44%
<b>Mean Annual Load</b>	<b>1,084</b>	<b>2,952</b>	<b>172.22%</b>

## Pollutant Export Analysis Using Regression and Hydrograph Separation

Hydrology is the driving force for the LSPC general water quality module (GQUAL). Because wastewater is exported out of the Lake Tahoe Basin, nonpoint sources represent the major source of pollutant loading to Lake Tahoe streams. Stream bank erosion has also been shown to represent another source of sediment loading (and possibly, associated nutrients) to Lake Tahoe streams; for total sediment, stream bank erosion might actually be higher than land loading in certain streams (Simon et al. 2003). There are no known point source pollutant dischargers in the basin. The GQUAL module requires that loading rates or concentrations be specified for groundwater, interflow, and surface runoff for each land use in each subwatershed. A statistical data-mining exercise was performed (1) to understand the seasonality and trends observed in both in-stream and stormwater monitoring data, (2) to represent nutrient species distribution and loading patterns in base flow versus storm flow samples, (3) to estimate organic and inorganic nutrient quantities, (4) to characterize particulate- and sediment-associated nutrient mass, and (5) to derive land-use-specific loading rates to apply in the watershed model.

The primary source of in-stream monitoring is a high-resolution historical water quality dataset collected at numerous sites by the LTIMP, USGS, UCD, and NDEP. The constituents that have been monitored include ammonia ( $NH_4$ ), total Kjeldahl nitrogen

(TKN), nitrate (NO<sub>3</sub>), soluble reactive phosphorus (SRP), total phosphorus (TP), and total suspended sediment (TSS). For the purpose of this investigation, the data have been aggregated into five categories: TSS, TN, TP, dissolved nitrogen (inorganic: NO<sub>3</sub> + NH<sub>4</sub>), and dissolved phosphorus (SRP). TN is the sum of TKN and NO<sub>3</sub>. Nitrite levels, while measured, are so low that they are of no consequence to inorganic nitrogen loading in the Lake Tahoe Basin. Table 4-4 is a summary of the LTIMP monitoring data available from the Ward Creek monitoring station.

**Table 4-4. Summary of monitoring data collected at the Ward Creek outlet**

Water Quality Constituent	Monitoring		Number of Samples	Average Sample Frequency (every # days) <sup>a</sup>
	Start Date	End Date		
Total suspended sediment (mg/L)	12/20/1972	9/19/2003	534	21
Total nitrogen (mg/L)	10/16/1983	9/19/2003	406	18
Total phosphorus (mg/L)	10/10/1988	9/19/2003	402	14
Dissolved <sup>b</sup> nitrogen (mg/L)	10/16/1983	9/19/2003	404	18
Dissolved <sup>b</sup> phosphorus (mg/L)	10/10/1988	9/19/2003	402	14

<sup>a</sup>As noted in Figure 4-6, sampling is clustered around the periods of high flow to better represent loading.

<sup>b</sup>*Dissolved* assumes inorganic nutrient portions (NO<sub>3</sub> + NH<sub>4</sub>, SRP).

## Estimating Seasonal Pollutant Loading Patterns in the Streams

Hydrograph separation used in conjunction with log-transform regression allows the assessment of base flow (the portion of the stream flow from groundwater) and surface runoff volumes and associated nutrient yield. The USGS hydrograph separation algorithms (HYSEP) were used to perform hydrograph separation on the observed flow time series (Sloto and Crouse 1996). Figure 4-8 presents the results of the hydrograph separation and shows that stream flow in the Lake Tahoe Basin tends to be groundwater-dominated.

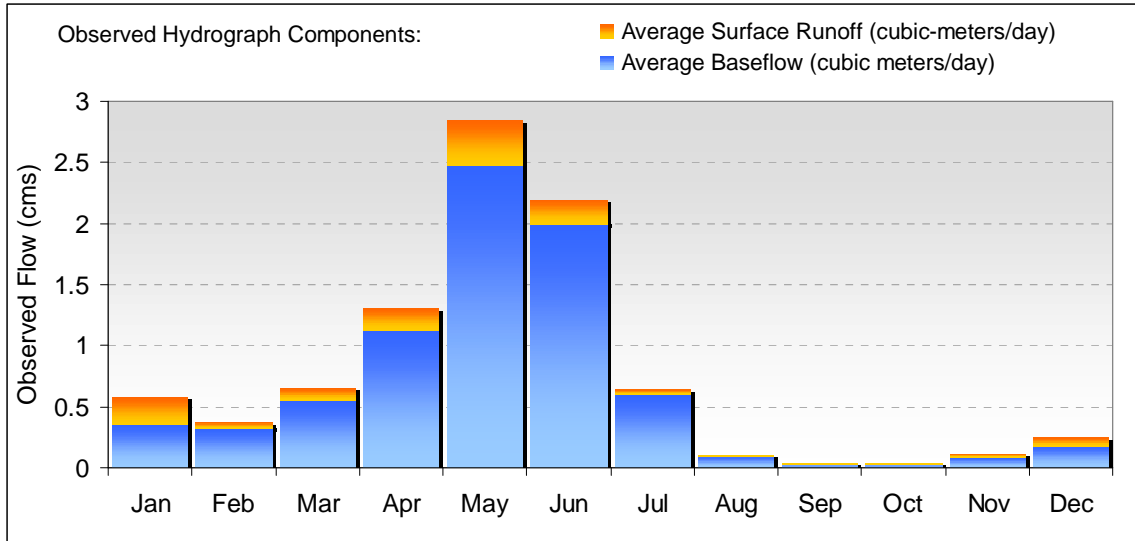


**Figure 4-8. Hydrograph separation for Ward Creek (USGS 10336676) using historical flow data collected between 10/1/1972 and 9/30/2003.**

Because there are no direct point source contributions of nutrients to the streams, the sediment and nutrient yields at the monitoring station are assumed to have come from upstream nonpoint sources. The following assumptions were applied for this analysis:

- Reasonable base flow and surface runoff volumes can be obtained using the HYSEP sliding-interval method.
- Because flow-versus-load regressions have errors that are normally distributed in log space, it is reasonable to use rating curves in conjunction with MVUEs to develop base flow and surface runoff load relationships in linear space.
- TN and TP represent all transportable nitrogen and phosphorus from upstream sources.
- Base flow load is primarily groundwater-driven, and storm flow load is primarily surface-runoff-driven.
- Base-flow-associated samples are composed primarily of dissolved forms of pollutants (DN and DP, inorganic nutrients).
- TN and TP base flow samples represent total dissolved nutrients, which include both organic and inorganic forms.
- TSS, which is primarily associated with surface runoff, includes organic material that contains nutrients.
- Base flow rating curves can be used in conjunction with total flow rating curves to back-calculate surface runoff nutrient yields.
- Surface runoff pollutant mass is primarily composed of particulate constituents.
- Particulate nutrient mass is primarily composed of organic material.
- Particulate-nutrient-mass-to-sediment-mass ratios represent sediment-associated nutrients.

For each LTIMP gage, a set of 10 regression rating curves was developed using the monitoring data. For each water quality constituent, base flow (BF) and storm flow

(runoff [RO]) curves were derived using the separated hydrograph. Example equations are presented in Table 4-5. For the development of the rating curves, each in-stream sample had to be classified as a BF sample or an RO sample using the daily separated hydrograph time series. It was reasonable to assume that the BF classification could be assigned to any sample for which the base-flow-to-total-flow ratio was greater than 50 percent. Therefore, this sample classification analysis was performed for each threshold value between 50 and 100 percent to see which threshold value resulted in the best correlation for both the BF and RO rating curves. The  $r^2$  correlation value served as the performance measure for goodness of fit.

**Table 4-5. Base flow and storm flow sediment and nutrient rating curve summary**

Constituent and Sample Type <sup>a</sup>		Number of Samples	Base-flow Threshold	Log of Intercept	Slope	R <sup>2</sup>
Sediment	BF	77	98%	6.326	1.354	0.863
	RO	457	98%	7.473	1.769	0.811
Total nitrogen	BF	69	99%	2.165	1.149	0.915
	RO	337	99%	2.609	1.144	0.880
Total phosphorus	BF	90	96%	0.571	0.982	0.940
	RO	312	96%	1.339	1.211	0.829
Dissolved nitrogen	BF	76	98%	-0.213	1.066	0.907
	RO	328	98%	0.220	1.081	0.843
Dissolved phosphorus	BF	295	58%	-0.659	0.856	0.925
	RO	107	58%	-0.098	0.870	0.900

<sup>a</sup>BF indicates base flow samples, and RO indicates storm flow samples (collected during runoff events).

The rating curves were used to develop loading estimates and summarized to produce seasonal trends and loading distributions. Figure 4-15 is an example of the results. To validate this methodology independently, dissolved organic nitrogen (DON) and dissolved organic phosphorus (DOP) values were compared against independently computed fractions (Coats and Goldman 2001); the values were found to be in agreement.

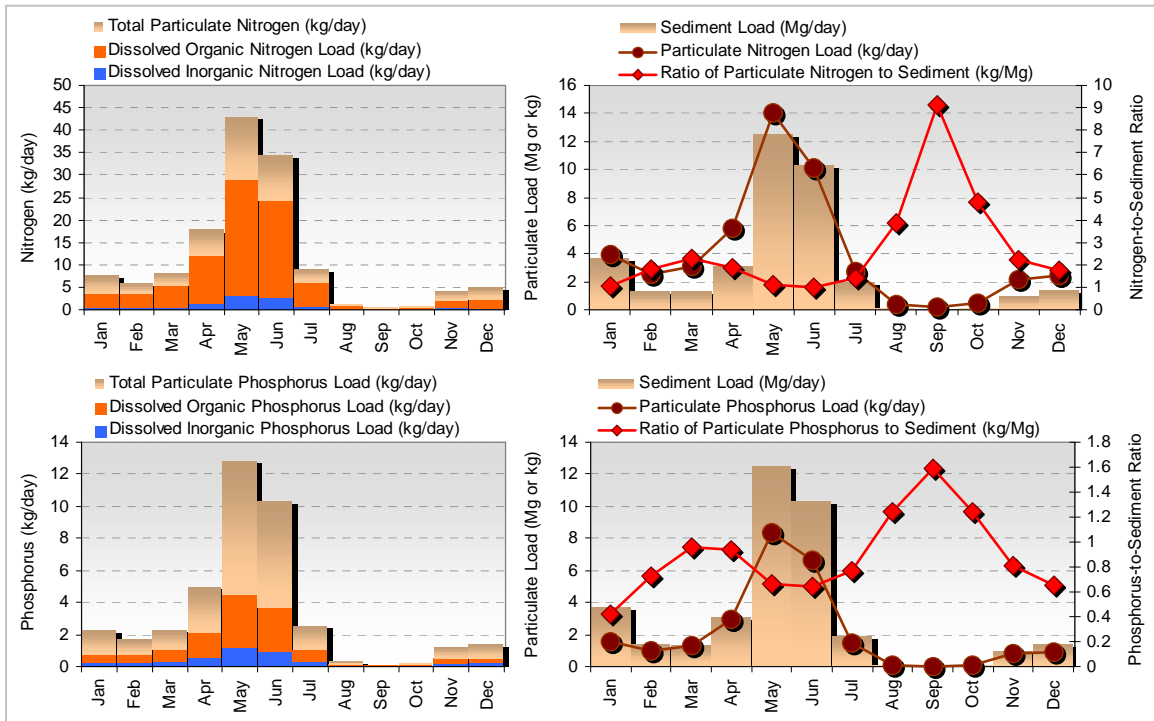


**Figure 4-9. Seasonal nitrogen and phosphorus constituent distribution for Ward Creek water quality sampling data collected between 1972 and 2003, derived from hydrograph separation and regression.**

The insights gained from this statistical data-mining exercise provide guidance for selecting appropriate source loading parameters for the deterministic watershed simulation model. Some interesting observations from reviewing the results are presented below:

- About 70 percent of the total annual sediment, nitrogen, and phosphorus load is delivered to the stream during the snowmelt months (April, May, and June).
- On average, 8.5 percent of TN and 12 percent of TP are inorganic.
- Of the 91.5 percent of TN are organic and 88 percent of TP are either organic or sediment associated, 62 percent and 30 percent, respectively, are dissolved.
- Although the months of August, September, and October yield the lowest amount of sediment and nutrients, the ratio of particulate nutrient mass to total sediment mass shows a distinct 2 to 4 times increase, suggesting that the organic matter (in terms of percentage of total sediment) increases during those months.
- Comparison of total nitrogen distribution and loading to an independent analysis performed using the same dataset shows good agreement in estimated loads for Ward Creek (Coats and Goldman 2001, estimate about 1.5 kg-N/ha/yr for Ward Creek, compared to 1.6 kg-N/ha/yr for this analysis).

An estimate of TN and TP loads was developed for each of the 10 calibration watersheds using this method. Table 4-6 is a summary of the results.

**Table 4-6. Annual estimates of total nitrogen and phosphorus loads for calibration streams developed using in-stream water quality data**

Watershed	Total Nitrogen (kg/year)	Total Phosphorus (kg/year)
Third Creek	3,930	1,170
Incline Creek	2,190	553
Glenbrook Creek	638	137
Logan House Creek	241	21
Edgewood Creek	1,030	214
General Creek	3,160	398
Blackwood Creek	9,170	2,710
Ward Creek	5,660	1,760
Trout Creek	5,390	954
Upper Truckee River	25,300	4,160

### Model Parameterization by Land Use

Following the data-mining analysis, monthly variable base flow and surface concentrations were directly computed using the various loading components and their associated flow volumes. Particulate nutrient mass was modeled as a sediment-associated fraction using the derived nutrient-to-sediment mass ratios. Because water quality parameters are specified at the land use level for each subwatershed, supplemental information was required to associate representative components of the estimated bulk load with each land use unit.

Recent research completed on nutrient and suspended sediment concentrations in stormwater runoff in the Lake Tahoe Basin to support the TMDL effort was used to estimate watershed-specific loading ratios for a number of land uses. In this research, runoff mean concentrations were related to watershed characteristics and land use through multiple linear regression analyses. It was found that particulate species of nitrogen and phosphorus were the most abundant sources of nutrients in stormwater and that they were especially high in commercial land uses. Population density and residential yard maintenance play key roles in nutrient and sediment concentrations for residential land uses (Gunter 2005).

In addition, a review of the National Stormwater Quality Database (Pitt et al. 2004) and the Tahoe Research Group Stormwater Monitoring Dataset (Heyvaert 1988) provided further guidance regarding the relative loading rates for sediment and nutrients from different land use categories. Table 4-7 summarizes the relative concentrations for land

use categories represented in the Lake Tahoe watershed model. See Appendix B for a description of how these concentrations were determined.

**Table 4-7. Relative pollutant concentrations for modeled land uses (Note: Appendix B describes how these numbers were determined).**

Modeled Land Use	Total Suspended Solids <sup>a</sup>	Total Nitrogen <sup>a</sup>	Dissolved Nitrogen <sup>a</sup>	Total Phosphorus <sup>a</sup>	Dissolved Phosphorus <sup>a</sup>
Residential SFP <sup>b,c</sup>	47	1.46	0.12	0.39	0.12
Residential MFP <sup>b,c</sup>	125	2.37	0.35	0.49	0.12
CICU Pervious <sup>d</sup>	247	2.06	0.24	0.59	0.07
Ski Runs Pervious					
- Heavenly	39	0.30	0.11	0.10	0.03
- Homewood	47	0.41	0.01	0.14	0.04
- Diamond Peak	5,238	2.17	1.97	1.47	0.05
Vegetated Unimpacted	0.7	0.14	0.01	0.03	0.02
Vegetated Recreational	383	0.86	0.01	0.52	0.17
Vegetated Burned <sup>e</sup>					
- Wildfire <sup>e</sup>	<i>Equivalent Roaded Area (ERA) Methodology<sup>e</sup></i>				
- Prescribed Burns <sup>e</sup>					
Vegetated Harvest <sup>e</sup>					
Vegetated Turf	10	4.06	0.41	1.25	0.22
Residential SFI <sup>b,c</sup>	47	1.46	0.12	0.39	0.12
Residential MFI <sup>b,c</sup>	125	2.37	0.35	0.49	0.12
CICU Impervious <sup>d</sup>	247	2.06	0.25	0.59	0.07
Roads Primary	793	3.27	0.60	1.65	0.08
Roads Secondary	793	3.27	0.60	1.65	0.08
Roads Unpaved	846	1.95	0.01	1.27	0.40

<sup>a</sup>Values are in milligrams of N or P per liter.

<sup>b</sup>P = pervious; I = impervious.

<sup>c</sup>SF = single-family, MF = multi-family.

<sup>d</sup>CICU = Commercial/Institutional/Communications/Utilities.

<sup>e</sup>Concentrations equal to unpaved roads, but areas will be adjusted based on ERA values.

In addition to the EMCs, the fraction of the TSS comprised of fine sediment (< 63 µm) was estimated for each urban land use category using available stormwater sampling information (Hayvaert, et. al 2007). The same urban sediment distribution was applied to all landuses of the same type in all subwatersheds. The remaining non-urban land uses were assigned a uniform distribution of fine sediment based on in-stream sediment distributions that varied by subwatershed. Table 4-8 shows the fine sediment distributions by land use and subwatershed.

**Table 4-8. Percent fines by land use and subwatershed as applied in the watershed model**

Landuse Type	Landuse Name or Subwatershed	Runoff Fines Distribution		
		(< 63 um)	(20 - 63 um)	(< 20 um)
Urban	Residential_SF	76.3%	40.6%	35.7%
Urban	Residential_MF	88.4%	30.7%	57.7%
Urban	CICU	85.4%	22.3%	63.1%
Urban	Roads_Primary	85.4%	22.3%	63.1%
Urban	Roads_Secondary	85.4%	22.3%	63.1%
Non-Urban	Third Creek	31.0%	21.5%	9.5%
Non-Urban	Incline Creek	67.0%	46.6%	20.4%
Non-Urban	Glenbrook Creek	80.0%	55.4%	24.6%
Non-Urban	Logan House Creek	75.0%	51.6%	23.4%
Non-Urban	Edgewood Creek	59.0%	41.2%	17.8%
Non-Urban	General Creek	29.0%	20.3%	8.7%
Non-Urban	Blackwood Creek	45.0%	31.4%	13.6%
Non-Urban	Ward Creek	47.0%	32.3%	14.7%
Non-Urban	Trout Creek	38.0%	26.3%	11.7%
Non-Urban	Upper Truckee River	44.0%	30.6%	13.4%

Once the water quality parameters were initially set-up in the model, the model was run and the results of the annual average loads by calibration watershed were compared with the annual loads obtained using the available data. After this initial comparison was made, two things were noted. First, the modeled fine sediment loads were too low for those areas with a large percent of volcanic soils and second, fine sediment loads were too high for those areas dominated by granitic soils. A regression was developed that correlates the required multiplying factor for the pervious land uses and the percent volcanic soils in the watershed. This regression is presented in Figure 4-10. Each point in the graph represents a calibration watershed. It can be observed that the higher the fraction of volcanic soils in the watershed, the higher the multiple required for the TSS EMCs.

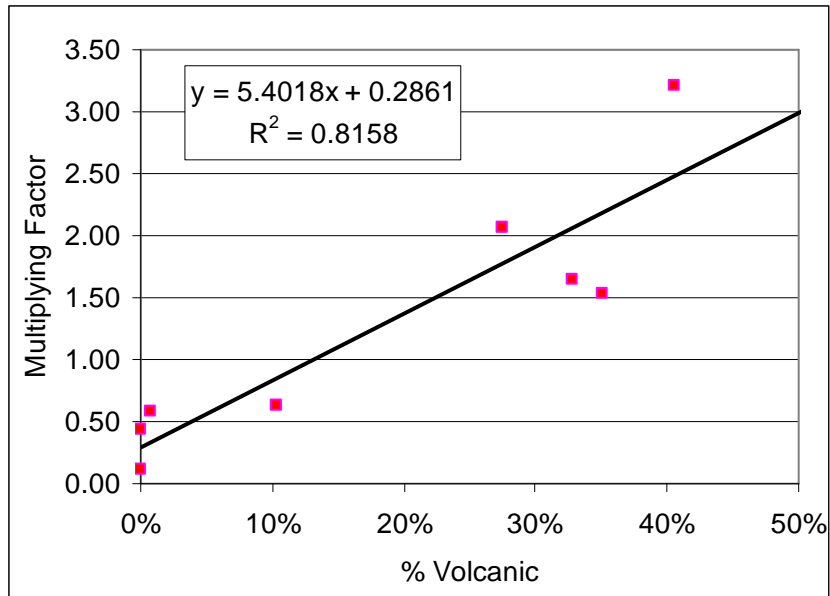


**Figure 4-10. EMC multiplying factor for pervious land uses relative to percent volcanic**

After the soil variability was taken into account, the model was run again, and a second observation was made. This observation was related to the differences in the fine-load estimates by quadrant of the watershed. The model’s estimate was low for the northern and western quadrants and high for the southern and eastern ones. This error was minimized by applying the following scaling factors to the EMCs for all land uses (Table 4-9). Similar Scaling factors were also derived for total nitrogen and total phosphorus following the quadrant method.

**Table 4-9. Multiple for TSS EMCs by quadrant**

QUAD ID	QUAD Name	Ratio
1	North	1.59
2	East	0.11
3	South	0.74
4	West	1.45

A summary of the results of the water quality calibration is shown in Tables 4-10, 4-11 and 4-12.

**Table 4-10. Results of water quality calibration for upland fine sediment**

Name	Overland Flow (m <sup>3</sup> /year)	Baseflow (m <sup>3</sup> /year)	Modeled: Upland Fines (tonnes/year)	Target: Upland Fines (tonnes/year)	Fines Ratio (target / modeled)
Third Creek	1,070,000	5,600,000	190	229	<b>1.21</b>
Incline Creek	1,270,000	6,380,000	357	318	<b>0.89</b>
Glenbrook Creek	587,000	3,220,000	25	17	<b>0.71</b>
Logan House Creek	258,000	1,210,000	4	7	<b>2.02</b>
Edgewood Creek	1,430,000	2,630,000	21	24	<b>1.16</b>
General Creek	3,390,000	11,700,000	60	62	<b>1.04</b>
Blackwood Creek	3,730,000	25,700,000	837	1,150	<b>1.38</b>
Ward Creek	4,980,000	18,900,000	1,430	1,110	<b>0.78</b>
Trout Creek	3,980,000	28,400,000	205	189	<b>0.92</b>
Upper Truckee River	22,900,000	78,800,000	1,010	1,030	<b>1.02</b>
<b>TOTAL</b>	<b>43,600,000</b>	<b>183,000,000</b>	<b>4,140</b>	<b>4,140</b>	<b>1.00</b>

**Table 4-11. Results of water quality calibration for total nitrogen**

Name	Overland Flow (m <sup>3</sup> /year)	Baseflow (m <sup>3</sup> /year)	Modeled: Total Nitrogen (kg/year)	Target: Total Nitrogen (kg/year)	Ratio TN (target / modeled)
Third Creek	1,070,000	5,600,000	2,820	3,930	<b>1.39</b>
Incline Creek	1,270,000	6,380,000	3,300	2,190	<b>0.66</b>
Glenbrook Creek	587,000	3,220,000	383	638	<b>1.67</b>
Logan House Creek	258,000	1,210,000	157	241	<b>1.53</b>
Edgewood Creek	1,430,000	2,630,000	1,370	1,030	<b>0.75</b>
General Creek	3,390,000	11,700,000	3,150	3,160	<b>1.01</b>
Blackwood Creek	3,730,000	25,700,000	8,400	9,170	<b>1.09</b>
Ward Creek	4,980,000	18,900,000	6,440	5,660	<b>0.88</b>
Trout Creek	3,980,000	28,400,000	6,540	5,390	<b>0.82</b>
Upper Truckee River	22,900,000	78,800,000	24,100	25,300	<b>1.05</b>
<b>TOTAL</b>	<b>43,600,000</b>	<b>183,000,000</b>	<b>56,700</b>	<b>56,700</b>	<b>1.00</b>

**Table 4-12. Results of water quality calibration for total phosphorus**

Name	Overland Flow (m <sup>3</sup> /year)	Baseflow (m <sup>3</sup> /year)	Modeled: Total Phosphorus (kg/year)	Target: Total Phosphorus (kg/year)	Ratio TP (target / modeled)
Third Creek	1,070,000	5,600,000	843	1,170	<b>1.38</b>
Incline Creek	1,270,000	6,380,000	877	553	<b>0.63</b>
Glenbrook Creek	587,000	3,220,000	143	137	<b>0.96</b>
Logan House Creek	258,000	1,210,000	26	21	<b>0.80</b>
Edgewood Creek	1,430,000	2,630,000	203	214	<b>1.05</b>
General Creek	3,390,000	11,700,000	517	398	<b>0.77</b>
Blackwood Creek	3,730,000	25,700,000	2,320	2,710	<b>1.17</b>
Ward Creek	4,980,000	18,900,000	2,030	1,760	<b>0.87</b>
Trout Creek	3,980,000	28,400,000	1,000	954	<b>0.95</b>
Upper Truckee River	22,900,000	78,800,000	4,110	4,160	<b>1.01</b>
<b>TOTAL</b>	<b>43,600,000</b>	<b>183,000,000</b>	<b>12,100</b>	<b>12,100</b>	<b>1.00</b>

Once the upland model was calibrated, a summary of average annual upland loads was obtained for each modeled stream. Simon provided an estimate of total fine sediment load vs. channel fine sediment load for each stream. From this information, the ratio of channel fines to total fines was applied to the modeled upland load as follows to obtain an estimate of total fine sediment loads for all streams:

$$\text{Total Fine Sediment Load} = \text{Upland Fines Load} / (1 - [\text{Channel Fines}/\text{Total Fines}])$$

From there, the channel fine sediment load becomes:

$$\text{Channel Fines Load} = \text{Total Fines Load} \times [\text{Channel Fines}/\text{Total Fines}]$$

Time series comparison revealed that the timing of streambank erosion was not linearly related to the timing of upland fines. Therefore, it was not representative to simply multiply the modeled upland fines load by the stream fines ratio. However, streambank erosion frequency appeared to vary closely with streamflow. Assuming a linear relationship between streambank erosion and stream flow, estimated channel loads were distributed according to modeled flows from the LSPC model to generate time series of channel fines sediments. This time series was superimposed over the original upland fines time series, resulting in a complete total fines time series representation.

After appropriate water quality parameters for the watershed model were selected, modeled results were compared against both the observed data points and the estimated pollutant loads. Figures 4-10 through 4-14 show LSPC model results versus observed data for TSS, TN, TP, DN, and DP.

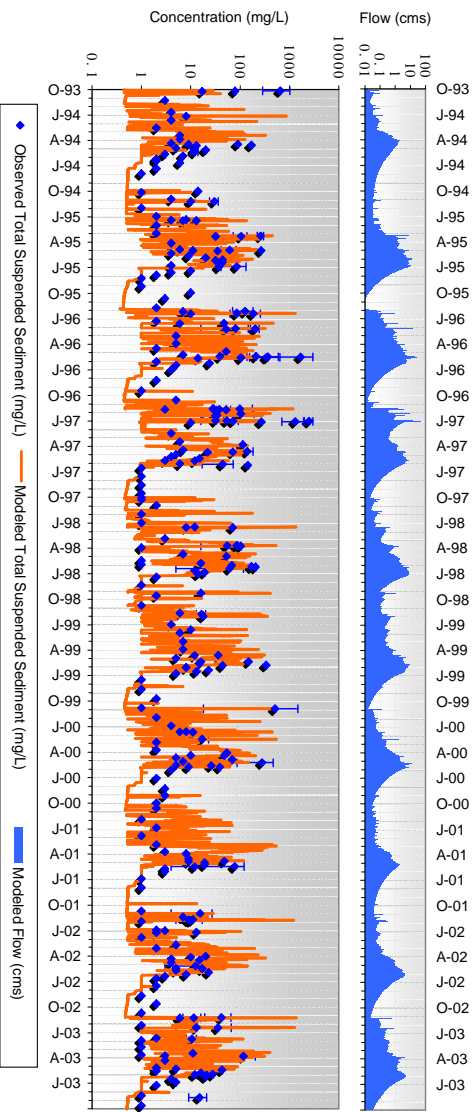


**Figure 4-10. LSPC model results vs. observed data for TSS at Ward Creek.**

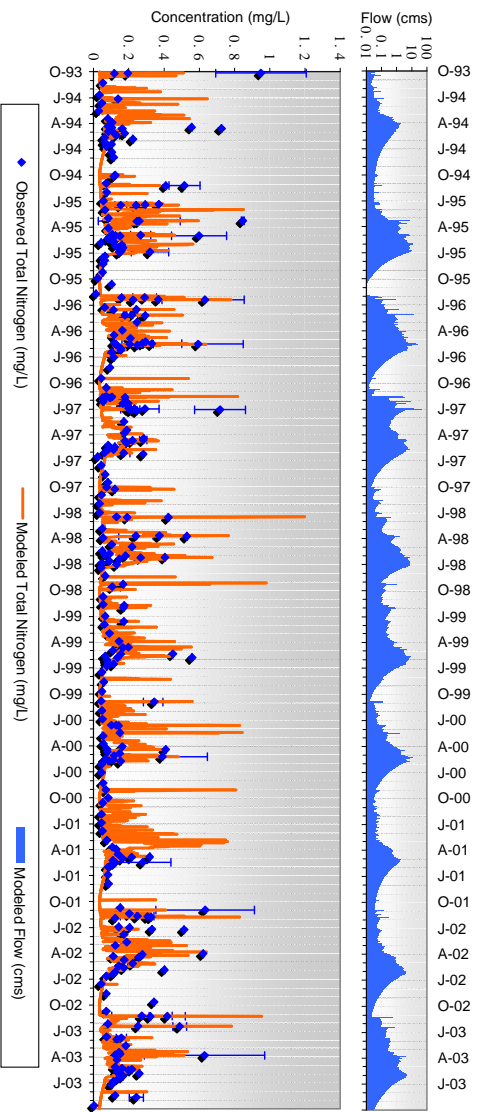


**Figure 4-11. LSPC model results vs. observed data for TN at Ward Creek.**

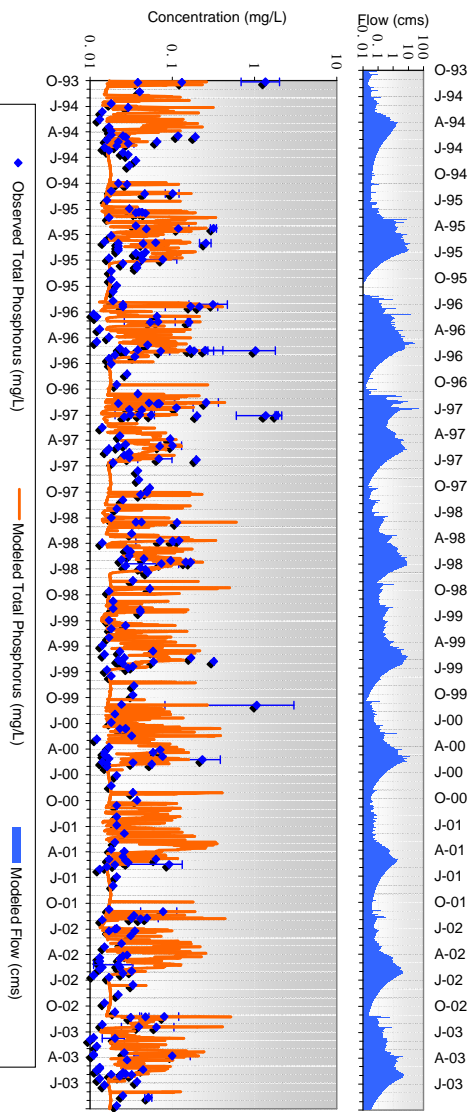


**Figure 4-12. LSPC model results vs. observed data for TP at Ward Creek.**

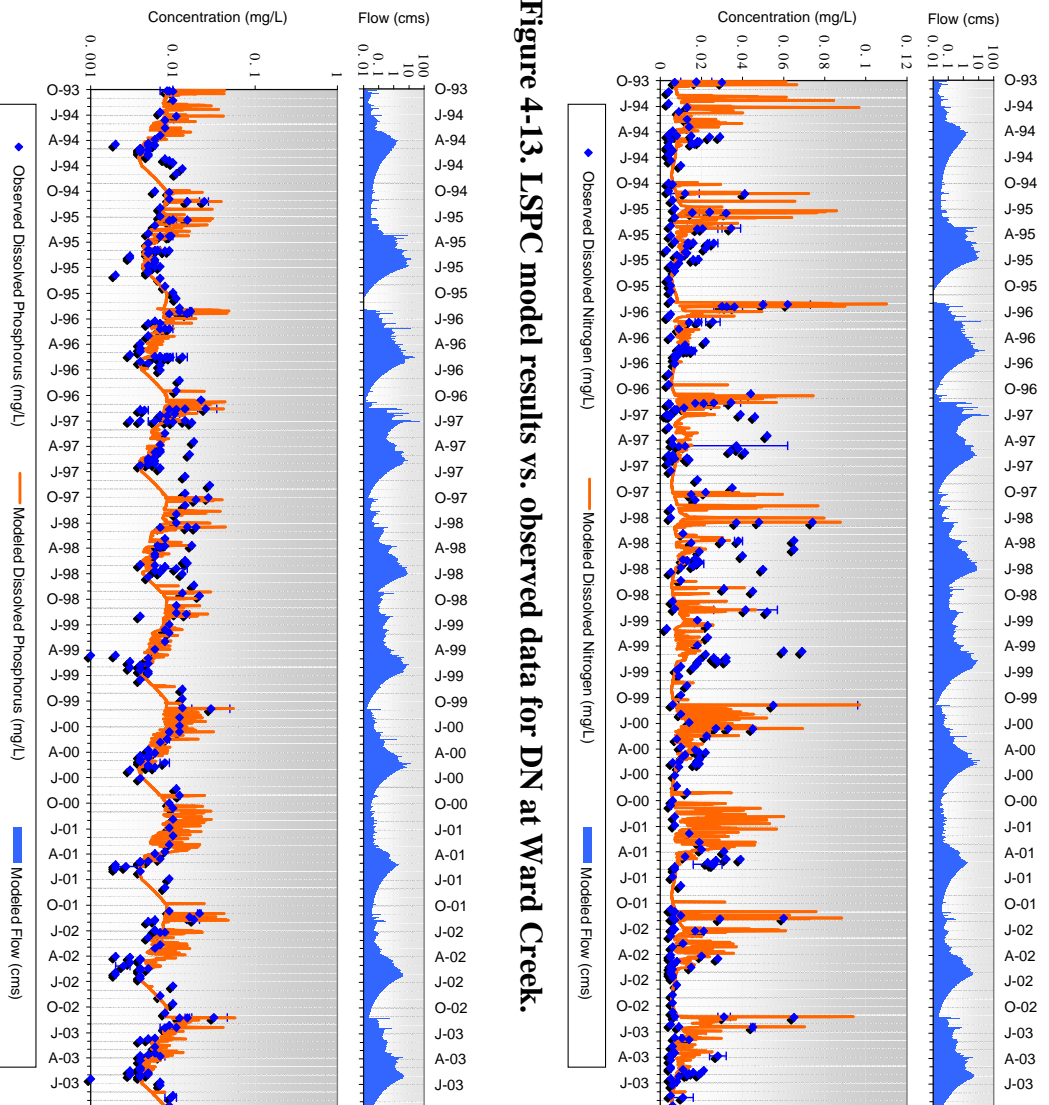


**Figure 4-13. LSPC model results vs. observed data for DN at Ward Creek.**

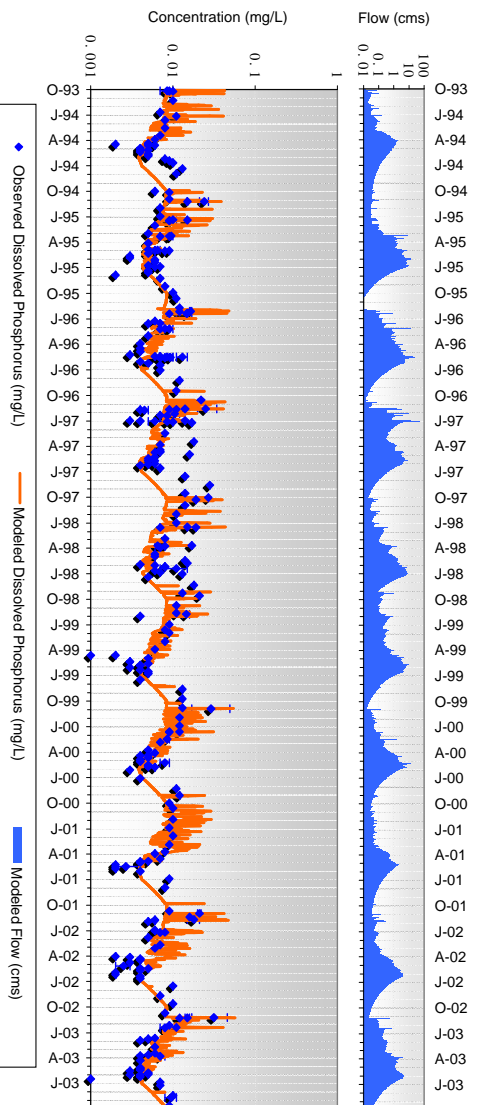


**Figure 4-14. LSPC model results vs. observed data for DP at Ward Creek.**

---

---



## 5. DISCUSSION OF MODEL RESULTS

---

Tables C-1 through C-8 and Figures C-1 through C-29 in Appendix C present a detailed summary of the Lake Tahoe Watershed Model results. Some general observations are described below regarding the influence of elevation, location, and landuse on the model predicted results for water yield, sediment, and nutrient loads. The last section of the results summary ranks the top ten contributors in terms of total load and unit-area yield for relative comparison and trend assessment.

### *Elevation*

Elevation has the biggest effect on predicted water yield. Higher elevations tend to receive higher amounts of snowfalls. In general, for subwatersheds in the same region, unit-area flow increases as elevation increases. Total flow volume, location, and landuse are factors that directly influence model-predicted loads.

### *Location*

The Lake Tahoe watershed has distinct orographic features that vary spatially. By categorizing the watershed into north, south, east, and west quadrants; one can see distinct spatially variable patterns. Unit area water yield varies by quadrant. The west quadrant is wettest while the east is the driest. The prevailing weather patterns in the basin are significantly influenced by the topographic relief. If one considers two subwatersheds with the same elevation on the west side and east side, the western subwatershed will typically experience over two times the volume of precipitation and water yield as its eastern counterpart. Total flow volume has a direct effect on the predicted model load.

### *Landuse*

Table 5-1 shows the percent of total contribution for Upland TSS, Upland Fines, Nitrogen and Phosphorus from each of the 20 landuse categories. Marked in bold are values for which a single landuse category contributes greater than 10% of the total load. A cursory review shows a fairly consistent correlation of flow yield with area. Table 5-1 also shows that the largest contributors are generally vegetated areas and roads. While roads represent a relatively small amount of area, they are impervious surfaces which they tend to serve as conduits of flow from surrounding areas. As modeled, concentrations from road surfaces are higher than those from other pervious and impervious areas. In general, while urban areas represent a relatively small percentage of the watershed area, they exhibit a disproportionately higher level of fine sediment and nutrient loads. Finally, it's noteworthy to mention that the "Water\_Body" landuse was

retained in the landuse list to complete the water balance. There are several smaller high elevation lakes that were not explicitly modeled. The associated water surface areas contribute flow from direct precipitation, but do not directly generate pollutant loads.

**Table 5-1. Landuse area distribution and percent contribution to the model predicted outputs**

Landuse	Area	Flow	Upland TSS	Upland Fines	Total Nitrogen	Total Phosphorus
Residential_SFP	4.0%	3.8%	1.7%	2.3%	5.4%	7.5%
Residential_MFP	1.0%	0.9%	1.3%	1.9%	1.5%	2.2%
CICU-Pervious	0.9%	0.7%	1.3%	1.9%	1.0%	1.5%
Ski_Runs-Pervious	0.5%	0.7%	4.1%	2.5%	0.6%	1.3%
Veg_EP1	5.7%	5.2%	0.1%	0.1%	2.3%	1.4%
Veg_EP2	<b>46.3%</b>	<b>41.1%</b>	4.0%	3.2%	<b>20.9%</b>	<b>13.4%</b>
Veg_EP3	<b>26.1%</b>	<b>27.0%</b>	<b>17.6%</b>	<b>13.5%</b>	<b>16.4%</b>	<b>12.4%</b>
Veg_EP4	8.9%	9.7%	<b>33.1%</b>	<b>25.9%</b>	6.4%	6.3%
Veg_EP5	0.2%	0.3%	4.0%	3.2%	0.2%	0.4%
Veg_Recreational	0.2%	0.2%	0.2%	0.2%	0.2%	0.3%
Veg_Burned	0.2%	0.2%	1.0%	0.8%	0.4%	0.8%
Veg_Harvest	0.2%	0.2%	0.8%	0.6%	0.2%	0.5%
Veg_Turf	0.5%	0.4%	0.0%	0.0%	0.9%	2.0%
Water_Body	1.7%	n/a	n/a	n/a	n/a	n/a
Residential_SFI	0.9%	1.3%	2.0%	2.7%	7.6%	8.4%
Residential_MFI	0.4%	0.5%	2.3%	3.5%	4.8%	4.0%
CICU-Impervious	0.5%	0.7%	5.0%	7.4%	5.2%	5.3%
Roads_Primary	0.3%	0.4%	<b>10.8%</b>	<b>16.2%</b>	5.4%	<b>12.2%</b>
Roads_Secondary	1.3%	2.1%	8.6%	<b>12.9%</b>	<b>20.2%</b>	<b>18.1%</b>
Roads_Unpaved	0.2%	0.2%	2.0%	1.4%	0.4%	2.0%

#### *TSS and Upland Fines Loads*

The largest overall Vegetated area sediment yields occurred in areas with the highest Erosion Potential. Urban areas, especially roads, also were high sediment producers. The largest sediment yields occur in the Blackwood Creek and Ward Creek regions, since they experience the highest levels of precipitation and unit-area water yield. As previously described, while urban areas represent a relatively small percentage of the watershed area, they exhibit a disproportionately higher level of fine sediment load. Examples of this are the developed areas surrounding Incline and Third Creeks, and the city of South Lake Tahoe. Figures C-13 and C-14 show unit-area total and fine sediment yield by subwatershed.

#### *Total Nitrogen & Total Phosphorus*

The trend for Nitrogen and Phosphorus appear to be most influenced by landuse and location. The wetter more urbanized subwatersheds and intervening zones on the west side are the largest contributors on a unit-area basis. The urbanized regions surrounding Incline and Third Creeks area, and the City of South Lake Tahoe also show high nutrient

---

---

yields. The lowest levels in the eastern quadrant, with even lower levels in less developed areas. Both TN and TP follow the same general trends. Figures C-15 and C-16 show unit-area TN and TP yields by subwatershed.

### *Ranking Analysis*

Included in the appendix are graphs of the top ten contributors for flow, sediment, and nutrients. In terms of total water volume or pollutant load, this correlated fairly well with the size of the watershed; however, looking at unit-area yield the member list often changes, sometimes dramatically. For example, while Upper Truckee is the largest sediment contributor in terms of total load, it drops out of the top ten subwatersheds when computed as sediment yield per drainage area. Another trend appears when looking at fine sediment versus total sediment. The four of the intervening zones make the top-ten list of fine sediment contributors, despite their relatively smaller size. These four have a higher concentration of urban landuses from where more fine sediment originate. Figures C17 through C29 show the top ten lists.

---

---



## **6. EXPLORATORY SCENARIO: POTENTIAL IMPACTS ASSOCIATED WITH CLIMATE CHANGE**

---

Understanding the potential effects of climate change on pollutant loading to Lake Tahoe is important to future management planning in the Basin. No regulations or pollutant loads were developed as a result of this analysis. This information is presented to inform land managers of the potential impact of climate change on the hydrology of the Basin and pollutant loading to Lake Tahoe. Although this information is presented for informational purposes it is critically important that additional analysis and climate monitoring be included as part of adaptive management changes in the future.

The calibrated watershed model provides a framework for evaluating the potential effects of climate change. As previously described, climate data, including precipitation, temperature, dew point, wind speed, and cloud cover serve as the raw data inputs. In addition, potential evapotranspiration (PEVT) and solar radiation are computed derivatives of these five weather datasets. The model used 8 discrete weather station datasets which were evenly distributed around the Basin; however, each of the 184 subwatersheds experiences a unique climate pattern because temperature data are corrected for elevation change using a lapse rate. Each subwatershed also has a unique land use distribution.

For process simulation, climate data drives the snowfall/snowmelt processes, land based hydrology, in-stream hydraulics and water quality. For this reason, changes in climate data will exhibit a direct response throughout all stages of the model. This section will focus on the effects of climate change on overall watershed hydrologic response.

### **Development of Climate Change Projections**

For this analysis, the USGS compiled a range of published results from 84 different climate and hydrology model simulations for different emissions scenarios and environmental sensitivities. The predicted climate changes are reflective of projected conditions for the year 2050. The USGS reviewed a substantial body of literature on climate change, paying specific attention to those papers published in peer-reviewed journals and/or reports to or from high-level government agencies with expertise in climatology. The goal was to identify a range of temperature and precipitation changes that are likely to occur in the northern and central parts of the Sierra Nevada mountain range in California and Nevada over the next 50 years. Changes in temperature and precipitation over these areas have the potential to affect snowpack depth and extent, the timing and volume of snowmelt runoff, and the balance of precipitation that falls as rain instead of snow. In a snow-dominated system like the Sierra, even small changes in the

---

---

amount, type, and timing of snowfall and/or snowmelt runoff could impact the hydrology of the Lake Tahoe Basin. This in turn has great potential to change the volume and timing of sediment and nutrient loading to Lake Tahoe. The central purpose of this effort to understand the climatologic and hydrologic changes at Tahoe is to develop scenario inputs for the TMDL watershed model.

Two important papers were identified in the literature review that integrated and synthesized the outputs of a wide variety of climate models and greenhouse gas emissions scenarios into ensembles of likely changes in temperature and precipitation. The first of these, a paper by Dettinger (2005) of the U.S. Geological Survey and Scripps Institute uses a resampling approach that converts the time series graphs of model-projected temperature and precipitation change into graphs representing the probability/projection distribution functions (PDFs) of these two types of climate change over time. This approach produces more than the usual confusing representation of overlapping lines typically generated by climate models that each trace out single-model-run results over time. Rather, this approach integrates all the results from three different scenarios run through 6 different coupled ocean-atmosphere global climate models. The resampling created over 20,000 data points spread over the entire 99-year time horizon and principal components analysis was used to understand the interactions between temperature and precipitation changes in the models. The PDFs produced with this method project a range of warming between +2°C and +7°C and precipitation changes between -30 to +25 centimeters per year (cm/yr), by 2099. The author also provides time slices from the PDFs which show that by 2050 – the time horizon of interest for this project – the temperature change PDF is centered at about +2.3°C and the precipitation PDF is centered between -5 to -10 cm/yr.

The second key paper (Cayan et al. 2006) is similar in approach, but does not produce PDFs of likely outcomes. It does, however, produce ensemble graphs of temperature and precipitation changes from projections made by 13 different model investigations of four families of emissions scenarios. The global model outputs were then downscaled to a grid of approximately 7 miles on a side. These ensemble analyses show results that do not differ dramatically from those in the Dettinger (2005) paper. Indeed, since they use somewhat different modeling, downscaling, and meta-analysis approaches, their close agreement provide greater confidence that such modeled changes are representative of what will occur if climate changes in the area.

This ensemble analysis concludes that California temperatures will increase by as little as 1.5°C in the lower emission scenario using the model with the lowest sensitivity to climate change through increased greenhouse gas emissions. The high end of increases is 4.5°C in the higher-emissions scenario and with a more sensitive model. These projections are run out to 2099, so halving them gives a reasonable estimate of 2-3°C by 2050. Most simulations show more warming in the summer than in winter, while the trend across the time horizon is approximately linear. While precipitation continues to occur primarily in the winter, the projections for changes in its absolute volume are widely varied, with little change expected when the average is calculated. The central estimate is a decrease of less than 5 cm/yr in total precipitation by mid-century. A

spreadsheet was compiled containing a set of combinations of temperature and precipitation changes that seem reasonable to use in creating inputs for the TMDL watershed model. One of these scenarios is to apply today's climate pattern with no projected change (Baseline Projection). The central estimate for temperature and precipitation changes from the Cayan et al. (2006) paper and the Dettinger (2005) paper were then used to create a Central Projection which includes a 2°C warming and a 10 percent decrease in total precipitation by mid-century. These scenarios then include temperature increases of one standard deviation on either side of that central estimate (1°C and 3°C increases above current temperatures) and precipitation changes one standard deviation above and below the central estimate (-25% and +15% of today's total precipitation, as well as a no change from today's precipitation). This method produced the matrix of projections presented Table 6-1. Table 6-2 describes each scenario in detail.

**Table 6-1. Matrix summary of climate change scenarios**

Precipitation Change	Temperature Change			
	0°C	+1°C	+2°C	+3°C
-25%	3	-	8	-
-10%	2	10	Central (1)	11
0%	Baseline (0)	5	6	7
+15%	4	-	9	-

**Table 6-2. Descriptions for climate change scenarios**

No.	Scenario Descriptions: <sup>a</sup>	Precipitation Change	Temperature Change
0	Baseline - - current climate conditions	+0%	+0°C
1	Central PROJ from 84 models	-10%	+2°C
2	Central PREC PROJ, no TEMP change	-10%	+0°C
3	1 SD below mean PREC PROJ, no TEMP change	-25%	+0°C
4	1 SD above mean PREC PROJ, no TEMP change	+15%	+0°C
5	No PREC change, 1 SD below mean TEMP PROJ	+0%	+1°C
6	No PREC change, central TEMP PROJ	+0%	+2°C
7	No PREC change, 1 SD above mean TEMP PROJ	+0%	+3°C
8	1 SD below mean PREC PROJ, central TEMP PROJ	-25%	+2°C
9	1 SD above mean PREC PROJ, central TEMP PROJ	+15%	+2°C
10	Central PREC PROJ, 1 SD below mean TEMP PROJ	-10%	+1°C
11	Central PREC PROJ, 1 SD above mean TEMP PROJ	-10%	+3°C

<sup>a</sup> PROJ = projection, PREC = precipitation, TEMP = temperature, SD = standard deviation

The climate data that were used in the model included detailed Snow Telemetry (SNOTEL) precipitation and temperature, while the other dataset requirements were compiled from the National Climatic Data Center (NCDC). The model evaluation period spanned a fifteen year time period from 1990 through 2004 that exhibited a natural

---

---

weather variations of wet and dry years. The climate data estimates are projected expectations for the year 2050. For this analysis, the climate data for each scenario was prepared by uniformly modifying the 15-year baseline condition according to the climate change projection matrix. For example, Scenario 1 Central Projection would have a applied a uniform 10percent reduction in precipitation volume and a uniform 2°C increase in temperature for the entire 15 year period. This approach not only preserves the natural year-to-year weather variation from the original data, but also, does not introduce any additional uncertainty associated with predicting the trajectory of how that 50-year climate change actually occurs. Also worth noting is that since precipitation changes are applied uniformly, they only change the magnitude and not the frequency of precipitation events.

For climate change simulation, 11 new sets of hourly weather files were generated using this uniform change approach. The matrix includes 3 precipitation changes and 3 temperature changes each applied to the 8 baseline SNOTEL timeseries. Also, since PEVT is a function of temperature, 3 new sets of timeseries were also generated at each of the eight SNOTEL locations. Since wind speed, dew point, and solar radiation are not as spatially sensitive as the other three timeseries, one averaged set was used for all conditions at all locations. All in all, between precipitation, temperature, and PEVT, 72 unique hourly timeseries over a 15 year evaluation period were generated in addition to the 19 original baseline timeseries. They were combined as specified by the matrix to create 11 projected weather conditions in addition to the baseline condition.

---

---

## Watershed Model Results - Hydrology

The model output can be represented at any intermediate temporal or spatial point during the course of the simulation. Considering the spatial and temporal extent of the dataset driving the simulation (184 subwatersheds, 20 landuses, 15 years of hourly simulation), the model yields approximately 500 million data points per output parameter. The nine output parameters selected for this analysis are presented in Table 6-3. These parameters reflect both direct and indirect effects of climate change at various stages throughout the simulated hydrologic cycle.

**Table 6-3. Selected model output parameters for climate change analysis**

Output Parameter	Description
PREC	Total precipitation volume
AIRTMP	Air temperature
SNOWF	Snowfall volume (a subset of precipitation)
WYIELD	Water yield from the snowpack (from melting or rain-on-snow)
PACK	Snowpack water equivalent depth
PERO	Total water outflow to streams (surface + baseflow)

While a high degree of spatial variation is both observed and modeled by the Lake Tahoe watershed model, it was theorized that the spatial variation relative to the baseline condition would hold fairly constant for all weather scenarios. To confirm this theory, annualized snowpack depth (PACK) and total water outflow from land (PERO) were computed for the 15 year simulation by subwatershed and normalized to the basin-wide average snowpack and water outflow for the baseline condition, respectively. Figure 6-1 illustrates spatial variation for the 11 scenarios relative to the baseline condition. Each point on the graph represents a subwatershed average divided by the basin-wide average for a given scenario. A value at (1,1) means that subwatershed's value equals the baseline basin-wide average, a point below indicates less than average, and points above indicate greater than average. A value at (2,1) on the left graph means that for that individual subwatershed, while the baseline snowpack was twice the basin-wide average, the climate change scenario predicted that subwatershed snowpack as equal to the baseline basin-wide average (a 50 percent reduction in snowpack relative to baseline). For scenarios where both precipitation and temperature are changed, there is greater variance in predicted snowpack, since elevation also influences snow prediction. When looking at total water outflow, the variance is masked by the presence of baseflow volumes. In general, subwatersheds with greater than average snowpack under baseline conditions will also have greater than average snowpack under climate change scenarios, even if the "slope" or magnitude changes. It is therefore reasonable to conclude that relative spatial variation is preserved for each scenario. For this reason, the focus of the following discussion will be basin-wide average values.

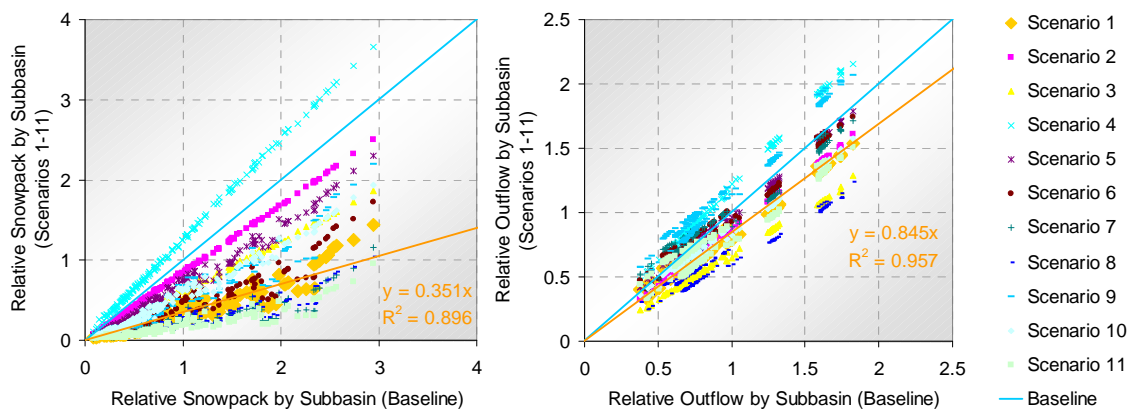


**Figure 6-1. Spatial variation of subwatershed snowpack and total flow for the 11 scenarios relative to the baseline condition.**

Comparing two transects of the climate change matrix (Table 6-1) shows model sensitivity in terms of (a) precipitation change alone with no temperature change (baseline vs. Scenarios 2, 3, and 4), and (b) temperature change alone with no precipitation change (baseline vs. Scenarios 5, 6, and 7). The “a” transect results proportionally altered the overall precipitation volume and subsequent processes. They are clearly distinguished as the pink, yellow and turquoise series in Figure 6-1, which show uniform spatial magnitude change. The “b” transect results preserved overall precipitation volume; however, the temperature changes resulted in a shift in the rainfall vs. snowfall distribution, a change in net water outflow, and noticeable shifts in the timing of snowfall and snowmelt sequences. Figure 6-2 illustrates the average snow/rainfall distributions as well as average subwatershed outflow for the “b” transect scenarios. Figure 6-3 shows the same data summaries plotted as a function of temperature change.

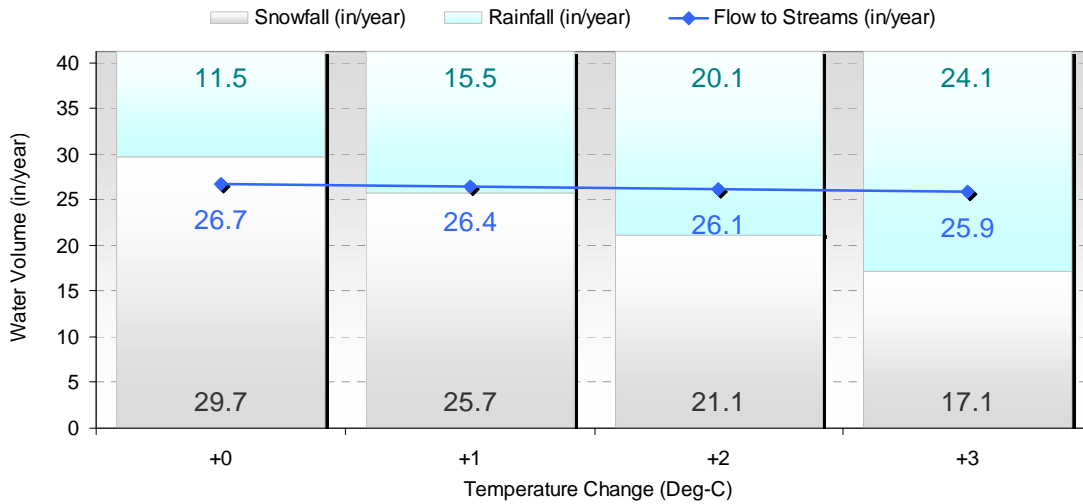


**Figure 6-2. Precipitation volume distribution and net water yield vs. temperature change for Scenarios 5, 6 and 7 relative to baseline.**

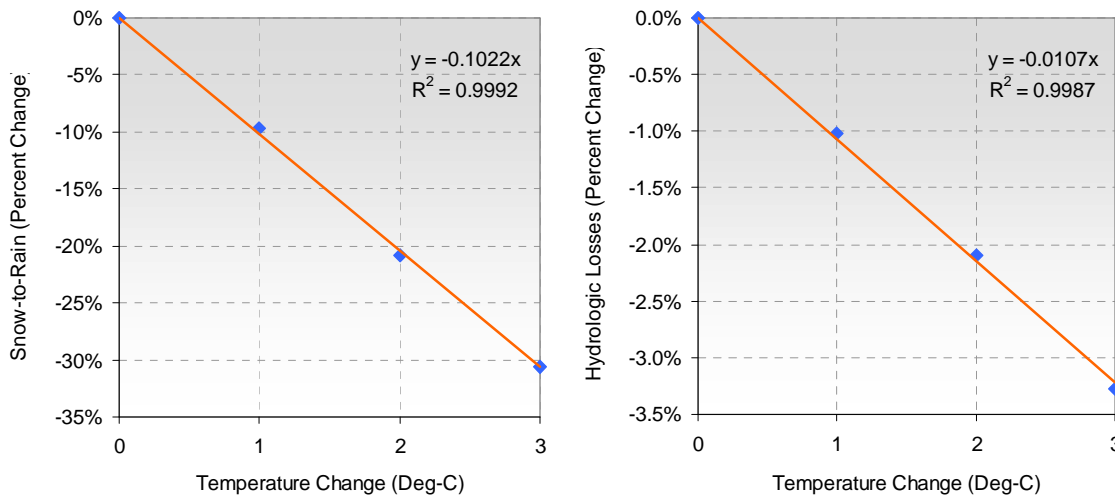


**Figure 6-3. Percent change in precipitation distribution and net water yield vs. temperature change for Scenarios 5, 6 and 7 relative to baseline.**

Figure 6-3 indicates a linear trend over the 3-degree sample space considered in this analysis. In general, a 1 degree C increase in temperature results in a 10 percent shift of water from snowfall to rainfall, and a 1 percent increase in hydrologic evaporative losses.

An indicator of interest is the effects of climate change on the shape, maximum depth and timing of the snowpack for all 11 scenarios relative to baseline. For each subwatershed,

PACK was area-weighted and aggregated on a daily basis to form an annualized daily snowpack profile. For example, PACK for first day of each year (1990 through 2004), are multiplied by watershed area, added together (15 values times 184 subwatersheds) and divided by total watershed area to get a representative January 1 value for the annualized profile. This process was repeated for every day in the simulation for each of the 11 scenarios as well as baseline. Table 6-4 is a summary of annualized snowpack characteristics for all scenarios relative to baseline. Figure 6-4 plots the annualized daily snowpack profiles for the 15 year simulation period. An interesting observation is that the January 1, 1997 extreme storm event is noticeable even after averaging over 15 years.

**Table 6-4. Summary of snowpack characteristics for all scenarios relative to baseline**

Scenario	Date			Relative to Baseline (Days)				Peak Percent Change
	Snowpack >0.5 in	Snowpack Peak	Snowpack <0.5 in	Pack Start	Peak Shift	Pack End	Duration	
Baseline	Oct 20	Mar 6	Jul 2	0	0	0	256	0%
Central (1)	Nov 10	Feb 27	May 11	+21	-8	-52	183	-61%
2	Oct 25	Mar 6	Jun 25	+5	0	-7	244	-14%
3	Oct 26	Mar 6	Jun 10	+6	0	-22	228	-35%
4	Oct 18	Mar 6	Jul 18	-2	0	+16	274	+22%
5	Oct 25	Mar 6	Jun 15	+5	0	-17	234	-29%
6	Oct 29	Feb 27	May 20	+9	-8	-43	204	-54%
7	Nov 17	Feb 24	Apr 27	+28	-11	-66	162	-72%
8	Nov 17	Feb 24	Apr 28	+28	-11	-65	163	-72%
9	Oct 26	Feb 27	Jun 1	+6	-8	-31	219	-42%
10	Nov 9	Feb 25	Jun 1	+20	-10	-31	205	-40%
11	Nov 25	Feb 24	Apr 22	+36	-11	-71	149	-77%

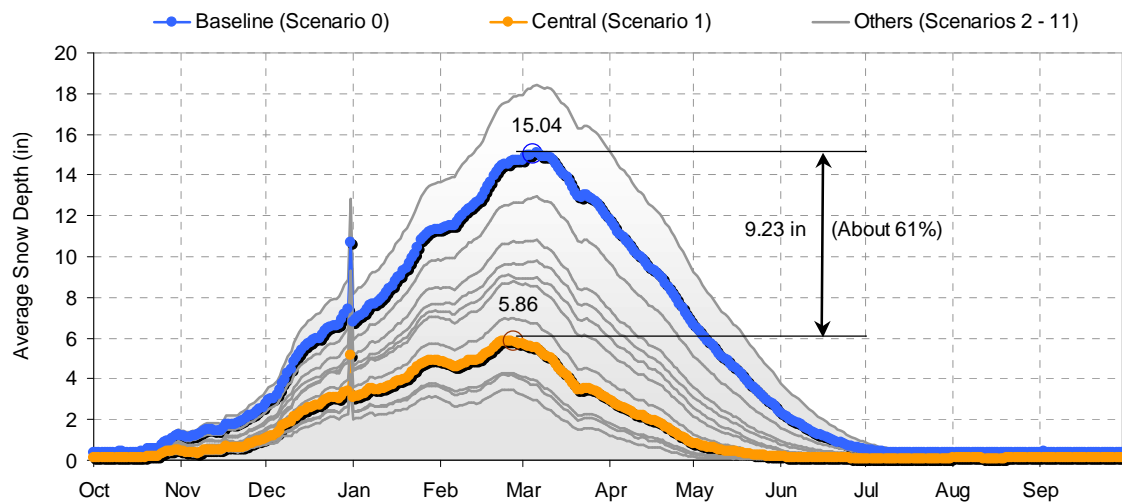


**Figure 6-4. Annualized snowpack profiles for all scenarios relative to baseline.**

---

---



## 7. REFERENCES

---

- Anderson, M., M.L. Kavvas, Z.Q. Chen, and J. Yoon. 2004. Lake Tahoe Basin Synthetic Atmospheric/Meteorologic Database. Hydrologic Research Laboratory, Department of Civil and Environmental Engineering, University of California, Davis. 30 pp.
- Bicknell, B.R., J.C. Imhoff, J.L. Kittle, Jr., A.S. Donigian, Jr., and R.C. Johanson. 1997. *Hydrological Simulation Program–FORTRAN, User's manual for version 11*. EPA/600/R-97/080. Athens, GA: U.S. Environmental Protection Agency.
- Bradu, D., and Y. Mundlak. 1970. Estimation in lognormal linear models. *J. Am. Stat. Assoc.* 65(329): 198–211.
- Cayan, D.R., E.P. Maurer, M.D. Dettinger, M. Tyree and K. Hayhoe. 2006. Climate Change Scenarios for the California Region. Submitted to: *Climatic Change*, 41 pages, July 2006.
- Coats, R.N., and C.R. Goldman. 2001. Patterns of nitrogen transport in streams of the Lake Tahoe Basin, California-Nevada. *Water Resources Research* 37(2): 405–416.
- Cohn, T.A., L.L. DeLong, E.J. Gilroy, R.M. Hirsch, and D.K. Wells. 1989. Estimating constituent loads. *Water Resources Research* 25(5): 937–942.
- Cohn, T.A., and E.J. Gilroy. 1991. Estimating Loads from Periodic Records. U.S. Geological Survey, Branch of Systems Analysis, Technical Memo 91.01.
- Cohn, T.A. 1995. Recent advances in statistical methods for the estimation of sediment and nutrient transport in rivers. *Reviews in Geophysics Supplement*, Vol. 33. <<http://www.agu.org/revgeophys/cohn01/cohn01.html>>.
- Crawford, H.H., and R.K. Linsley. 1966. Digital Simulation in Hydrology: Stanford Watershed Model IV. Stanford University, Department of Civil Engineering. Tech. Rep. 39.
- Dettinger, M.D. 2005. From climate-change spaghetti to climate-change distributions for 21st Century California. *San Francisco Estuary and Watershed Science*, 3(1).
- Finney, D.J. (1941). On the distribution of a variate whose logarithm is normally distributed. *J. R. Stat. Soc. Suppl.* 7: 155–161.

- 
- 
- Green, W.R., and B.E. Haggard. 2001. *Phosphorus and Nitrogen Concentrations and Loads at Illinois River South of Siloam Springs, Arkansas, 1997–1999*. Water-Resources Investigations Report 01-4217. Reston, VA : U.S. Geological Survey.
- Gunter, M.K. 2005. Characterization of Nutrient and Suspended Sediment Concentrations in Stormwater Runoff in the Lake Tahoe Basin. Master of Science in Hydrology thesis, University of Nevada, Reno.
- Hamon, W.R. 1961. Estimating potential evaporation. *Journal of Hydraulics Division, Proceedings of the American Society of Civil Engineers* 871: 107–120.
- Heyvaert, A. 1998. *The Biogeochemistry and Paleolimnology of Sediments from Lake Tahoe, California-Nevada*. Ph.D. thesis, University of California, Davis. 194 pp.
- Heyvaert, A., J. Reuter, G. Schladow. 2007. *Particle Size Distribution in Stormwater Runoff Samples at Tahoe*. Report to the Lahontan Regional Water Quality Control Board, Desert Research Institute, and UCD Tahoe Environmental Research Center.
- Jassby, A.D., C.R. Goldman and J.E. Reuter. 1995. Long-term Change in Lake Tahoe (California-Nevada, U.S.A.) and its Relation to Atmospheric Deposition of Algal Nutrients. *Arch. Hydrobiol.* 135(1): 1–21.
- Jensen, M.E., and H.R. Haise. 1963. Estimating evapotranspiration from solar radiation. *J. Irrig. Drainage Div. American Society of Civil Engineers* 89: 15–41.
- Lumb, A.M., R.B. McCammon, and J.L. Kittle, Jr. 1994. *User's Manual for an Expert System (HSPEXP) for Calibration of the Hydrological Simulation Program–FORTRAN*. Water-Resources Investigations Report 94-4168. Reston, VA: U.S. Geological Survey.
- MDNR and USGS (Maryland Department of Natural Resources and U.S. Geological Survey MD-DE-DC District). 2001. Chesapeake Bay Water-Quality Monitoring Program: River Input Nutrient Loading Trends Component. Quality Assurance Project Plan; July 1, 2001, to June 30, 2002.
- Minor, T., and M. Cablk. 2004. *Estimation of Hard Impervious Cover in the Lake Tahoe Basin Using Remote Sensing and Geographic Information Systems*. Reno, NV: Desert Research Institute.
- Penman, H.L. 1948. Natural Evaporation from Open Water, Bare Soil, and Grass. *Proceedings of the Royal Society of London, A*; 193: 120–145.
- Perez-Losada, J., 2001. A Deterministic Model for Lake Clarity. Application to Lake Tahoe (California, Nevada), USA. Ph.D. Dissertation, University of Girona, Spain. 239 pp.

- 
- 
- Pitt, R., A. Maestre, and R. Morquecho. 2004. *The National Stormwater Quality Database (NSQD, version 1.1)*. Dept. of Civil and Env. Eng., University of Alabama.
- Reuter, J.E., and D. Roberts. 2004. *An Integrated Science Plan for the Lake Tahoe TMDL*. Tahoe Environmental Research Center, University of California, Davis.
- Schladow, S.G., J. Perez-Losada, W.E. Fleenor, and P.E. Heald. 2004. Reference Manual for the Lake Model DLM –WQ and DLM-VOC. Department of Civil and Environmental Engineering. University of California, Davis.
- Schwab, G.O., D.D. Fangmeier, W.J. Elliot, and R.K. Frevert. 1993. *Soil and Water Conservation Engineering*. New York: John Wiley & Sons, Inc.
- Simon, A., E.J. Langendoen, R.L. Bingner, R. Wells, A. Heins, N. Jokay, and I. Jaramillo. 2003. *Lake Tahoe Basin Framework Implementation Study: Sediment Loadings and Channel Erosion*. Research Report No. 39. USDA-ARS National Sedimentation Laboratory. 377 pp.
- Sloto, R.A., and M.Y. Crouse. 1996. *HYSEP: A Computer Program for Streamflow Hydrograph Separation and Analysis*. Water-Resources Investigations Report 96-4040. Reston, VA: U.S. Geological Survey.
- Swift, T. J., 2004. *The Aquatic Optics of Lake Tahoe, CA-NV*. Ph.D. dissertation, University of California, Davis. 212 pp.
- Swift, T.J., J. Perez-Losada, S.G. Schladow, J.E. Reuter, A.D. Jassby, and C.R. Goldman (2006). Water clarity modeling in Lake Tahoe: Linking suspended matter characteristics to Secchi depth. *Aquatic Sciences*. Vol. 68, No. 1.
- USGS (U.S. Geological Survey). 2005. *Suspended Sediment Database: Daily Values of Suspended Sediment and Ancillary Data*. <<http://co.water.usgs.gov/sediment/bias.frame.html>>.
- Wischmeier, W.H., and D.D. Smith. 1978. *Predicting Rainfall Erosion Losses—A Guide to Conservation Planning*. Agricultural Handbook No. 537. Washington, D.C.: U.S. Department of Agriculture.

---

---

## **APPENDIX A: MODEL CALIBRATION RESULTS**

---

PLACEHOLDER for remaining calibration graphs and tables at the USGS/LTIMP gages. Ward Creek results are presented with detailed discussion in Section 4.

## APPENDIX B: LAKE TAHOE WATERSHED MODEL LAND USE RUNOFF PARAMETERIZATION

This section presents the runoff concentrations of the pollutants of concern that were used to parameterize the modeled land uses of the Lake Tahoe watershed model.

Water quality parameters are specified at the land use level for each subwatershed, and representative runoff concentrations are required to associate the components of the estimated bulk load with each land use unit. Recent research completed on nutrient and suspended sediment concentrations of runoff and streams in the Lake Tahoe Basin was used to estimate watershed-specific loading ratios for a number of land uses. The runoff concentrations used in the initial model run have been updated with more representative information. The new values are presented in Table B-1.

**Table B-1. Values recommended for use in the Lake Tahoe Watershed Model to represent concentrations from surface runoff from specific land use/land cover<sup>a</sup>**

Modeled Land Use	Total Suspended Solids	Total Nitrogen	Dissolved Nitrogen	Total Phosphorus	Dissolved Phosphorus
Residential SFP <sup>b,c</sup>	47	1.46	0.12	0.39	0.12
Residential MFP <sup>b,c</sup>	125	2.37	0.35	0.49	0.12
CICU Pervious <sup>d</sup>	247	2.06	0.24	0.59	0.07
Ski Runs Pervious					
- Heavenly	39	0.30	0.11	0.10	0.03
- Homewood	47	0.41	0.01	0.14	0.04
- Diamond Peak	5238	2.17	1.97	1.47	0.05
Vegetated Unimpacted	0.7	0.14	0.01	0.03	0.02
Vegetated Recreational	383	0.86	0.01	0.52	0.17
Vegetated Burned <sup>e</sup>					
- Wildfire <sup>e</sup>	<i>Equivalent Roded Area (ERA) Methodology<sup>e</sup></i>				
- Prescribed Burns <sup>e</sup>					
Vegetated Harvest <sup>e</sup>					
Vegetated Turf	10	4.06	0.41	1.25	0.22
Residential SFI <sup>b,c</sup>	47	1.46	0.12	0.39	0.12
Residential MFI <sup>b,c</sup>	125	2.37	0.35	0.49	0.12
CICU Impervious <sup>d</sup>	247	2.06	0.25	0.59	0.07
Roads Primary	793	3.27	0.60	1.65	0.08
Roads Secondary	793	3.27	0.60	1.65	0.08
Roads Unpaved	846	1.95	0.01	1.27	0.40

<sup>a</sup>Values are as milligrams N or P per liter.

<sup>b</sup>I = impervious, P = pervious.

<sup>c</sup>SF = single-family, MF = multiple-family.

<sup>d</sup>CICU = commercial/institutional/communications/utilities.

---

---

<sup>e</sup>Concentrations equal to unpaved roads, but areas will be adjusted based on ERA values.

The following information describes how the concentrations in Table B-1 were obtained:

- *Residential Single-Family, Residential Multi-Family, and CICU, Pervious and Impervious.* Concentrations were taken from EMC analysis of runoff data from the Tahoe Research Group Stormwater Monitoring Dataset (by Heyvaert, Thomas and Gunther). No distinction can be made at this time between runoff concentrations of pervious and impervious fractions
- *Ski Runs Pervious.* This land use includes lands in otherwise vegetated areas for which trees have been cleared to create a run. The three ski areas in the watershed—Heavenly, Homewood, and Diamond Peak—have very different runoff characteristics, and consequently they are modeled separately. The concentrations are based on stream data at each ski area, background values, and the area of the ski runs.
- *Vegetated Unimpacted.* These are forested areas that have been minimally impacted in the recent past. Concentrations are based on stormwater monitoring by A. Heyvaert.
- *Vegetated Recreational.* This land use includes lands that are primarily vegetated and are characterized by relatively low-intensity uses and small amounts of impervious coverage. These include the unpaved portions of campgrounds, visitor centers, and day use areas. Final values were calculated assuming the area is represented by 40 percent roads and 60 percent forest.
- *Vegetated Turf.* These are large turf areas with little impervious coverage, such as golf courses, large playing fields, and cemeteries, with potentially similar land management activities. Concentrations are based on application ratios and land turf areas for golf course versus residential. According to the U.S. Army Corps of Engineers Lake Tahoe Groundwater report, the ratio of fertilizer application for N and P for Residential:Golf Courses was approximately 2.5 assuming the Home Landscaping Guide instructions are followed. With the assumption that most N/P runoff from residential land comes from fertilizer applied to lawns and the estimate of total residential areas to lawns is 1.25:1.0, these values represent  $1.25 \times 2.5 = 3.125$  times the mean of Single-Family Residential. Estimates do not account for infiltration of N/P. The recommended TSS concentration is based on best professional judgment.
- *Roads Primary.* Concentrations obtained from data in Caltrans 2003 summary report (CTSW-RT-03-054.36.02), and a report from NDOT and DRI looking at highway stormwater runoff and BMP effectiveness on portions of SR 28 and US 50 in Nevada (Publication No. 41209).

- 
- 
- *Roads Secondary*. No direct data were available for secondary roads. Concentrations were assumed to be the same as primary roads.
  - *Roads Unpaved*. Concentrations were based on data from McKinney Rubicon Rd Forest Service data. Values shown are the median of 20 samples at the road. Independent calculation based on the Sierra Nevada Eco-system Project sediment loadings by road slope, returned 955 mg/L for TSS.
  - *Vegetated Burned*. These are areas that have been subject to controlled burns and/or wildfires in the recent past. The concentrations used are the same as unpaved roads, but the impact areas are adjusted based on the Equivalent Road Area obtained from the Forest Service for each event. To account for the diminishing impact of the event through time, a recession curve is used during the calibration years.
  - *Vegetated Harvest*. These are lands that management agencies have thinned in the recent past for the purpose of forest health and defensible space (areas cleared to reduce the spread of wildfire). The concentrations used are the same as unpaved roads, but the impact areas are adjusted based on the Equivalent Road Area obtained from the Forest Service for each event. To account for the diminishing impact of the event through time, a recession curve is used during the calibration years.

## APPENDIX C: WATERSHED MODEL RESULTS

Table C-1. Summary of annual surface, base and total flow volumes by watershed

Quad	Tributary	OUTLET SWS	Surface Flow (1000 m <sup>3</sup> )	Baseflow (1000 m <sup>3</sup> )	Total Flow (1000 m <sup>3</sup> )
1	IVZ1000	1000	1,130	1,660	2,800
1	MILL CREEK	1010	369	1,920	2,290
1	INCLINE CREEK	1020	1,270	6,380	7,640
1	THIRD CREEK	1030	1,070	5,600	6,670
1	WOOD CREEK	1040	387	1,810	2,200
1	BURNT CEDAR CREEK	1050	193	223	416
1	SECOND CREEK	1060	196	1,290	1,490
1	FIRST CREEK	1070	184	1,680	1,870
1	IVZ2000	2000	755	3,630	4,390
2	SLAUGHTER HOUSE	2010	935	3,730	4,670
1	BLISS CREEK	2020	82	427	509
1	SECRET HARBOR CREEK	2030	417	2,680	3,100
1	MARLETTE CREEK	2040	1,540	3,310	4,850
1	BONPLAND	2050	110	673	783
1	TUNNEL CREEK	2060	109	1,220	1,330
2	IVZ3000	3000	1,420	3,450	4,870
2	MCFAUL CREEK	3010	511	2,120	2,630
2	ZEPHYR CREEK	3020	222	955	1,180
2	NORTH ZEPHYR CREEK	3030	316	1,510	1,830
2	LINCOLN CREEK	3040	289	1,430	1,720
2	CAVE ROCK	3050	99	416	515
2	LOGAN HOUSE CREEK	3060	258	1,210	1,460
2	NORTH LOGAN HOUSE CREEK	3070	134	840	974
2	GLENBROOK CREEK	3080	587	3,220	3,810
3	IVZ4000	4000	1,990	2,210	4,210
3	BIJOU CREEK	4010	766	1,450	2,220
2	EDGEWOOD CREEK	4020	1,430	2,630	4,060
2	BURKE CREEK	4030	420	1,790	2,210
3	IVZ5000	5000	2,200	2,620	4,810
3	UPPER TRUCKEE RIVER	5010	22,900	78,800	102,000
3	TROUT CREEK	5050	3,980	28,400	32,400
4	IVZ6000	6000	768	3,990	4,750
4	IVZ6001	6001	805	1,420	2,230
4	GENERAL CREEK	6010	3,390	11,700	15,100

Quad	Tributary	OUTLET SWS	Surface Flow (1000 m <sup>3</sup> )	Baseflow (1000 m <sup>3</sup> )	Total Flow (1000 m <sup>3</sup> )
4	MEEKS	6020	4,130	12,500	16,700
4	SIERRA CREEK	6030	439	1,330	1,770
4	LONELY GULCH CREEK	6040	573	1,640	2,210
4	PARADISE FLAT	6050	295	955	1,250
4	RUBICON CREEK	6060	1,380	4,370	5,750
4	EAGLE CREEK	6080	2,350	10,100	12,500
3	CASCADE CREEK	6090	2,370	6,530	8,900
3	TALLAC CREEK	6100	630	3,350	3,980
3	TAYLOR CREEK	6110	17,800	27,700	45,500
4	UNNAMED CK	6120	146	397	542
4	IVZ7000	7000	1,610	2,860	4,470
4	BLACKWOOD CREEK	7010	3,730	25,700	29,400
4	MADDEN CREEK	7020	1,090	3,210	4,290
4	HOMEWOOD CREEK	7030	562	1,570	2,130
4	QUAIL LAKE CREEK	7040	773	2,230	3,000
4	MKINNEY CREEK	7050	2,620	7,100	9,720
4	IVZ8000	8000	1,560	2,960	4,510
1	DOLLAR CREEK	8010	92	958	1,050
1	UNNAMED CK LAKE FOREST 1	8020	215	562	777
1	UNNAMED CK LAKE FOREST 2	8030	113	878	991
1	BURTON CREEK	8040	258	4,570	4,830
1	TAHOE STATE PARK	8050	84	911	995
4	WARD CREEK	8060	4,980	18,900	23,900
1	IVZ9000	9000	1,470	4,790	6,260
1	KINGS BEACH	9010	95	362	457
1	GRIFF CREEK	9020	272	3,740	4,010
1	TAHOE VISTA	9030	560	3,970	4,520
1	CARNELIAN CANYON	9040	225	2,630	2,860
1	CARNELIAN BAY CREEK	9050	49	771	820
1	WATSON	9060	127	1,940	2,070

**Table C-2. Summary of annual upland TSS, upland fines, channel fines and total fines loads by watershed**

Quad	Tributary	OUTLET SWS	Upland TSS Load (tonnes)	Upland Fines Load (tonnes)	Channel Fines (tonnes)	Total Fines (tonnes)
1	IVZ1000	1000	435	336	0	336
1	MILL CREEK	1010	114	94	0	94
1	INCLINE CREEK	1020	546	420	16	436
1	THIRD CREEK	1030	292	211	23	234
1	WOOD CREEK	1040	98	70	0	71
1	BURNT CEDAR CREEK	1050	80	60	4	64
1	SECOND CREEK	1060	51	26	0	26
1	FIRST CREEK	1070	79	29	0	30
1	IVZ2000	2000	114	97	0	97
2	SLAUGHTER HOUSE	2010	11	9	1	10
1	BLISS CREEK	2020	10	8	0	9
1	SECRET HARBOR CREEK	2030	28	23	0	23
1	MARLETTE CREEK	2040	28	23	2	25
1	BONPLAND	2050	3	2	0	2
1	TUNNEL CREEK	2060	4	3	0	3
2	IVZ3000	3000	28	23	0	23
2	MCFAUL CREEK	3010	2	1	0	2
2	ZEPHYR CREEK	3020	1	1	0	1
2	NORTH ZEPHYR CREEK	3030	1	1	0	1
2	LINCOLN CREEK	3040	3	2	0	2
2	CAVE ROCK	3050	1	0	0	0
2	LOGAN HOUSE CREEK	3060	5	4	0	4
2	NORTH LOGAN HOUSE CREEK	3070	2	1	0	1
2	GLENBROOK CREEK	3080	32	26	22	47
3	IVZ4000	4000	292	248	0	248
3	BIJOU CREEK	4010	85	71	0	71
2	EDGEWOOD CREEK	4020	26	22	5	27
2	BURKE CREEK	4030	7	6	0	6
3	IVZ5000	5000	150	122	0	122
3	UPPER TRUCKEE RIVER	5010	2,219	1,309	2,259	3,569
3	TROUT CREEK	5050	257	205	3	208
4	IVZ6000	6000	122	96	0	96
4	IVZ6001	6001	129	103	0	103

Quad	Tributary	OUTLET SWS	Upland TSS Load (tonnes)	Upland Fines Load (tonnes)	Channel Fines (tonnes)	Total Fines (tonnes)
4	GENERAL CREEK	6010	160	59	48	107
4	MEEKS	6020	137	54	12	66
4	SIERRA CREEK	6030	35	23	0	23
4	LONELY GULCH CREEK	6040	36	25	0	25
4	PARADISE FLAT	6050	11	7	0	7
4	RUBICON CREEK	6060	90	59	3	62
4	EAGLE CREEK	6080	40	22	0	22
3	CASCADE CREEK	6090	20	13	0	13
3	TALLAC CREEK	6100	52	31	0	32
3	TAYLOR CREEK	6110	272	137	3	139
4	UNNAMED CK	6120	16	11	0	11
4	IVZ7000	7000	469	304	0	304
4	BLACKWOOD CREEK	7010	1,816	839	873	1,712
4	MADDEN CREEK	7020	918	268	0	269
4	HOMEWOOD CREEK	7030	908	272	0	272
4	QUAIL LAKE CREEK	7040	405	123	0	123
4	MKINNEY CREEK	7050	192	88	0	88
4	IVZ8000	8000	524	405	0	405
1	DOLLAR CREEK	8010	113	51	1	51
1	UNNAMED CK LAKE FOREST 1	8020	92	65	0	65
1	UNNAMED CK LAKE FOREST 2	8030	92	47	0	47
1	BURTON CREEK	8040	366	117	1	118
1	TAHOE STATE PARK	8050	57	32	0	32
4	WARD CREEK	8060	2,994	1,439	485	1,924
1	IVZ9000	9000	679	468	0	468
1	KINGS BEACH	9010	57	29	0	29
1	GRIFF CREEK	9020	300	114	5	119
1	TAHOE VISTA	9030	489	223	2	225
1	CARNELIAN CANYON	9040	168	70	0	70
1	CARNELIAN BAY CREEK	9050	39	14	0	14
1	WATSON	9060	119	39	0	39

**Table C-3. Summary of annual surface, base and total nitrogen loads by watershed**

Quad	Tributary	OUTLET SWS	Surface TN Load (kg)	Baseflow TN Load (kg)	Total TN Load (kg)
1	IVZ1000	1000	2,631	280	2,911
1	MILL CREEK	1010	593	341	934
1	INCLINE CREEK	1020	2,173	1,127	3,300
1	THIRD CREEK	1030	1,846	978	2,824
1	WOOD CREEK	1040	651	311	962
1	BURNT CEDAR CREEK	1050	465	38	502
1	SECOND CREEK	1060	230	220	450
1	FIRST CREEK	1070	118	285	403
1	IVZ2000	2000	502	582	1,084
2	SLAUGHTER HOUSE	2010	140	249	389
1	BLISS CREEK	2020	33	69	102
1	SECRET HARBOR CREEK	2030	108	438	546
1	MARLETTE CREEK	2040	132	541	673
1	BONPLAND	2050	20	109	129
1	TUNNEL CREEK	2060	23	218	240
2	IVZ3000	3000	1,039	229	1,268
2	MCFAUL CREEK	3010	131	217	349
2	ZEPHYR CREEK	3020	52	98	150
2	NORTH ZEPHYR CREEK	3030	33	156	189
2	LINCOLN CREEK	3040	31	147	179
2	CAVE ROCK	3050	20	43	63
2	LOGAN HOUSE CREEK	3060	34	124	157
2	NORTH LOGAN HOUSE CREEK	3070	12	56	69
2	GLENBROOK CREEK	3080	166	216	383
3	IVZ4000	4000	4,062	192	4,254
3	BIJOU CREEK	4010	1,455	126	1,581
2	EDGEWOOD CREEK	4020	1,154	217	1,371
2	BURKE CREEK	4030	350	189	539
3	IVZ5000	5000	2,484	316	2,800
3	UPPER TRUCKEE RIVER	5010	13,981	10,133	24,115
3	TROUT CREEK	5050	4,046	2,492	6,538
4	IVZ6000	6000	870	929	1,799
4	IVZ6001	6001	1,990	232	2,221
4	GENERAL CREEK	6010	1,201	1,944	3,145

4	MEEKS	6020	1,376	2,084	3,460
4	SIERRA CREEK	6030	380	221	601
4	LONELY GULCH CREEK	6040	578	273	851
4	PARADISE FLAT	6050	175	159	334
4	RUBICON CREEK	6060	982	725	1,707
4	EAGLE CREEK	6080	444	2,479	2,923
3	CASCADE CREEK	6090	213	853	1,067
3	TALLAC CREEK	6100	291	421	712
3	TAYLOR CREEK	6110	1,872	3,512	5,384
4	UNNAMED CK	6120	188	65	254
4	IVZ7000	7000	4,390	462	4,852
4	BLACKWOOD CREEK	7010	1,850	6,553	8,402
4	MADDEN CREEK	7020	419	533	952
4	HOMEWOOD CREEK	7030	360	260	619
4	QUAIL LAKE CREEK	7040	364	371	735
4	MKINNEY CREEK	7050	1,949	1,177	3,126
4	IVZ8000	8000	5,588	514	6,102
1	DOLLAR CREEK	8010	111	166	277
1	UNNAMED CK LAKE FOREST 1	8020	487	97	584
1	UNNAMED CK LAKE FOREST 2	8030	196	152	348
1	BURTON CREEK	8040	61	805	866
1	TAHOE STATE PARK	8050	108	160	268
4	WARD CREEK	8060	2,883	3,561	6,444
1	IVZ9000	9000	3,196	823	4,019
1	KINGS BEACH	9010	191	62	254
1	GRIFF CREEK	9020	308	669	978
1	TAHOE VISTA	9030	1,078	695	1,773
1	CARNELIAN CANYON	9040	267	463	730
1	CARNELIAN BAY CREEK	9050	28	135	164
1	WATSON	9060	66	350	416

**Table C-4. Summary of annual surface, base and total phosphorus loads by watershed**

Quad	Tributary	OUTLET SWS	Surface TP Load (kg)	Baseflow TP Load (kg)	Total TP Load (kg)
1	IVZ1000	1000	772	60	831
1	MILL CREEK	1010	159	66	224
1	INCLINE CREEK	1020	657	221	877
1	THIRD CREEK	1030	632	211	843
1	WOOD CREEK	1040	166	67	232
1	BURNT CEDAR CREEK	1050	131	8	139
1	SECOND CREEK	1060	49	47	96
1	FIRST CREEK	1070	29	61	90
1	IVZ2000	2000	180	82	263
2	SLAUGHTER HOUSE	2010	31	110	141
1	BLISS CREEK	2020	14	10	23
1	SECRET HARBOR CREEK	2030	29	62	91
1	MARLETTE CREEK	2040	33	76	109
1	BONPLAND	2050	3	15	18
1	TUNNEL CREEK	2060	4	42	45
2	IVZ3000	3000	169	102	270
2	MCFAUL CREEK	3010	22	30	52
2	ZEPHYR CREEK	3020	9	14	23
2	NORTH ZEPHYR CREEK	3030	7	21	29
2	LINCOLN CREEK	3040	8	20	28
2	CAVE ROCK	3050	4	6	9
2	LOGAN HOUSE CREEK	3060	9	17	26
2	NORTH LOGAN HOUSE CREEK	3070	4	25	29
2	GLENBROOK CREEK	3080	47	96	143
3	IVZ4000	4000	739	21	760
3	BIJOU CREEK	4010	260	14	273
2	EDGEWOOD CREEK	4020	134	69	203
2	BURKE CREEK	4030	43	26	69
3	IVZ5000	5000	477	42	519
3	UPPER TRUCKEE RIVER	5010	2,782	1,328	4,110
3	TROUT CREEK	5050	728	272	1,000
4	IVZ6000	6000	439	135	574
4	IVZ6001	6001	639	26	665
4	GENERAL CREEK	6010	302	215	517

Quad	Tributary	OUTLET SWS	Surface TP Load (kg)	Baseflow TP Load (kg)	Total TP Load (kg)
4	MEEKS	6020	324	231	555
4	SIERRA CREEK	6030	125	24	149
4	LONELY GULCH CREEK	6040	163	30	193
4	PARADISE FLAT	6050	45	18	62
4	RUBICON CREEK	6060	311	80	391
4	EAGLE CREEK	6080	112	356	468
3	CASCADE CREEK	6090	45	111	156
3	TALLAC CREEK	6100	69	55	125
3	TAYLOR CREEK	6110	367	462	829
4	UNNAMED CK	6120	60	7	67
4	IVZ7000	7000	1,717	53	1,770
4	BLACKWOOD CREEK	7010	821	1,503	2,324
4	MADDEN CREEK	7020	351	59	410
4	HOMEWOOD CREEK	7030	398	29	427
4	QUAIL LAKE CREEK	7040	183	41	224
4	MKINNEY CREEK	7050	508	130	638
4	IVZ8000	8000	2,858	92	2,950
1	DOLLAR CREEK	8010	53	36	88
1	UNNAMED CK LAKE FOREST 1	8020	136	21	157
1	UNNAMED CK LAKE FOREST 2	8030	65	33	98
1	BURTON CREEK	8040	34	174	209
1	TAHOE STATE PARK	8050	41	35	76
4	WARD CREEK	8060	1,443	591	2,034
1	IVZ9000	9000	951	176	1,127
1	KINGS BEACH	9010	48	13	61
1	GRIFF CREEK	9020	117	146	263
1	TAHOE VISTA	9030	489	150	640
1	CARNELIAN CANYON	9040	99	100	199
1	CARNELIAN BAY CREEK	9050	14	29	43
1	WATSON	9060	23	77	100

**Table C-5. Summary of basin-wide annualized surface and baseflow volumes by land use**

<b>Landuse ID</b>	<b>Land Use Name</b>	<b>Surface Flow (1000 m<sup>3</sup>)</b>	<b>Baseflow (1000 m<sup>3</sup>)</b>
1	Residential_SFP	2,610	14,400
2	Residential_MFP	465	3,370
3	CICU-Pervious	370	2,760
4	Ski_Runs-Pervious	819	2,410
5	Veg_ep1	3,350	20,300
6	Veg_ep2	26,800	157,000
7	Veg_ep3	18,700	102,000
8	Veg_ep4	6,070	37,900
9	Veg_ep5	260	1,250
10	Veg_Recreational	127	607
11	Veg_Burned	201	861
12	Veg_Harvest	94	664
13	Veg_Turf	219	1,720
14	Water_Body	19,800	0
15	Residential_SFI	5,740	0
16	Residential_MFI	2,240	0
17	CICU-Impervious	3,040	0
18	Roads_Primary	1,810	0
19	Roads_Secondary	8,970	0
20	Roads_Unpaved	164	688

**Table C-6. Summary of annual upland TSS, upland fines loads by land use and flow-weighted basin-wide average concentration**

<b>Landuse ID</b>	<b>Land Use Name</b>	<b>Upland TSS (tonnes/year)</b>	<b>Upland Fines (tonnes/year)</b>	<b>Upland TSS Concentration (mg/L)</b>	<b>Upland Fines Concentration (mg/L)</b>
1	Residential_SFP	269	205	103	78
2	Residential_MFP	194	172	418	370
3	CICU-Pervious	205	175	555	474
4	Ski_Runs-Pervious	695	227	848	278
5	Veg_ep1	21	9	6	3
6	Veg_ep2	691	290	26	11
7	Veg_ep3	3,050	1,230	163	66
8	Veg_ep4	5,810	2,360	957	388
9	Veg_ep5	686	288	2,640	1,110
10	Veg_Recreational	41	17	326	135
11	Veg_Burned	189	69	941	342
12	Veg_Harvest	142	54	1,520	577
13	Veg_Turf	7	3	34	12
14	Water_Body	n/a	n/a	n/a	n/a
15	Residential_SFI	319	243	56	42
16	Residential_MFI	358	316	160	141
17	CICU-Impervious	788	673	260	222
18	Roads_Primary	1,720	1,470	950	811
19	Roads_Secondary	1,380	1,180	154	131
20	Roads_Unpaved	354	126	2,150	770

**Table C-7. Summary of annual surface and baseflow total nitrogen loads and flow-weighted basin-wide average concentrations by land use**

<b>Landuse ID</b>	<b>Land Use Name</b>	<b>Surface TN (kg/year)</b>	<b>Baseflow TN (kg/year)</b>	<b>Surface TN Concentration (mg/L)</b>	<b>Baseflow TN Concentration (mg/L)</b>
1	Residential_SFP	4,920	1,980	1.883	0.138
2	Residential_MFP	1,310	484	2.813	0.144
3	CICU-Pervious	891	373	2.407	0.135
4	Ski_Runs-Pervious	415	352	0.507	0.146
5	Veg_ep1	459	2,530	0.137	0.125
6	Veg_ep2	4,430	22,100	0.165	0.141
7	Veg_ep3	3,840	17,000	0.206	0.166
8	Veg_ep4	1,300	6,910	0.214	0.182
9	Veg_ep5	65	246	0.250	0.198
10	Veg_Recreational	153	89	1.207	0.147
11	Veg_Burned	431	110	2.143	0.128
12	Veg_Harvest	165	82	1.757	0.123
13	Veg_Turf	842	232	3.847	0.135
14	Water_Body	n/a	n/a	n/a	n/a
15	Residential_SFI	9,440	n/a	1.644	n/a
16	Residential_MFI	5,860	n/a	2.616	n/a
17	CICU-Impervious	6,380	n/a	2.103	n/a
18	Roads_Primary	6,740	n/a	3.718	n/a
19	Roads_Secondary	25,100	n/a	2.794	n/a
20	Roads_Unpaved	470	106	2.863	0.154

**Table C-8. Summary of annual surface and baseflow total phosphorus loads and flow-weighted average concentrations by land use**

<b>Landuse ID</b>	<b>Land Use Name</b>	<b>Surface TP (kg/year)</b>	<b>Baseflow TP (kg/year)</b>	<b>Surface TP Concentration (mg/L)</b>	<b>Baseflow TP Concentration (mg/L)</b>
1	Residential_SFP	1,950	343	0.745	0.024
2	Residential_MFP	565	92	1.215	0.027
3	CICU-Pervious	384	63	1.037	0.023
4	Ski_Runs-Pervious	370	51	0.452	0.021
5	Veg_ep1	77	344	0.023	0.017
6	Veg_ep2	780	3,290	0.029	0.021
7	Veg_ep3	910	2,870	0.049	0.028
8	Veg_ep4	700	1,270	0.115	0.034
9	Veg_ep5	82	44	0.316	0.035
10	Veg_Recreational	90	13	0.713	0.021
11	Veg_Burned	234	19	1.166	0.022
12	Veg_Harvest	126	16	1.342	0.024
13	Veg_Turf	528	47	2.411	0.027
14	Water_Body	n/a	n/a	n/a	n/a
15	Residential_SFI	2,500	n/a	0.436	n/a
16	Residential_MFI	1,160	n/a	0.517	n/a
17	CICU-Impervious	1,570	n/a	0.518	n/a
18	Roads_Primary	3,640	n/a	2.007	n/a
19	Roads_Secondary	5,400	n/a	0.602	n/a
20	Roads_Unpaved	614	18	3.739	0.026

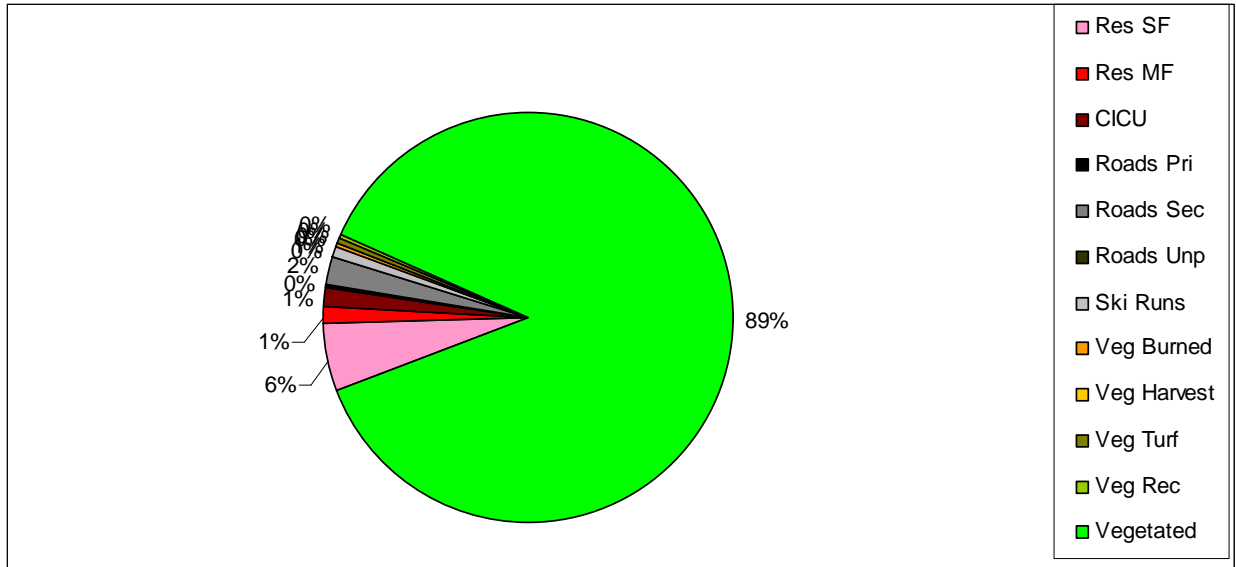


Figure C-1. Pie chart of percent of total flow (m<sup>3</sup>) contributed by land use.

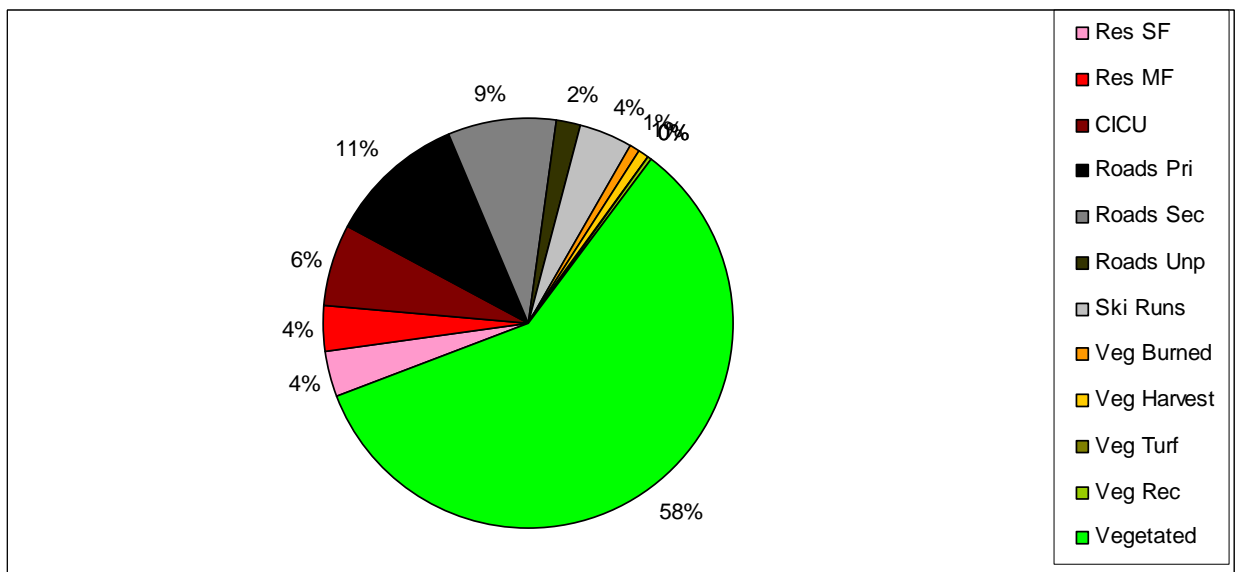


Figure C-2. Pie chart of percent of upland TSS (tonne) contributed by land use.

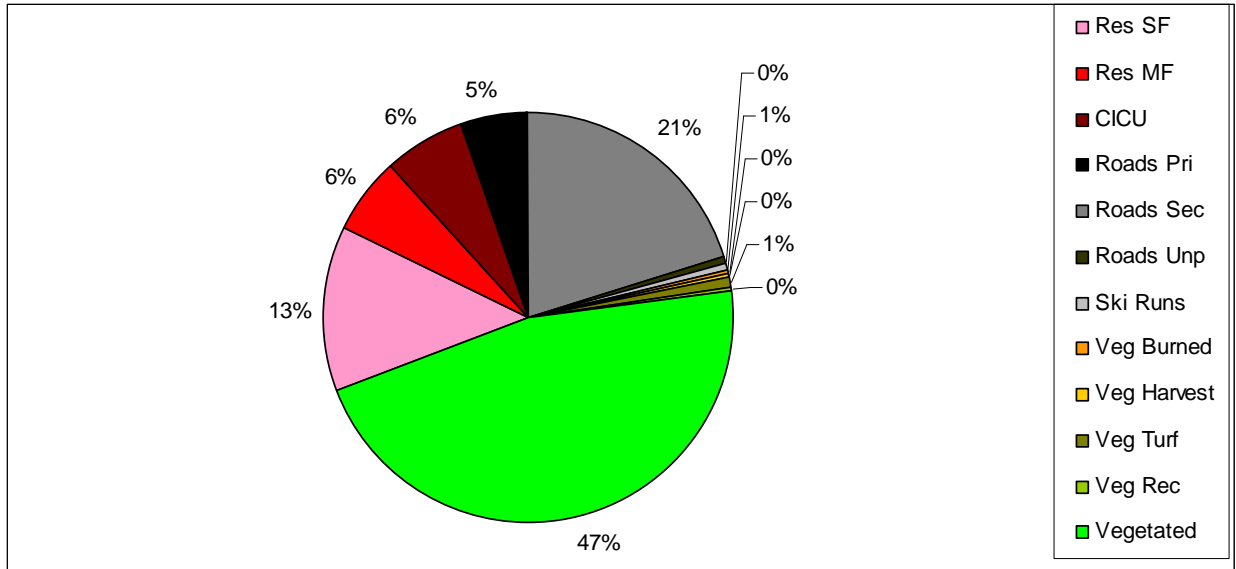


Figure C-3. Pie chart of percent of total nitrogen (kg) contributed by land use.

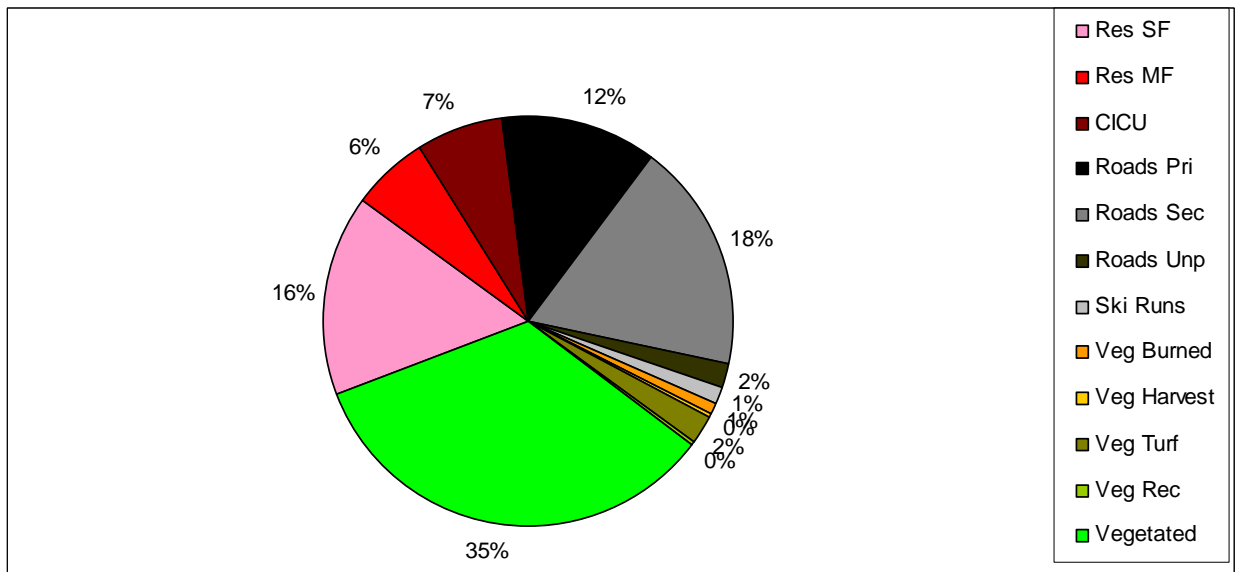


Figure C-4. Pie chart of percent of total phosphorus (kg) contributed by land use.

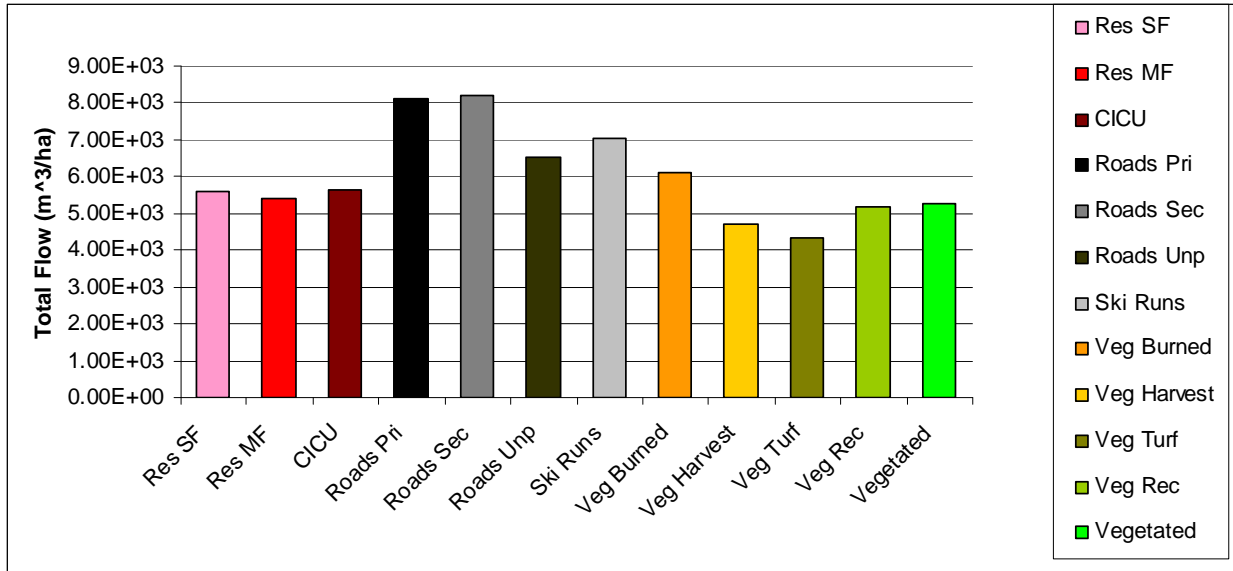


Figure C-5. Average unit area flow (m³/ha) by land use.

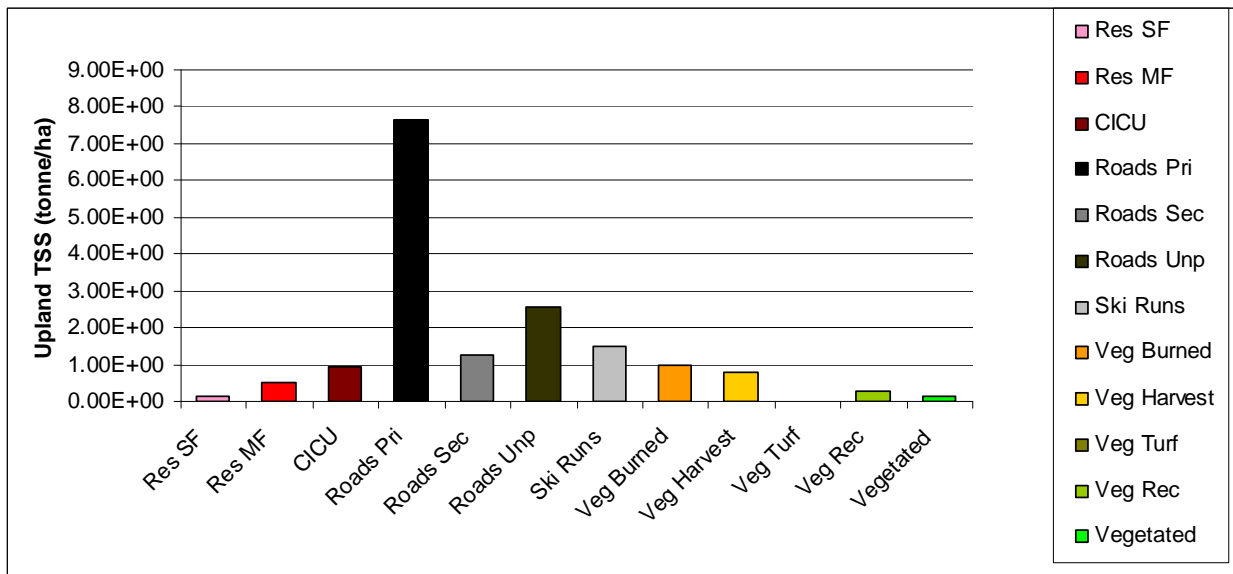


Figure C-6. Average unit area TSS (tonnes/ha) by land use.

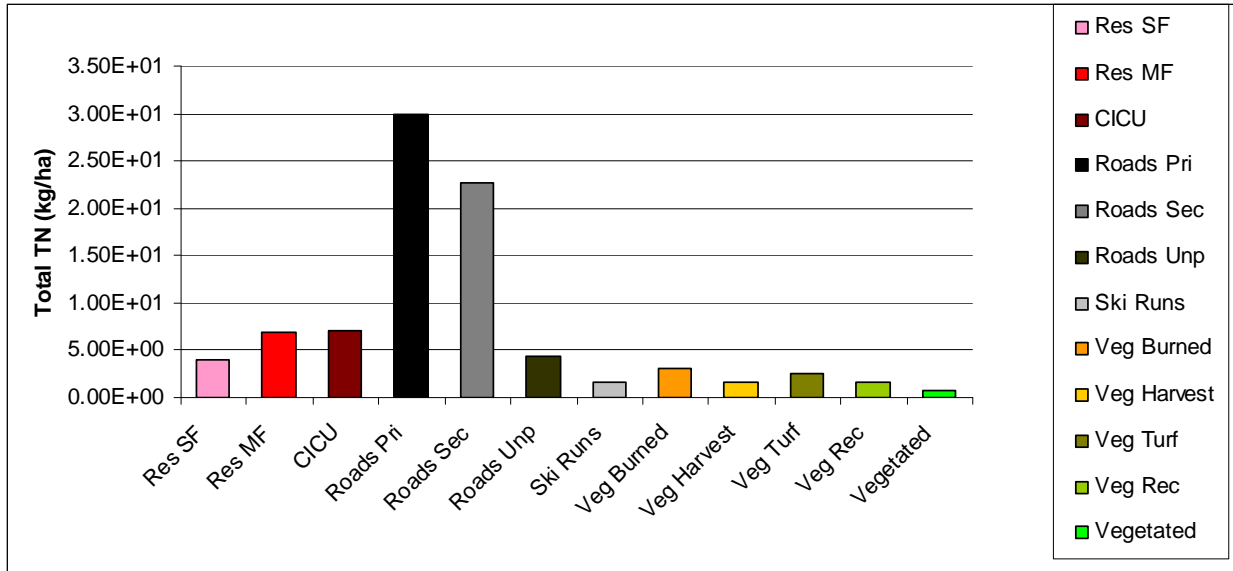


Figure C-7. Average unit area total nitrogen (m<sup>3</sup>/kg) by land use.

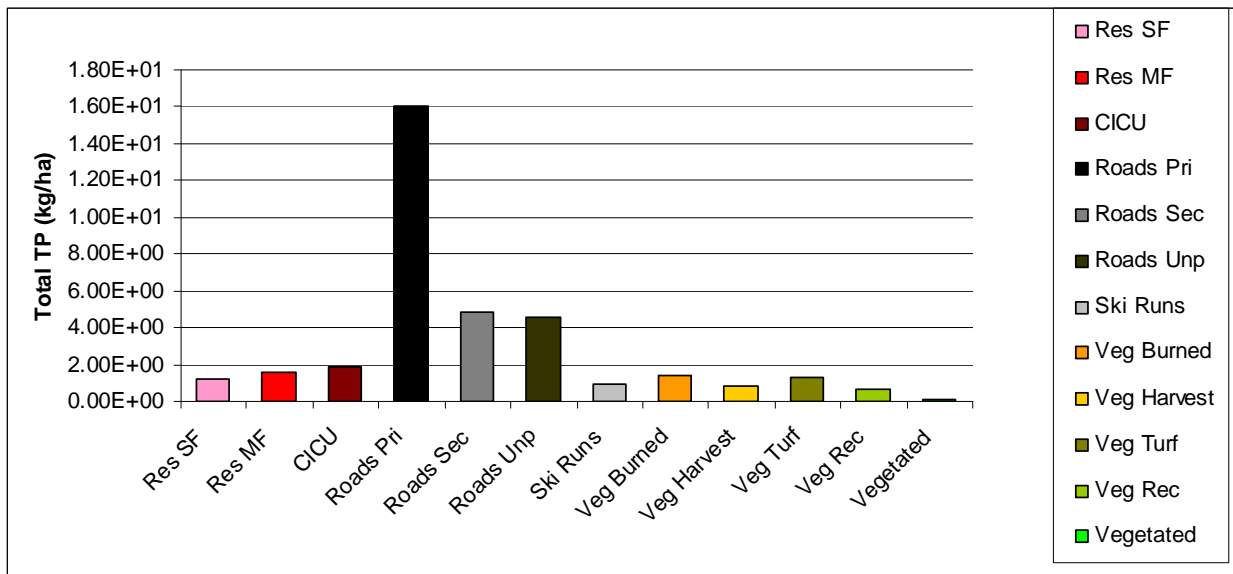


Figure C-8. Average unit area total phosphorus (m<sup>3</sup>/kg) by land use.

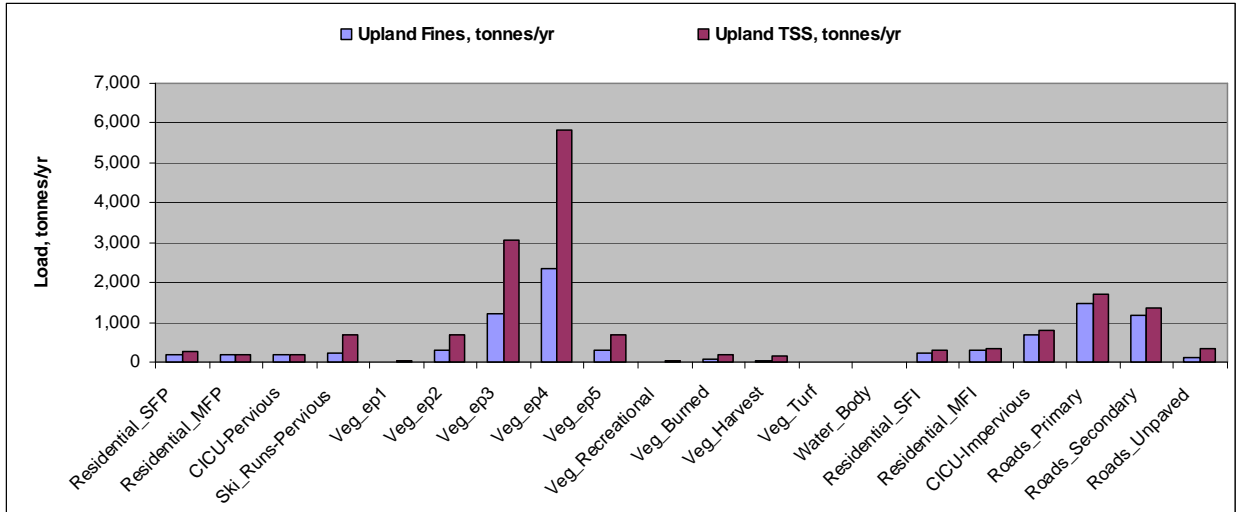


Figure C-9. Upland TSS and upland fines loads by land use.

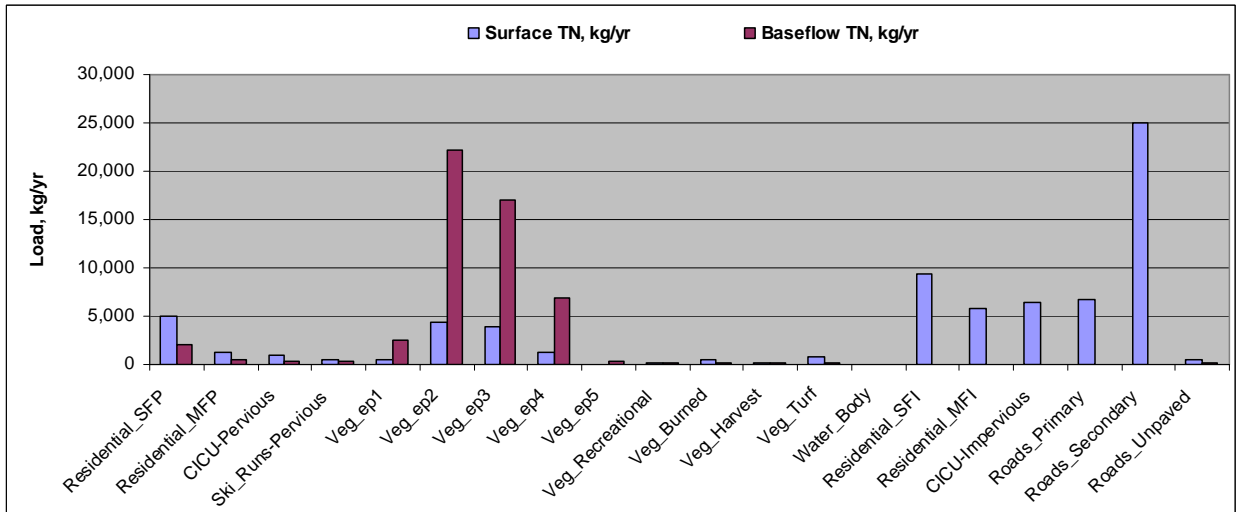
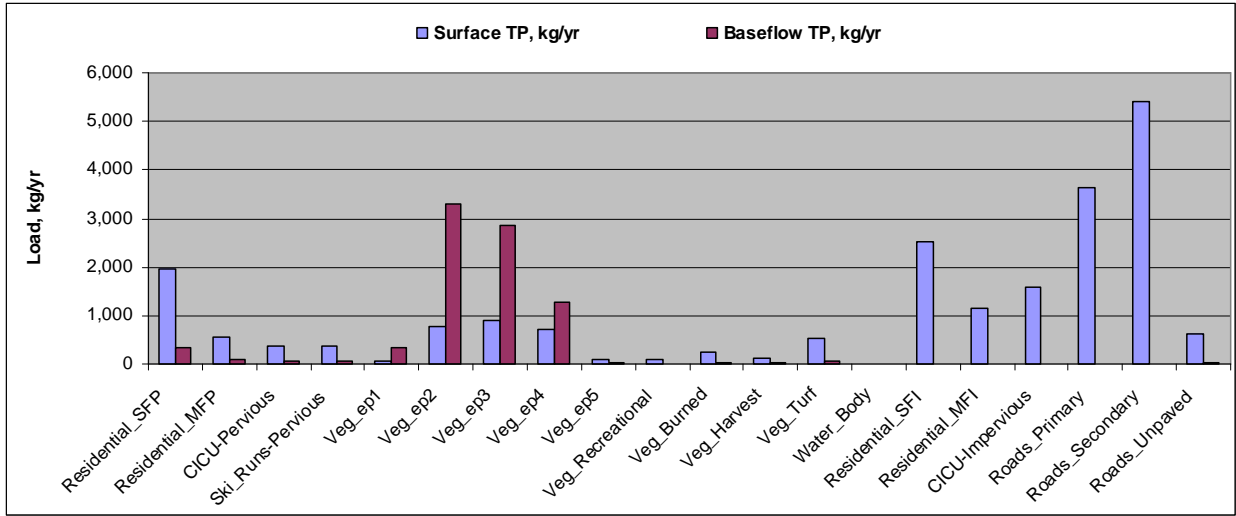
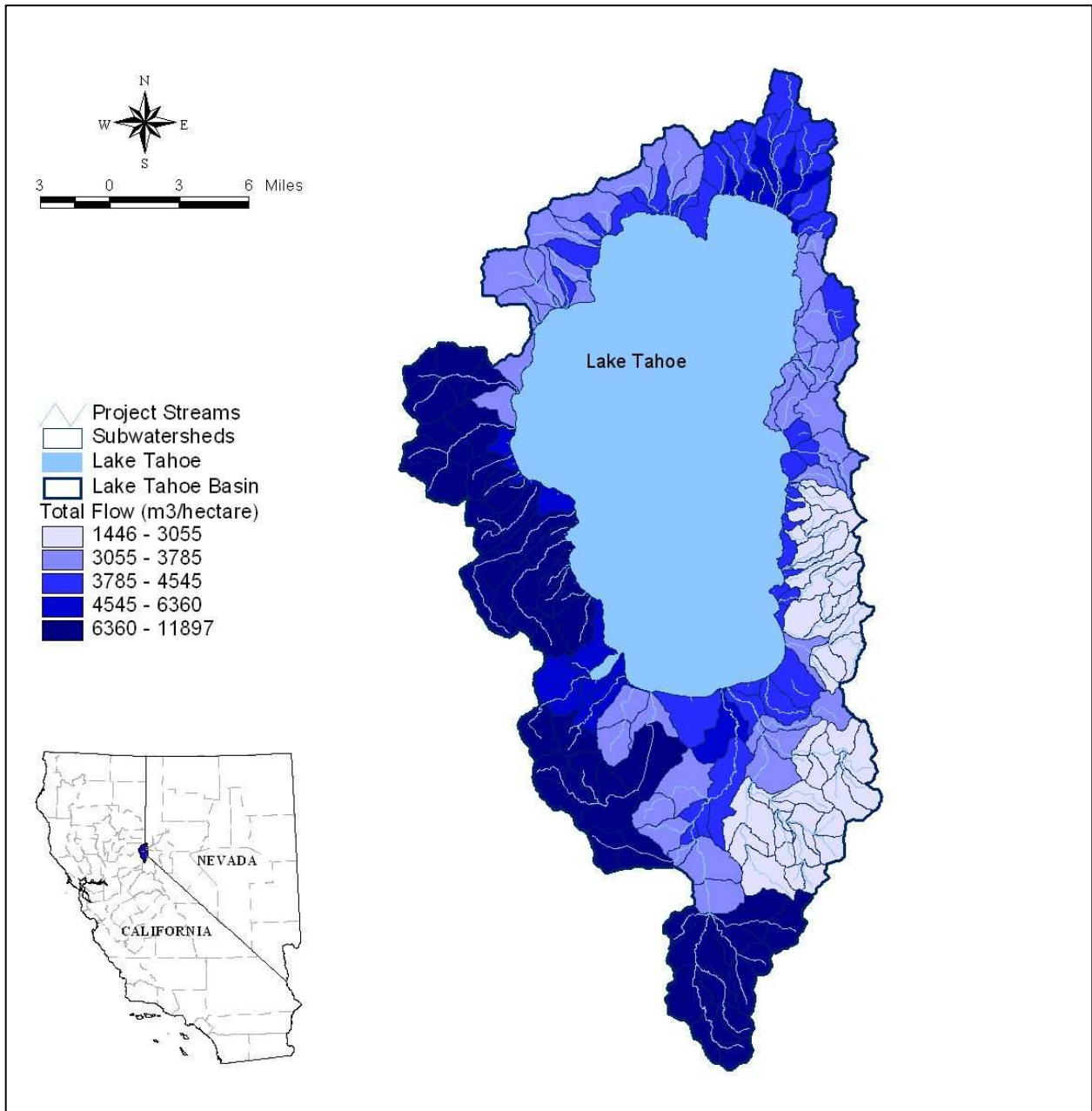


Figure C-10. Surface and baseflow total nitrogen loads by land use.



**Figure C-11. Surface and baseflow total phosphorus loads by land use.**



**Figure C-12. Unit-area annual water yield (m<sup>3</sup>/ha) by subwatershed.**

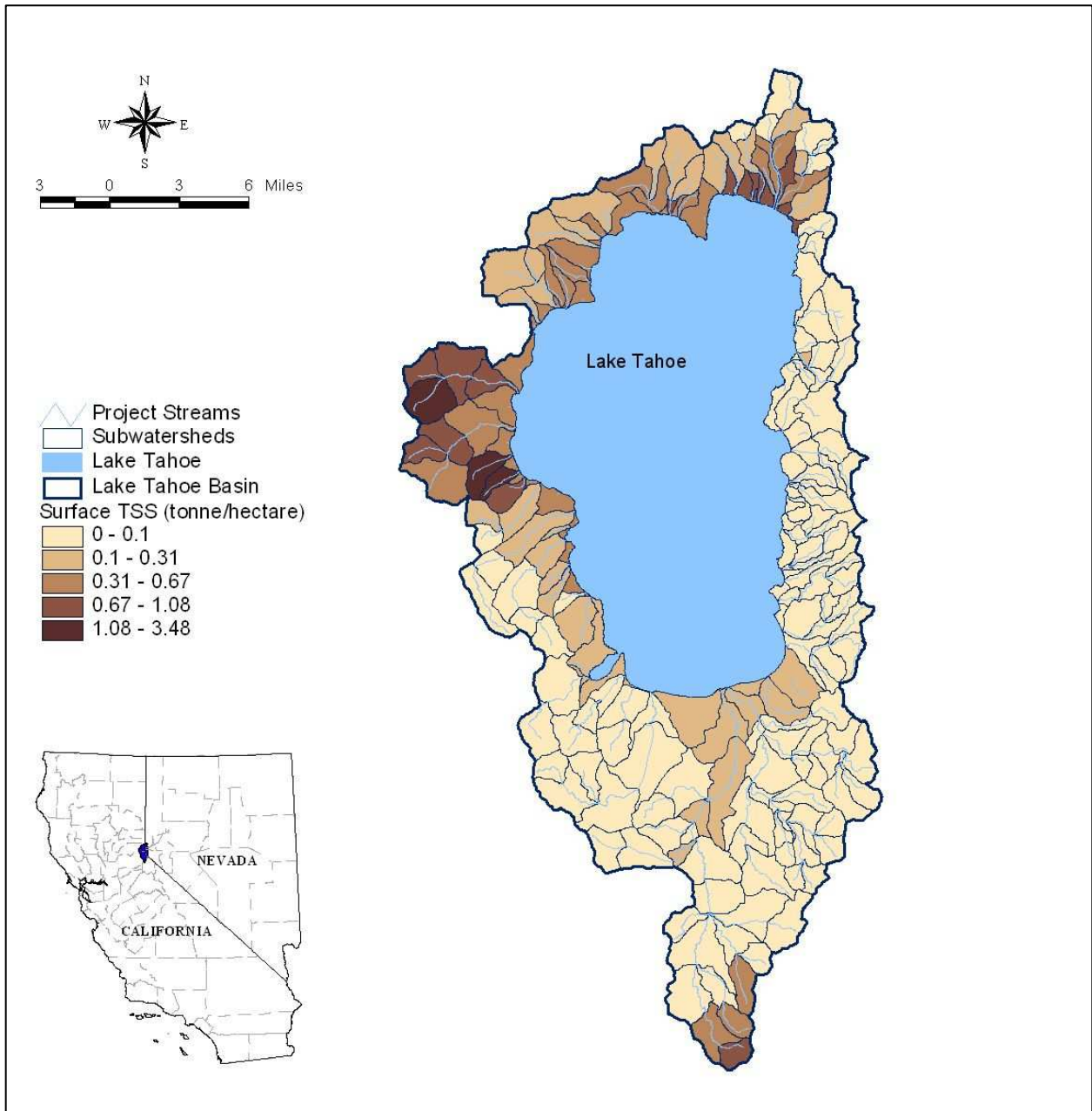


**Figure C-13. Unit-area annual total sediment yield (tonnes/ha) by subwatershed.**

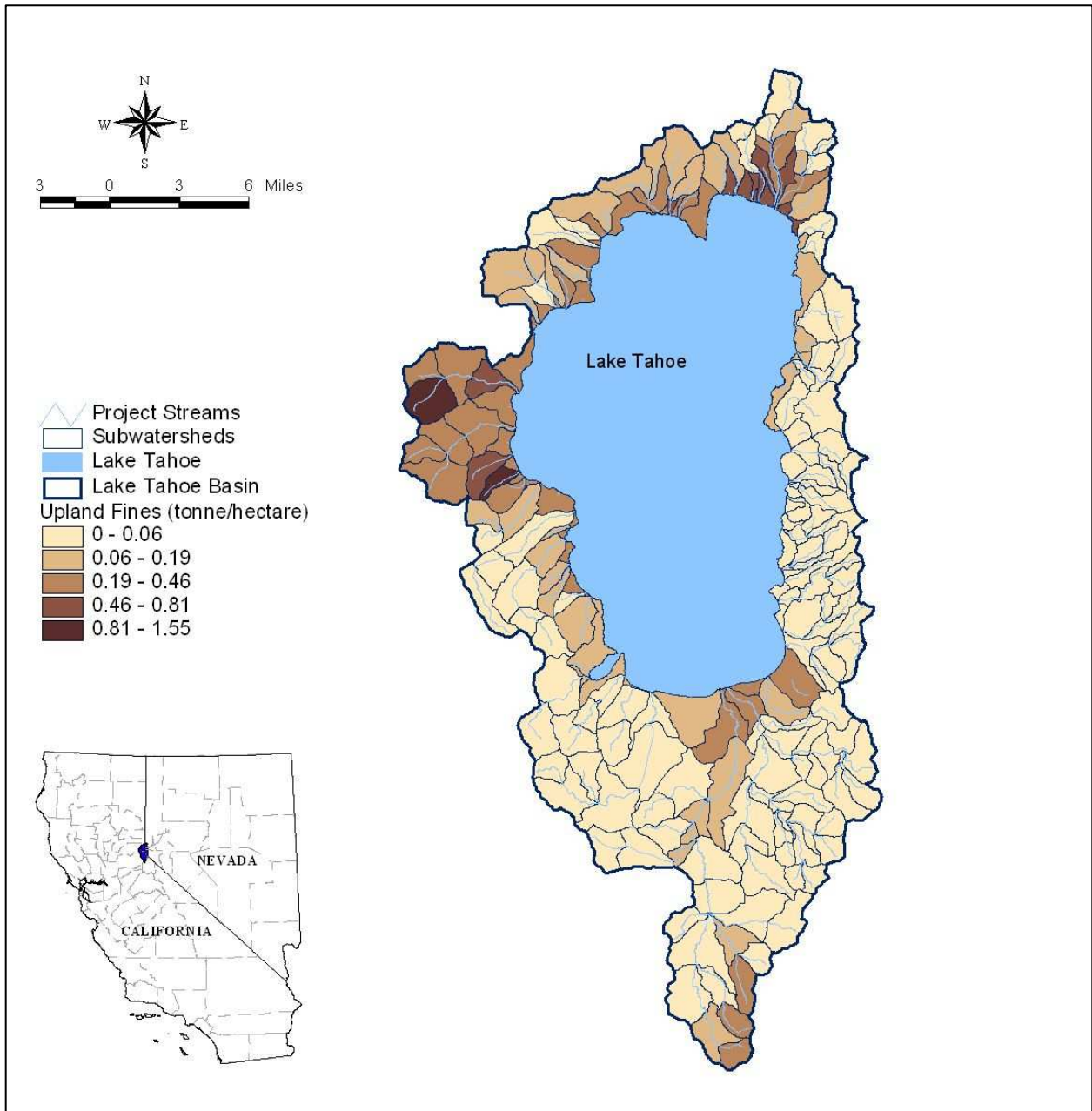


**Figure C-14. Unit-area annual fine sediment yield (tonnes/ha) by subwatershed.**

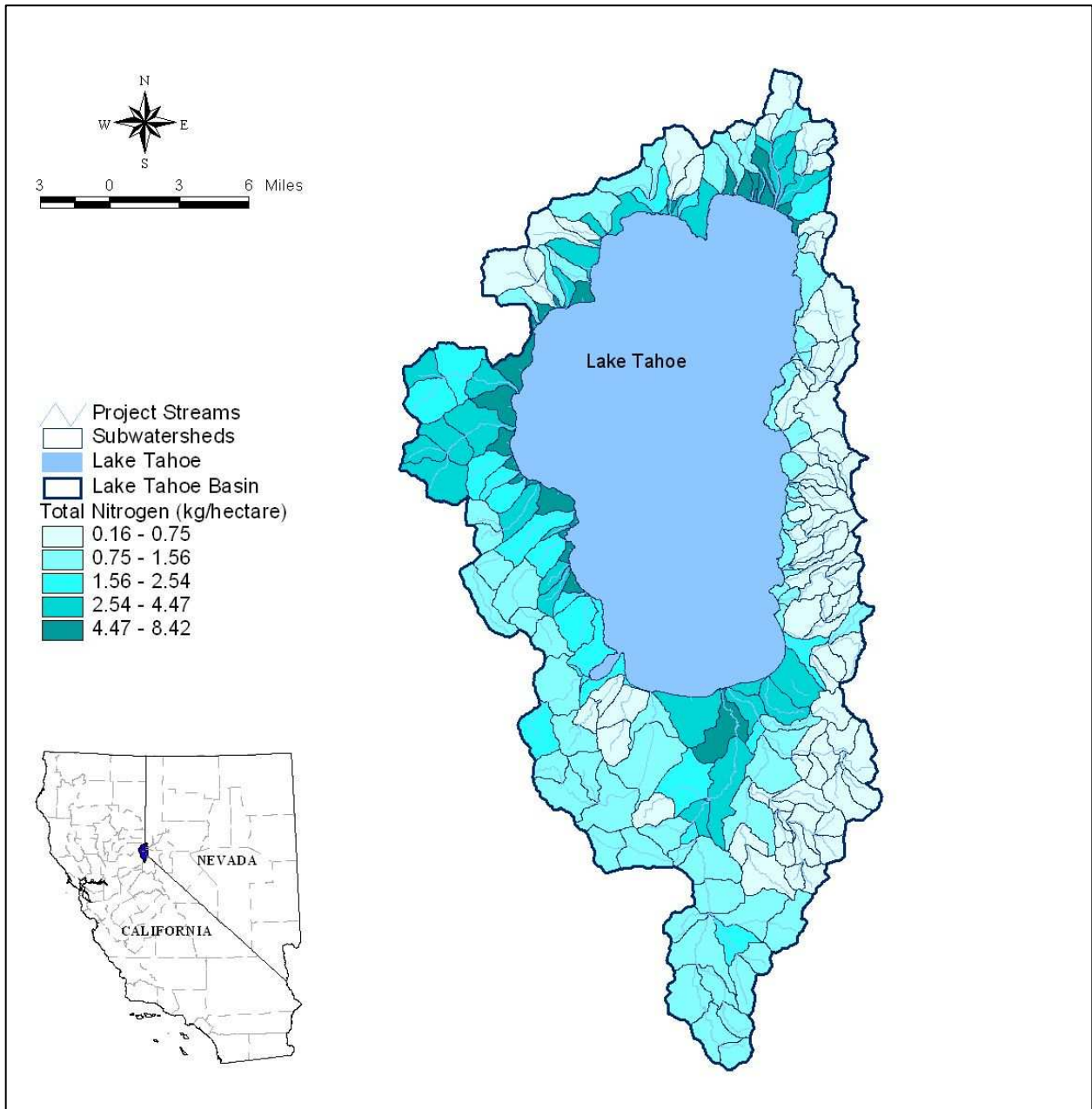


**Figure C-15. Unit-area total nitrogen yield (kg/ha) by subwatershed.**

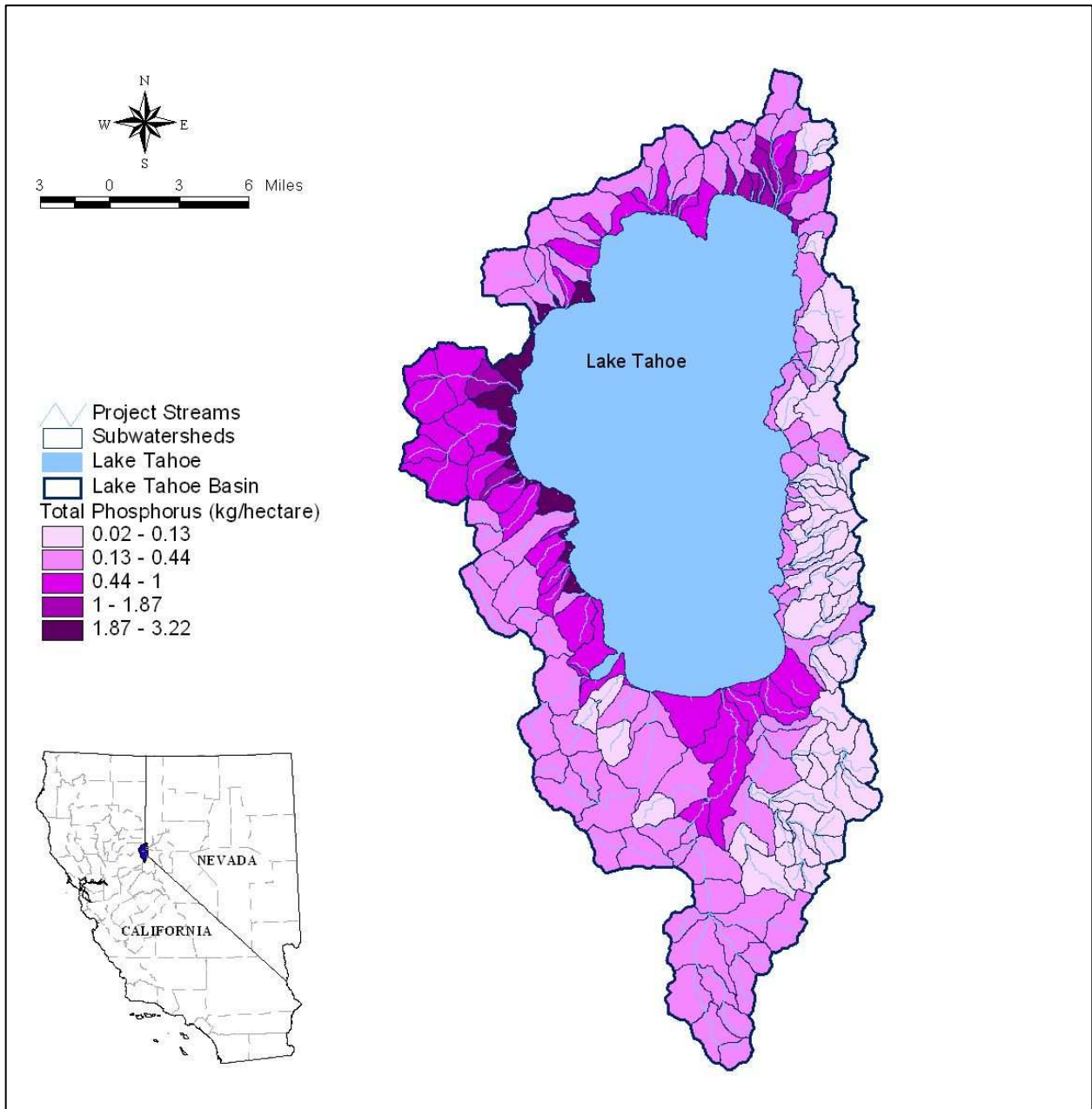


**Figure C-16. Unit-area total phosphorus yield (kg/ha) by subwatershed.**

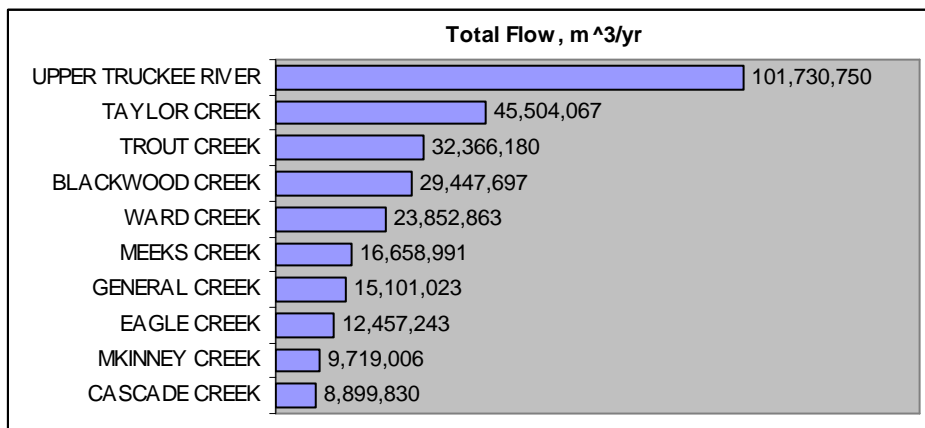


**Figure C-17. Top ten total flow contributors.**

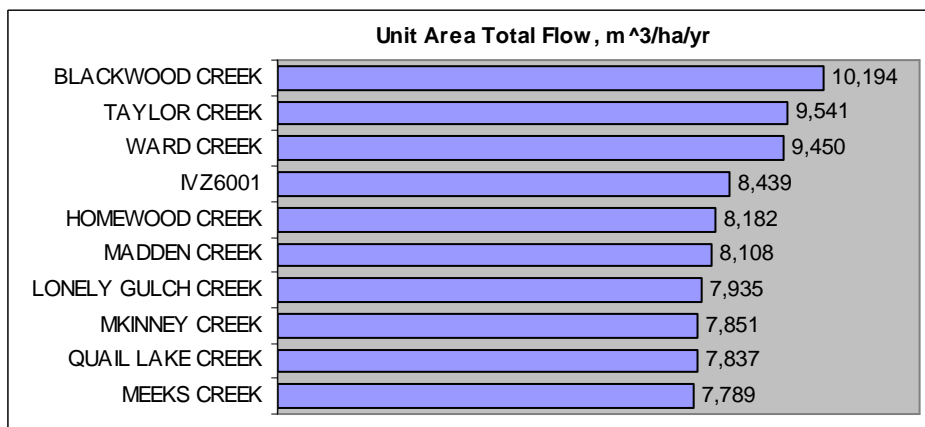


**Figure C-18. Top ten unit-area water yield contributors.**

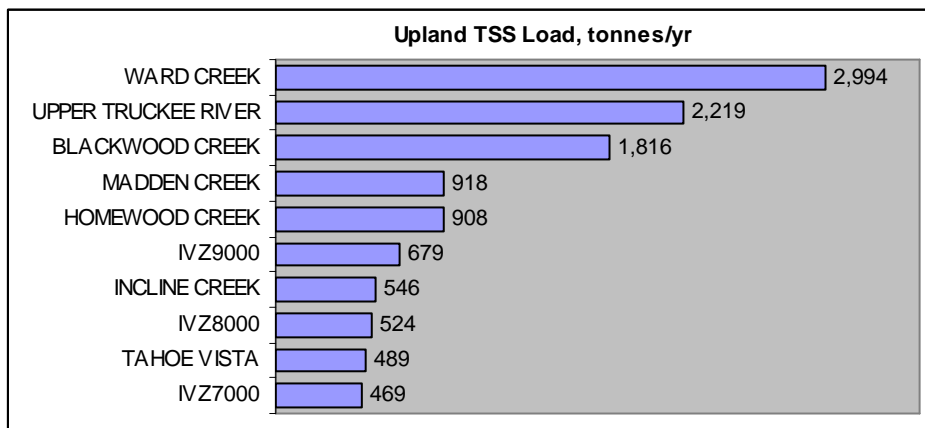


**Figure C-19. Top ten total upland sediment contributors.**

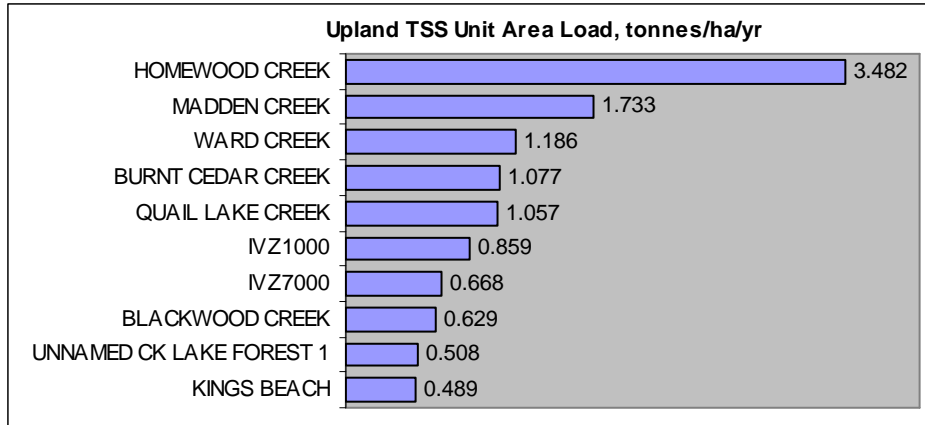


**Figure C-20. Top ten unit-area upland sediment contributors.**

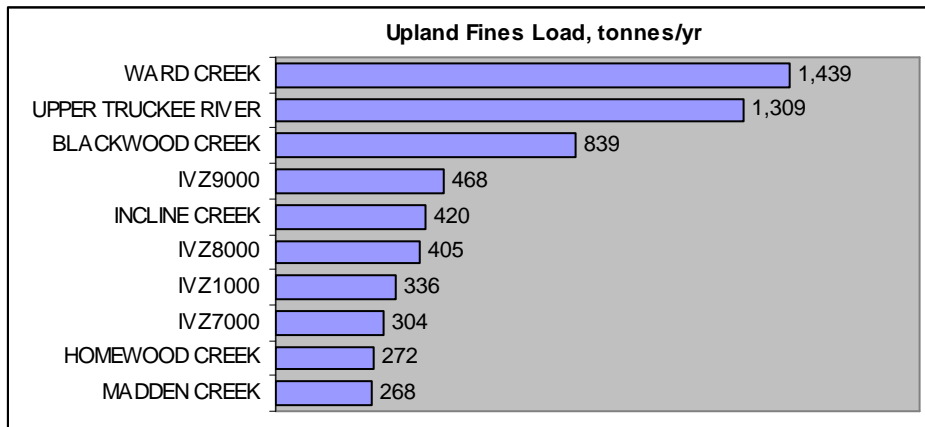


**Figure C-21. Top ten total upland fine sediment contributors.**

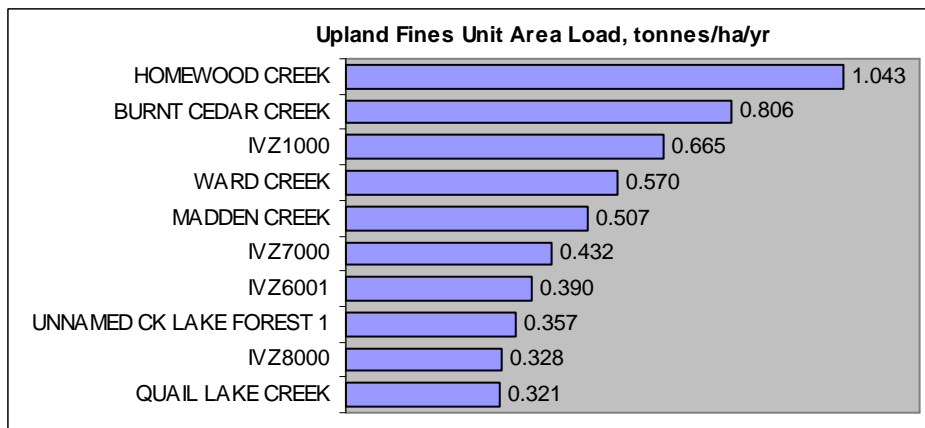


**Figure C-22. Top ten unit-area upland fine sediment yield contributors.**

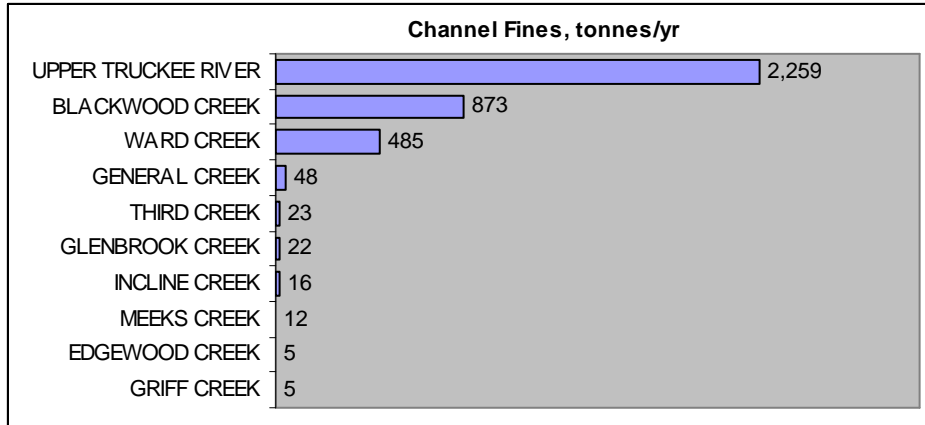


**Figure C-23. Top ten total channel fine sediment contributors.**

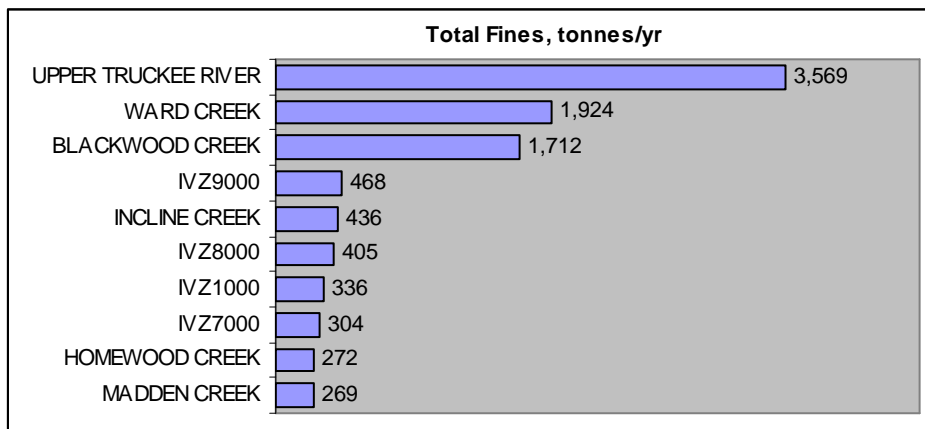


**Figure C-24. Top ten total fine sediment contributors.**

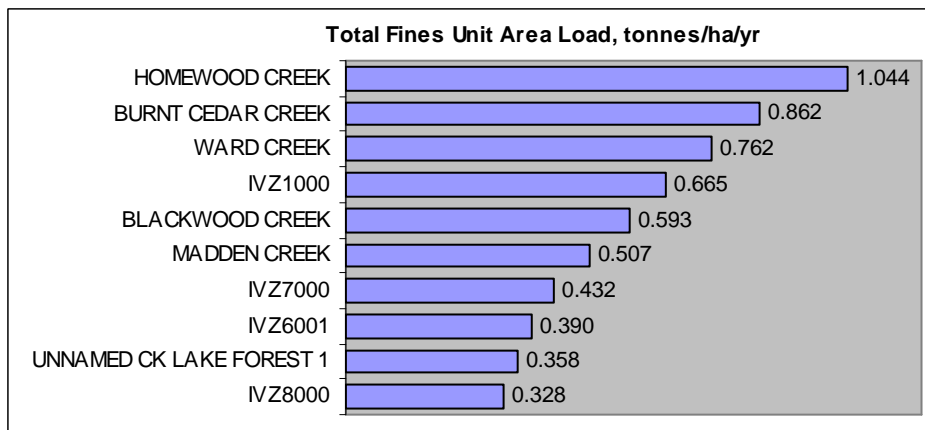


**Figure C-25. Top ten unit-area total fine sediment yield contributors.**

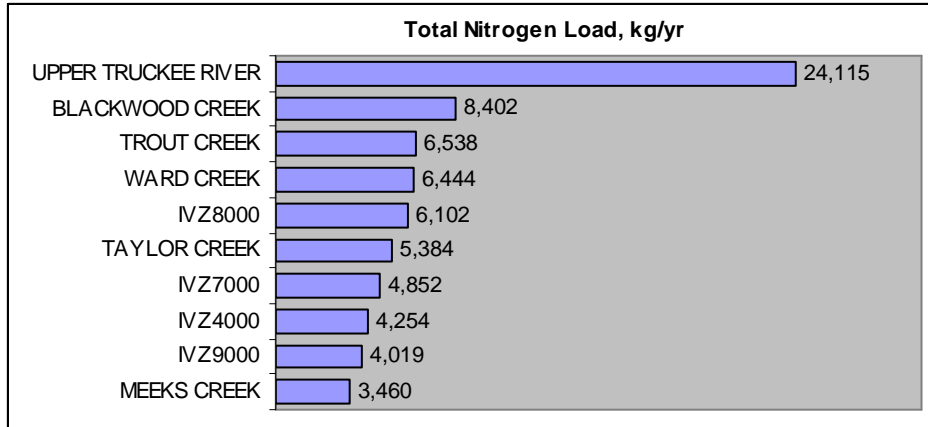


**Figure C-26. Top ten total nitrogen contributors.**

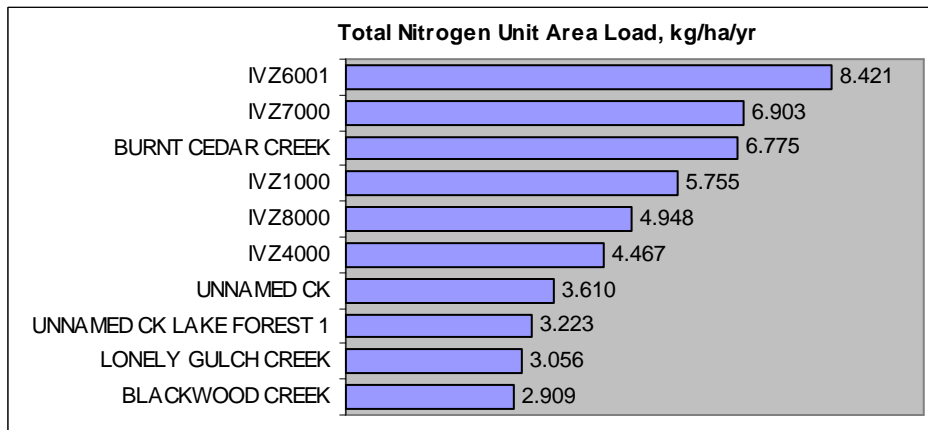


**Figure C-27. Top ten unit-area total nitrogen yield contributors.**

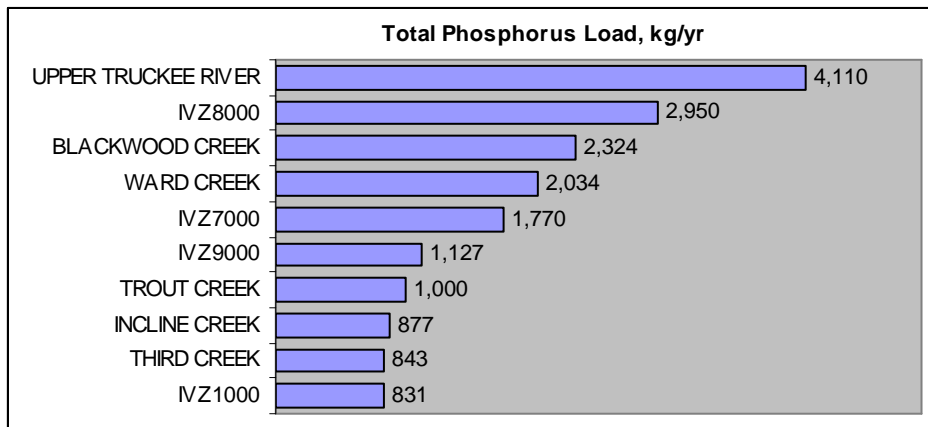


**Figure C-28. Top ten total phosphorus contributors.**

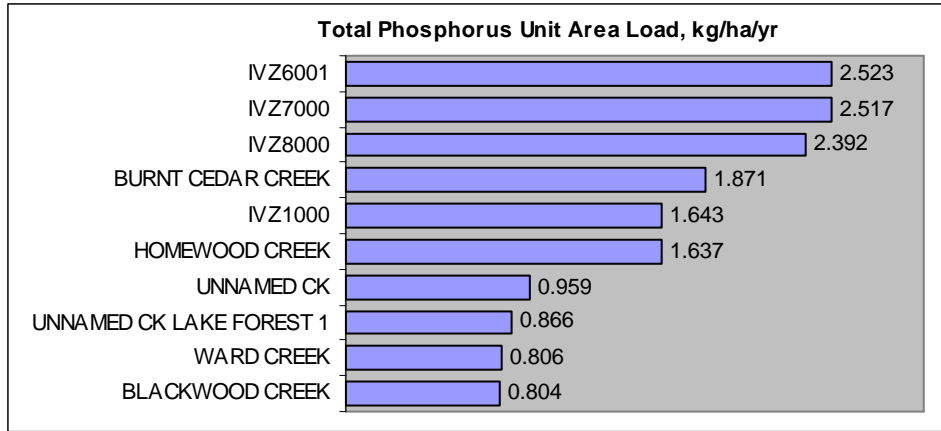


**Figure C-29. Top ten unit-area total phosphorus contributors.**